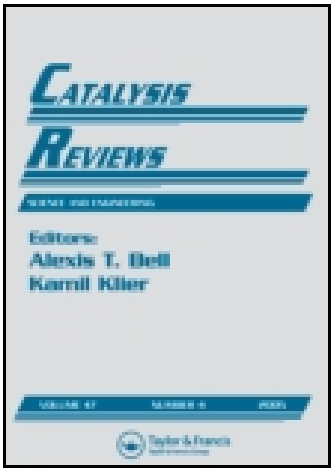

Catalysis Reviews: Science and Engineering
Publication details, including instructions for authors and subscription information:
http://www.tandfonline.com/loi/lctr20

Recent Advances in Reactions of Alkylbenzenes Over Novel Zeolites: The Effects of Zeolite Structure and Morphology

Sulaiman Al-Khattaf[a], Syed A. Ali[a], Abdullah M. Aitani[a], Naděžda Žilková[b], David Kubička[c] & Jiří Čejka[ab]

[a] Center of Research Excellence in Petroleum Refining and Petrochemicals, King Fahd University of Petroleum and Minerals, Dhahran, Saudi Arabia

[b] J. Heyrovský Institute of Physical Chemistry, Academy of Sciences of the Czech Republic, v.v.i., Prague, Czech Republic

[c] Research Institute of Inorganic Chemistry - UniCRE-RENTECH, Litvínov, Czech Republic

Published online: 25 Sep 2014.

To cite this article: Sulaiman Al-Khattaf, Syed A. Ali, Abdullah M. Aitani, Naděžda Žilková, David Kubička & Jiří Čejka (2014) Recent Advances in Reactions of Alkylbenzenes Over Novel Zeolites: The Effects of Zeolite Structure and Morphology, Catalysis Reviews: Science and Engineering, 56:4, 333-402, DOI: 10.1080/01614940.2014.946846

To link to this article: http://dx.doi.org/10.1080/01614940.2014.946846

Catalysis Reviews: Science and Engineering, 56:333–402, 2014

ISSN: 0161-4940 print / 1520-5703 online
DOI: 10.1080/01614940.2014.946846

Recent Advances in Reactions of Alkylbenzenes Over Novel Zeolites: The Effects of Zeolite Structure and Morphology

Sulaiman Al-Khattaf[1], Syed A. Ali[1], Abdullah M. Aitani[1], Naděžda Žilková[2], David Kubička[3], and Jiří Čejka[1,2]

[1]Center of Research Excellence in Petroleum Refining and Petrochemicals, King Fahd University of Petroleum and Minerals, Dhahran, Saudi Arabia
[2]J. Heyrovský Institute of Physical Chemistry, Academy of Sciences of the Czech Republic, v.v.i., Prague, Czech Republic
[3]Research Institute of Inorganic Chemistry – UniCRE-RENTECH, Litvínov, Czech Republic

Alkylbenzenes form an important segment of petrochemical industry for the manufacture of widely used commodities and specialty products. Since the last review on this topic (8), numerous new zeolite-based catalysts have been synthesized, characterized and evaluated in various transformations of aromatic hydrocarbons. This comprehensive review covers major reactions of mono-, di-, and tri-alkylbenzenes such as disproportionation, alkylation, transalkylation, isomerization, etc., over different zeolite-based acid catalysts. During the last decade, significant progress was made in the synthesis and structure determination of novel zeolites, mesoporous single crystals, hierarchic zeolites and two-dimensional zeolites. These developments have enhanced the understanding of the role of zeolites (effects of structural type, morphology, acid sites, accessibility of acid sites, shape selectivity factors) in transformations of aromatics. In this review, the emphasis is on the influence of the type of acid sites, zeolite topology, and reaction conditions on the activity, selectivity and pathways of these reactions. Thermodynamics and reaction kinetics of transformations of aromatic hydrocarbons are also discussed. This article covers mostly literature published during the period of 2002–2013.

Keywords Alkyl aromatics, Dialkyl aromatics, Zeolites, Molecular sieves, Reaction kinetics

Received 3 April 2014; accepted 8 July 2014.

Address correspondence to Jiří Čejka, J. Heyrovský Institute of Physical Chemistry, Academy of Sciences of the Czech Republic, v.v.i., Prague, Czech Republic. E-mail: jiri.cejka@jh-inst.cas.cz

Color versions of one or more of the figures in the article can be found online at www.tandfonline.com/lctr.

1. INTRODUCTION

Transformations of aromatic hydrocarbons are at the "heart" of the industrial petrochemistry having zeolites as the most important large-scale catalysts (1,2). Numerous papers were devoted to this topic in the last two decades of the 20th century (3,4,5,6,7) and most of the knowledge up to 2002 was reviewed by Čejka and Wichterlová (8). As for the transformations of aromatic hydrocarbons, one can hardly imagine this important industrial segment without using zeolites as catalysts. The main advantages of zeolites include:

i. higher activities and selectivities in comparison with the now obsolete aluminum trichloride or solid phosphoric acid catalysts (1);

ii. lower reaction temperatures enabling to perform reactions in liquid phase; and

iii. environmental tolerance of zeolites in contrast to the other above-mentioned catalysts (8).

The demand for benzene, toluene and xylenes in 2012 was estimated to be 42.5, 29.0, and 35.0 million tons per year, respectively, evidencing the importance of aromatic hydrocarbons on the global market (9). Some industrial aspects of the application of zeolites in the aromatics segment were nicely described by Vermeiren and Gilson (5).

The first decade of the 21st century experienced a significant progress in the development of new zeolites or zeolite-based materials (10,11) that are closely related to the transformations of aromatic hydrocarbons. This is due to the fact that aromatic transformations are not only industrially relevant reactions but are frequently used as model reactions to characterize zeolite channel systems and architectures (8). The individual types of the novel materials can be divided into three main categories:

i. novel zeolites including e.g., new 10-ring zeolites (TUN (12), IMF (13), -SVR (14), PCR (15)) or extra-large-pore zeolites (UTL, IRR, -ITV);

ii. hierarchic zeolites prepared either by forming of nanozeolite particles and assembling them to mesoporous structure (16), synthesized with secondary templates of mesopore size (17), or by post-synthesis treatments like desilication (18); and

iii. so-called two-dimensional (2D) zeolites with the thickness of the layers in the range of several nanometers (19,20).

The early period of the synthetic and catalytic efforts related to micro/mesoporous ("hierarchic") molecular sieves was discussed by Čejka and Mintova (21). All these zeolite-related catalysts offer interesting advantages

for the transformations of aromatic hydrocarbons that will be discussed here in detail. On the other hand, mesoporous molecular sieves will not be discussed here and the interested reader can refer to, for example, Kresge and Roth (22) and Perego Millini (23).

The main objective of this article is to review the understanding of the effects of chemical and textural properties of novel zeolite-based catalysts, namely those possessing new structural types, micro/mesoporous catalysts (hierarchic systems), and 2D zeolites, on the activity, selectivity, and long-term stability in alkylation, isomerization, disproportionation, and transalkylation reactions of aromatic hydrocarbons. This review particularly focuses on the new achievements since 2002.

2. ZEOLITE MOLECULAR SIEVES AND NEW STRUCTURES

Zeolite research in the synthesis addressed two different areas in the last decade in particular. The first involves an extensive effort (i) to prepare zeolites with new topologies, which either can be highly active or selective in transformations of aromatic hydrocarbons and (ii) to synthesize zeolites with larger pores enabling the upgrading of more bulky feedstocks, for which the current zeolite pores are too small. The second approach focuses on the tailored synthesis of zeolite-based materials exhibiting higher accessibility of the active sites. In this way, particularly micro/mesoporous composites (mesoporous zeolite single crystals) introducing mesoporosity to zeolite crystals and 2D zeolites with easily accessible active sites on their external surface were investigated.

The Structural Commission of IZA approved 218 topologies of zeolites early 2014, dozens of which were synthesized during the last decade. From the application of zeolites for transformations of aromatic hydrocarbons point of view, the new zeolites can be divided into the following groups: (i) 10-ring zeolites (TUN, IMF, -SVR) potentially showing *para*-selectivity due to the pore dimensions in the range of kinetic diameters of products (similarly to MFI zeolites); (ii) large and extra-large pore zeolites for transformations of more bulky aromatics; (iii) hierarchical zeolites of different structural types inherently exhibiting easier diffusion due to the presence of mesopores; and (iv) 2D zeolites with similar catalytic advantages as hierarchical zeolites. Due to the existence of a high number of recent reviews or books on zeolites, zeolites are not discussed here in detail and only some new zeolites are reported in the following sections (2,10).

2.1. Novel Zeolites Relevant to the Synthesis and Transformations of Alkyl Benzenes

Based on the kinetic diameter of alkyl and polyalkyl aromatic hydrocarbons, zeolites with pore sizes larger than 0.5 nm have to be used for their transformations. With the increasing number and length of alkyl chains, the

size of the pores should be larger or morphology of zeolites shall be properly adjusted. Here, several new conventional three-dimensional (3D) zeolites tested already for transformations of aromatic hydrocarbons are mentioned and for some reactions they are compared with 2D–layered zeolite analogs. Schematic pictures of their structures are provided in Fig. 1 and structural characteristics in Table 1.

2.1.1. *Medium-Pore Zeolites (10-Rings)*

In the last decade, several new medium-pore zeolites were successfully synthesized and their structures determined. Some of them, TUN (12,24), IMF (25,26), and –SVR (14), represent rather complex structures with unexpected properties, which substantially slowed down the process of

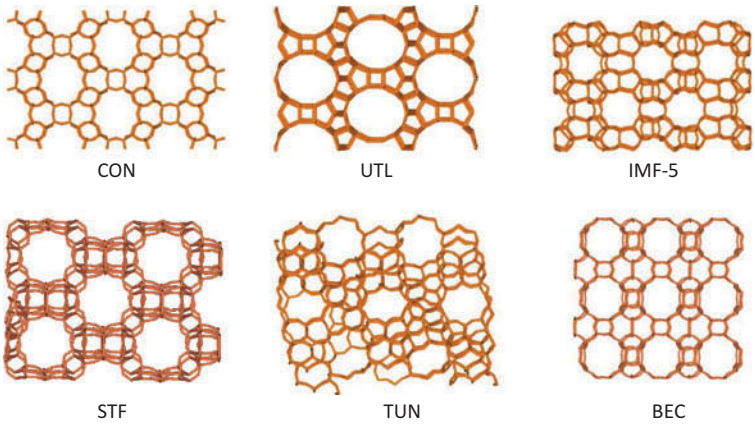

Figure 1: Schemes of structures of some zeolites discussed in this review.

Table 1: Structural characteristics of zeolites discussed in this review.

Code	Name	Channel System	Channel size (Å)				
*BEA	Beta	12-12	6.6x6.7	5.6x5.6			
CON	SSZ-33	12-12-10	6.4x7.0	7.0x5.9	5.1x4.5		
FAU	Faujasite	12	7.4x7.4				
IMF	IM-5	10-10-10-10-10	5.5x5.6	5.3x5.4	5.3x5.9	4.8x5.4	5.1x5.3
–ITV	ITQ-37	30	4.3x19.3				
IWR	ITQ-24	12-10-10	5.8x6.8	4.6x5.3	4.6x5.3		
IWW	ITQ-22	12-10-8	6.0x6.7	4.9x4.9	3.3x4.6		
	ITQ-33	18-10-10	12.2	5.6			
MFI	ZSM-5	10-10	5.1x5.5	5.3x5.6			
MOR	Mordenite	12-8	6.5x7.0	2.6x5.7			
MWW	MCM-22	10-10	4.0x5.5	4.1x5.1			
PCR	IPC-4	8-10	4.5x3.6	5.8x3.8			
–SVR	SSZ-74						
TUN	TNU-9	10-10	5.6x5.5	5.4x5.5			
UTL	IM-12	14-12	7.1x9.5	5.5x8.5			

structure determination. These zeolites possess 3D systems of intersecting 10-ring channels, although in the case of IMF this third dimension is limited. All the zeolites were synthesized with 1,*x*-bis-(N-methyl-pyrrolidinium) as structure-directing agent, where *x* stands for 4 (TUN), 5 (IMF), or 6 (-SVR). Structurally similar is also zeolite SSZ-57 combining 10-rings with some 12-rings in the structure (27,28).

2.1.2. Large-Pore Zeolites (12-Rings)

MSE (MCM-68) (29) and CON (SSZ-33) (30) belong to new zeolites with large pores at least in one dimension (1D). MSE has a 3D system of interconnected one 12- and two 10-ring channels. In contrast, CON (SSZ-33) possesses two 12- and one 10-ring channel system. Their catalytic propertis were investigated mainly in toluene and biphenyl alkylations (31).

2.1.3. Extra-Large-Pore Zeolites (> 12-Rings)

The successful synthesis of extra-large pore zeolites is substantially connected with the introduction of germanium oxide to the reaction mixtures. The presence of GeO_2 influences the preferential presence of single (S4R) and double-4-rings (D4R) and has an important structure-directing effect. Several new zeolites having larger than 12-ring channels were successfully prepared, namely UTL (14 x 12-ring (32,33)) and ITQ-33 (18 x 10 x 10-ring (34,35)). After introduction of aluminum (36,37), these zeolites show high activity in transformations of aromatic hydrocarbons providing more accessible acid sites than large- or medium-pore zeolites (38). High-throughput synthesis seems to accelerate the discoveries of new types of zeolites including extra-large pore ones (39).

2.2. Hierarchical Zeolites — Formation of Mesopores

The limited access to active sites and strong diffusion limitations inside the zeolite channels are the two most important disadvantages for catalysis on zeolites generally, and for transformations of bulky hydrocarbons including polyalkylbenzenes, in particular. One possible solution is the decrease in the zeolite crystal size resulting in a substantial increase in the external surface area, which is usually proportional to the increase in the number of the accessible active sites. The second approach is based on the formation of mesopores inside the zeolite crystals.

Hierarchic zeolites are characterized by the combination of micropores and mesopores enhancing the mass transport in zeolite crystals. As a result, higher activities and sometimes even higher selectivities are achieved in transformations of different organic reactants (18). In principle, two different strategies can be employed for the synthesis of hierarchic zeolites. Either, crystallization of zeolites is carried out with two different templates, a classical one for the

synthesis of that particular zeolite and a secondary one applied for the formation of mesopores (17). This approach is sometimes called the bottom-up approach. Carbon black particles, nanotubes, or some other removable carbon species are used as secondary templates. Their soaking in the reaction mixture is a critical step to form reasonable amount of mesopores, which are not ordered like in mesoporous molecular sieves. In addition to the classical hydrothermal synthesis of mesoporous zeolites (e.g., MFI), microwave irradiation was successfully used providing high pore volumes up to 0.8 cm^3/g (40). Zeolite materials prepared by secondary templating are usually called mesoporous zeolite crystals stressing the importance of the direct preparation with hydrothermal (solvothermal) procedure. The mesopore volume is formed as soon as the template is removed by calcination at temperatures around 550–600°C. Other synthetic methods involve application of appropriate organosilanes combining a silica source and a supramolecular template (41,42,43). These methods enable to prepare mesoporous zeolite single crystals of different structural types and modifiable acidity. Up until now, no solvent-free synthesis of mesoporous zeolite crystals was reported (44).

2.3. Two-Dimensional Zeolites and Expanded Structures

For decades, zeolites were considered as microporous crystals with 3D networks not easily transformable when already synthesized. During the last two decades, it has been shown that some zeolites can be prepared as 2D precursors (the third dimension being equal to the unit cell dimensions). These precursors allow preparing of conventional 3D zeolites, some of them being not synthesized directly (20,45). The best described family of 2D zeolites is MWW family (including several distinguishable materials, MCM-22P, MCM-36, ITQ-2, or EMM-10 (20)). 2D zeolites usually exhibit sizes of dozen (hundreds) of nanometers in two dimensions and larger BET areas than conventional zeolites. They are interesting for surface chemistry studies, mainly due to the fact that the easily accessible silanol groups on the external surface can be used for anchoring of organic or organometallic groups for different adsorption and catalytic applications. While the first 2D zeolites were synthesized accidentally and not immediately recognized (46,47,48,49,50), further studies resulted in a breakthrough in designing templates for the synthesis of 2D zeolites (19) or in post-synthesis hydrolysis followed by organization of layers and their condensation (51). Despite the synthesis procedure leading to 2D zeolitic layers, they can be organized in different ways, using delamination (52), swelling (53), interlayer expansion and pillaring (11,54,55), and last but not least preparation of 3D zeolites (15). The preparation of novel zeolites, IPC-4 (PCR) and IPC-2 (OKO), using top-down approach to prepare individual silica layers from UTL zeolite by hydrolysis, followed by organization with appropriate templates and finally by condensation, proceeds according to the ADOR (A – assembly, D – dis-assembly, O – organization, R – re-assembly) mechanism (15).

3. XYLENES

This section describes various routes for the formation of xylenes, via toluene disproportionation or its alkylation with methanol, and toluene and trimethylbenzene transalkylation. The catalysts used in these reactions are mainly zeolites of different structural types and properties (8). The main objective of most studies was to investigate catalyst properties and reaction conditions enabling selective production of *p*-xylene in the C_8 aromatics stream (ethylbenzene, *m*-xylene, *o*-xylene and *p*-xylene), i.e., deviating from the chemical equilibrium. *p*-Xylene is the most important xylene isomer being used for the production of terephthalic acid (PTA) or dimethyl terephthalate (DMT), further on applied to prepare polyester fibers, resins, films and plasticizers (5,9,56,57). *o*-Xylene is used for the production of phthalic anhydride mainly for polymer industry. The primary source of xylene isomers in the world is the catalytic reformate providing more than 70% of xylenes in 2011 followed by 17% via transalkylation, 7% by toluene disproportionation, and 4% extracted from pyrolysis gasoline. Table 2 presents data of the world demand and the main uses of the three xylene isomers. The main driver for xylenes growth is their consumption in Asia accounting for about 70% of the world production in 2011 and it is assumed to continue in the future (9).

3.1. Toluene Disproportionation

Toluene disproportionation is an industrial process converting toluene to a mixture of xylenes and benzene. The process can be either a conventional toluene disproportionation (CTDP, yielding equilibrium mixture of xylenes) or a selective one (STDP, with an enhanced selectivity to *p*-xylene). Most of the studies on the CTDP were conducted over MFI, MWW, and MOR zeolites while the STDP studies were mainly conducted over modified MFI zeolites (58,59). Although the equilibrium xylene mixture contains approximately 24% *p*-xylene, 54% *m*-xylene and 22% *o*-xylene in the temperature

Table 2: World demand and main use of xylene isomers in 2011. Adapted from Lidback (9), Copyright 2012, IHS.

Xylene Isomer	World Demand, million tons/yr	Expected Growth: 2012 to 2016, %/yr	Intermediate Uses	End Uses
p-Xylene	35.9	5.7	Terephthalic acid (PTA); dimethyl terephthalate (DMT)	Polyethylene terephthalate, fibers, films, resins
o-Xylene	3.2	3.5	Phthalic anhydride	Phthalate plasticizers
m-Xylene	0.45	4.8	Isophthalic acid	Unsaturated polyester resins

range of 250–450°C, over the modified MFI zeolites *para*-selectivity higher than 90% can be achieved. At 30% toluene conversion, STDP yields 41 wt% *p*-xylene, 46 wt% benzene and less than 2 wt% of light by-products per pass (58,59,60).

Acid sites on the external surface and in the pore entrances of the zeolites reduce the *para*-selectivity in toluene disproportionation. To enhance *p*-xylene selectivity and to limit its secondary isomerization, methods of deactivation of the external surface of zeolite crystals were investigated. They include liquid or vapor deposition of silica, selective dealumination of the external active sites, and modification with metal oxides (58). The measurement of the acid sites amount and strength of nanoscale MFI and modified MFI showed that only acid sites with acid strength $H_0 \leq +2.27$ can be related to the catalytic activity in toluene disproportionation. However, the concentration of the acid sites is not linearly related to the reactivity in TDP (61,62).

The external surface and pore mouth regions of MFI samples with different crystal sizes were modified by chemical liquid deposition (CLD) using tetraethoxy silane (TEOS) (63). Multi-cycle silylation was necessary to narrow the pore mouths and to deactivate the external acid sites of the small crystals to enhance their *para*-selectivity. In the case of cylinder-shaped MFI extrudates, TEOS was proven to be a more efficient silylating agent than the conventional polysiloxanes (64). The catalyst exhibited *p*-xylene selectivity of 91.1% at conversion of 25.6%. SEM analyses confirmed the formation of a layer of amorphous silica on the external surface of MFI zeolite crystals. Table 3 shows the performance of catalysts treated with different CLD cycles and the amounts of TEOS used in each cycle. It can be seen that whatever the amount of TEOS used for each CLD (0.1 or 0.3 ml/g catalyst), repeated CLD treatments improved *p*-xylene selectivity remarkably. A detailed investigation of CLD modification of MFI revealed that the deposition of polysiloxane is an acid-catalyzed degradation process associated with thermal pyrolysis, followed by oxidation at high temperatures (65). The total concentration of acid sites in the modified MFI zeolite dropped gradually with the increasing amount of siloxane applied, however, the acid strength distribution remained almost unchanged compared with the parent MFI. As shown in Table 4, high selectivity to *p*-xylene up to 96.2% was obtained over the modified MFI, compared with 24.3% over the parent MFI.

Table 3: Effect of chemical liquid deposition (CLD) cycle and amount of tetraethoxysilane (TEOS) on MFI zeolite on the reactivity of toluene disproportionation. Adapted from Teng et al. (64), Copyright 2011, Elsevier.

CLD Cycle	–	**1**	**2**	**3**	**1**	**2**
Amount of TEOS, ml/g catalyst	–	**0.1**	**0.1**	**0.1**	**0.3**	**0.3**
Toluene conversion, %	48.7	32.9	28.6	22.6	29.3	24.4
p-Xylene selectivity, %	24.0	34.8	56.6	79.2	52.1	75.0

Table 4: Conversion and selectivity in toluene disproportionation over modified MFI by silica deposition. Adapted from Zhu et al. (65), Copyright 2007, Elsevier.

	Unmodified	One Cycle	Two Cycles	Three Cycles	Four Cycles
p-Xylene selectivity, %	24.3	47.1	78.0	89.5	96.2
Toluene conversion, %	48.6	41.5	36.2	32.4	27.1
Deposited silica, wt%	0	4.8	7.7	9.8	11.4

More sophisticated modifications of MFI zeolites include covering the external surface with silicate layer or preparation of wash-coated monoliths (66). MFI crystals coated with a thin layer of silicalite-1 showed higher *para*-selectivity than the parent catalysts due to the inhibition of isomerization on their external surface. It is expected that the diffusion of reactants/products is not decreased due to the same channel structure of silicalite-1 while the active sites on the external surface of zeolite crystals are eliminated. In another study (67), the selectivity for *p*-xylene was enhanced over MFI/silicalite-1 core/shell composites by passivating acid sites on the external surface of MFI using non acidic silicalite-1 membrane, as well as the shape-selective diffusion of *p*-xylene inside silicalite-1 pores. The drop in toluene conversion was due to the additional diffusion resistance from the silicalite-1 membrane (67).

MFI zeolite was also modified with a metal oxide, Sb_2O_3, strongly interacting with the hydroxyl groups of the zeolite (68). Only a small amount of Sb_2O_3 penetrated into the zeolite pores while the main fraction of Sb_2O_3 was deposited on the external surface of the MFI crystals. Selectivity to *p*-xylene increased from 33% (3.3 wt% Sb_2O_3) to 68% (10.2 wt% Sb_2O_3) with the simultaneous decrease in conversion to half of the original value when compared with the parent zeolite. Al-Khattaf and co-workers (69) showed that toluene conversion over MFI zeolite modified with Mo-oxide increased with increasing pressures (10–50 bar) and reaction temperatures (375–425°C). Figure 2 shows

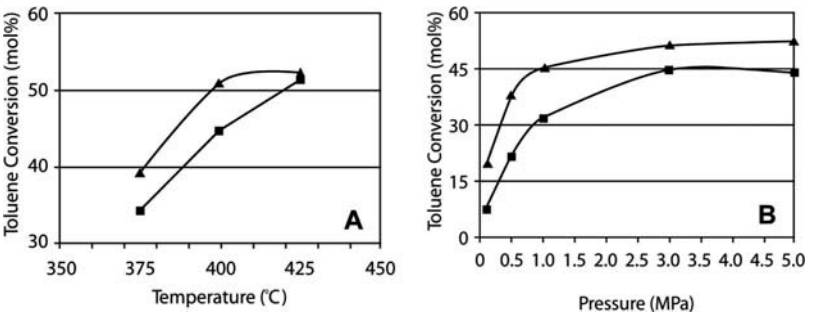

Figure 2: Conversion of toluene using hydrogen (■) and nitrogen (▲) carrier gases as a function of: (A) temperature at 3.0 MPa and (B) pressure at 400°C over Mo-MFI catalyst. Reproduced from Al-Khattaf et al. (69), Copyright 2008, with permission from the American Chemical Society.

that the initial toluene conversion using hydrogen as carrier gas was lower as compared with nitrogen. In contrast, with the increasing reaction time, catalyst deactivation was more profound in the experiments with nitrogen.

The advantages and disadvantages of mesoporous MFI in toluene disproportionation were investigated using one conventional and two mesoporous MFI zeolites differing in the mesopore volume but with a similar Si/Al ratio (70). No substantial differences among the three samples were observed as for the type and concentration of Brønsted and Lewis acid sites as well as their location in the zeolite channels or on the external surface of the zeolite crystals. Toluene conversion increased with increasing volume of mesopores in the MFI zeolite while the selectivity to xylenes increased due to a shorter contact time. In contrast, the *para*-selectivity decreased (70). The data evidence that diffusion pathways of a certain length are needed to increase the *para*-selectivity, which is not fulfilled in mesoporous MFI zeolites.

Ryoo and coworkers (71) compared conventional MFI zeolite with lamellar (2D) MFI samples prepared by specially designed organic templates (72,73). The conventional MFI zeolite exhibited a higher conversion (25% at 500°C, 15 min TOS) than the lamellar materials (lamellar MFI – 18 %) while the selectivity to *p*-xylene was comparable over both MFI catalysts.

MFI wash-coated monoliths with zeolite loading ranging from 10–60 wt.% showed an increase in toluene conversion with increasing temperature (74). The selectivity for *p*-xylene increased with a decrease in the temperature, space time, and wash-coat thickness. This high selectivity indicates that *p*-xylene is easily removed from the zeolite pores in the thin wash-coat preventing further isomerization. A further improvement in *p*-xylene yield depended on the type of a metal oxide (MgO, CaO, La_2O_3, or CeO_2) on the monolith and wash-coat thickness comprising MFI (75). In general, the addition of modifiers lowered the total acidity of MFI and enhanced the diffusive constraint in the zeolite pores due to entry of some metal ions into the pores of the zeolite. The 10% La- MFI washcoated monolith having an average thickness of 23 μm showed the highest *p*-xylene yield. Figure 3 shows the distribution of the xylene isomers in the product for the differently modified MFI catalysts at 500°C at an average conversion of 22%. The selectivity as well as the yield of *p*-xylene decreased with the decreasing washcoat thickness (75).

Molecular simulations revealed that the diffusion characteristics of TDP reactants and products over MFI, MEL, and MTW zeolites were sensitive to the pore dimensions and architectures of these zeolites (76). MFI showed a significant selectivity for *p*-xylene because the diffusion energy barriers for all aromatic molecules in the sinusoidal channels of MFI were higher than those in the straight channel zeolites. The calculated diffusion energy barriers for MEL were uniformly higher than for MFI due to the smaller pore dimensions of MEL showing an efficient shape-selectivity to *p*-xylene. While *p*-xylene selectivity over MFI and MEL were almost the same, the lowest one was over MTW as predicted from their diffusion energy barriers (76).

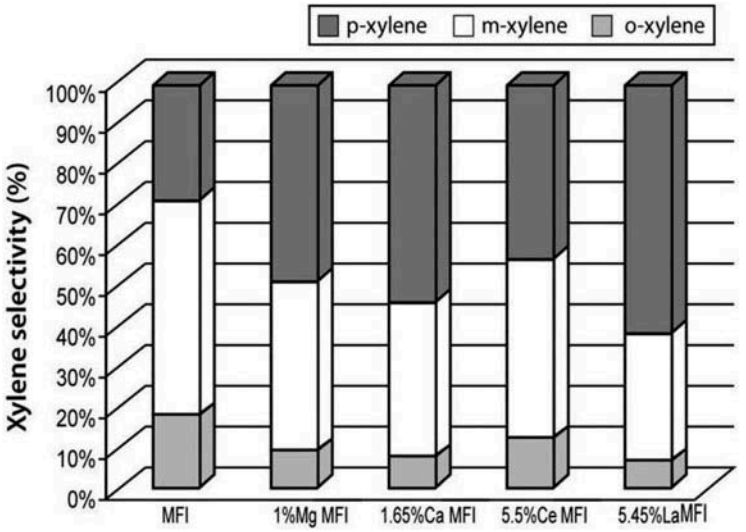

Figure 3: Distribution of xylene isomers for metal oxide-loaded and pure MFI washcoated monoliths at 500°C and 22% conversion. Reproduced from Mitra and Kunzru (75), Copyright 2011, with permission from Springer.

Žilková and coworkers (77) investigated the catalytic performance of various zeolites differing in channel architecture and acidity. The results showed that a general relationship for increasing zeolite activity with increasing pore diameter and pore connectivity was not valid when comparing different 10- and 12-zeolites with 1D or 3D channel systems. As shown in Table 5, toluene conversion over seven zeolites matched neither with the decreasing order of the concentrations of Brønsted acid sites nor with the total amount of acid (Brønsted plus Lewis) sites. As a result, final conversions/selectivities were controlled by a combination of chemical/structural/textural parameters of zeolites studied without a clear preference for any of them.

Table 5: The order of zeolites with respect to the concentration and strength of acid sites, as well as toluene conversion after 60 min TOS (at 500°C). Adapted from Žilková et al. (77), Copyright 2009, Elsevier.

Concentration of Acid Sites			Strength of Acid Sites			Toluene Conversion
Brønsted	**Lewis**	**All Sites**	**Brønsted**	**Lewis**	**All Sites**	
MOR	BEA	MOR	CON	IFR	IFR	MOR
MSE	CON	BEA	STF	MOR	MOR	CON
IFR	MSE	MSE	IFR	STF	STF	IFR
BEA	MFI	CON	MSE	MSE	MSE	MSE
CON	STF	IFR	MFI	CON	CON	STF
STF	IFR	STF	MOR	BEA	MFI	BEA
MFI	MOR	MFI	BEA	MFI	BEA	MFI

The medium pore TUN zeolite (12) exhibits unique shape selectivity as compared with MFI, MWW, MOR, and BEA zeolites. At 300°C and WHSV 7.2 h^{-1}, TUN provides toluene conversion 38% after 240 min TOS. The initial activity of TUN zeolite was comparable with large-pore zeolites MOR and BEA. An array of different zeolites (TUN, CON, MFI and MOR) varying in the channel architecture and acidity was investigated using fluidized-bed and fixed-bed reactors (see Figure 4) (78,79,80). Toluene conversion in the fixed-bed reactor was found to be higher than in the fluidized-bed reactor over all zeolites in the temperature range 300–400°C. Toluene conversion increased in the following order: MFI < MOR-A (Si/Al = 180) < CON < MOR-B (Si/Al = 18) < TUN. Figure 5 presents the product selectivity during toluene disproportionation over MFI, TUN, MOR-A, MOR-B, and CON at conversion level 16%. The selectivity to the sum of xylenes over the different zeolite catalysts under study follows the order: MOR-B < CON < TUN < MFI ≈ MOR-A.

Dealumination, desilication and silylation of TUN zeolite were investigated and related to its catalytic behavior in TDP (81). Only negligible concentration of acid sites was identified on the "external" surface of the parent TUN zeolite. Desilication resulted in a simultaneous decrease in the concentration of Brønsted acid sites and increase in the concentration of Lewis acid sites. Silylation narrowed the channel entrances and probably plugged some of them providing higher selectivity towards xylenes, higher xylene/benzene ratios, as well as higher selectivity to *p*-xylene.

MWW (Si/Al = 15) and its modification with a metal oxide or isomorphous substitution with trivalent atoms have been studied as an alternative to MFI type catalysts for the selective *p*-xylene production (82). Over MWW

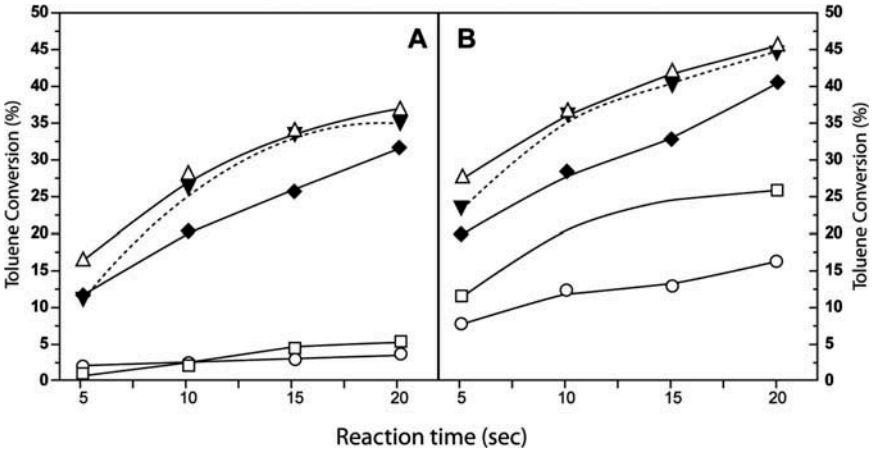

Figure 4: Effect of reaction time on toluene conversion for TDP over MFI (○), MOR-A (□), MOR-B (▼), CON (♦), TUN (△) in a fluidized-bed reactor at: (A) 300°C and (B) 400°C. Reproduced from Odedario et al. (78), Copyright 2011, with permission from the American Chemical Society.

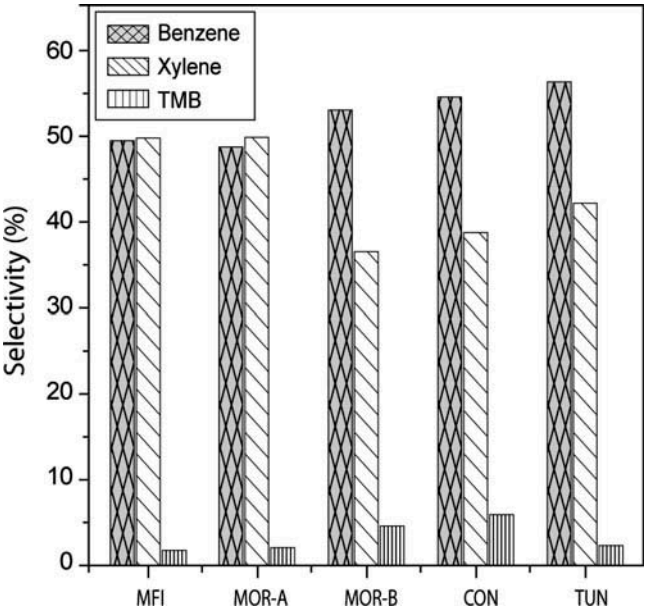

Figure 5: Product selectivity of toluene disproportionation over the different catalysts at 16% toluene conversion (toluene/methanol, 1:1 mol ratio; reactor = fluidized-bed; catalyst/feed = 5; reaction temperature 300, 350, and 400°C). Reproduced from Odedario et al. (78), Copyright 2011, with permission from the American Chemical Society.

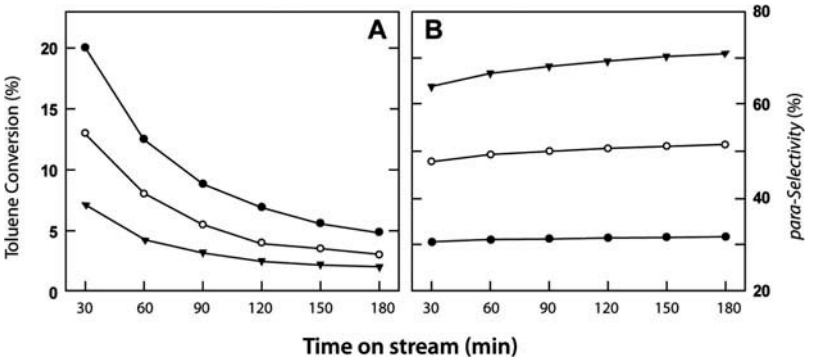

Figure 6: Conversion of toluene as a function of time (TOS) on stream over MWW (●) and its dealuminated samples (○, ▼) at 350°C. Reproduced from Park and Rhee (82), Copyright 2003, with permission from Taylor and Francis.

zeolite, *p*-xylene was primarily produced within the micropores, while secondary isomerization of *p*-xylene occurred on the external acid sites, reducing *para*-selectivity. The dealumination of MWW removed selectively the acid sites from the external surface and suppressed the secondary isomerization of *p*-xylene (82). Figure 6 shows the impact of MWW dealumination on the increase in the *para*-selectivity. FTIR analysis revealed that dealumination by steaming

followed by acid leaching selectively removed the acid sites from the external surface. For MWW zeolite with Si/Al = 31.7, only about 9% of acid sites exist on the external surface compared with 20.1 % for the parent MWW zeolite.

The modification of MWW zeolite using mild alkaline concentrations (~0.1–0.2 M NaOH) led to a partial desilication of the zeolite framework with the formation of some mesopores (83). The accessibility/availability of Lewis acid sites increased after the treatment while the concentration of Brønsted acid sites decreased. A higher toluene conversion was assigned to a faster diffusion. The concentration of Lewis acid sites increased with increasing base concentration. In contrast, at higher alkaline concentrations (e.g., 0.50 M NaOH) toluene conversion decreased due to a partial destruction of the MWW structure.

A shape-selective core/shell-structured Al-MWW (core)/B-MWW (external surface) composite catalyst was synthesized by adding B-containing reaction mixture to Al-MWW crystals (84). The growth of borosilicate enlarged the thickness of the platelet crystallites of MWW and increased the surface Si/Al ratio from 16 to 222. As shown in Fig. 7, the composite catalyst exhibited significantly enhanced *p*-xylene selectivity in comparison with normal MWW as a result of suppression of *p*-xylene isomerization on the external surface.

Characterization of channel systems and accessibility of acid sites in UTL zeolite was carried out using toluene disproportionation. UTL zeolite (14- x 12-ring channel system) was successfully synthesized with different concentrations of three-valent elements (38) and used in toluene

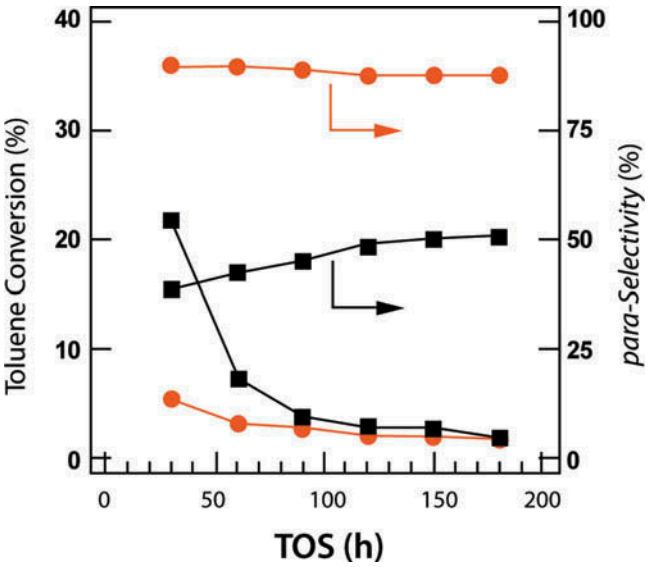

Figure 7: Effect of time on stream (TOS) on toluene conversion over Al-MWW (■) and Al-MWW/B-MWW (●) at 300°C. Reproduced from Ji et al. (84), Copyright 2011, with permission from Elsevier.

disproportionation (36). For isomorphously substituted UTL zeolites (Al, Ga, Fe) with similar crystal sizes, toluene conversion decreased in the order Al > Ga > Fe, i.e., with decreasing acid strength of the acid sites.

3.2. Toluene Alkylation with Methanol

Toluene alkylation with methanol is an attractive potential route for industrial application since it can selectively produce *p*-xylene without benzene co-product as in toluene disproportionation (58,85). Recently, Sinopec Yangzi Petrochemical announced the completion of the construction of the first toluene methanol alkylation plant (based on its MTX technology) with a production capacity of 200,000 tons/year *p*-xylene (86). Similarly, SABIC and CB&I's Lummus Technology announced plans for developing a new technology for *p*-xylene production based on MTX (86). It indicates that the toluene methylation becomes more and more competitive for *p*-xylene production. This route has the potential of increasing *p*-xylene production throughput and lowering the operating and capital cost via the adoption of single-stage crystallization for *p*-xylene purification.

In principle, toluene alkylation with methanol over acid catalysts produces virtually exclusively xylenes as styrene and ethylbenzene are formed by side-chain alkylation only over basic catalysts (Scheme 1).

Selectivity to *p*-xylene is a function of acidity, specific surface area, pore and crystal size, reaction temperature and toluene to methanol ratio (60). Mostly, metal-modified zeolites MFI and MWW were investigated in toluene methylation aiming to enhance the product *para*-selectivity (87). Other zeolite modifications include: (i) addition of an oxide, such as MgO, ZnO, or P_2O_5, (ii) precoking by high-temperature treatment with a carbonaceous material, and (iii) silanization. Each treatment resulted in some extent of blocking of the external surface, modification of the transport properties of xylene isomers, and reduction of the concentration of Brønsted acid sites in the pore entrances.

Breen et al. (88) demonstrated that it was possible to produce *p*-xylene with 99.9% selectivity by optimizing process variables over MFI zeolite (Si/Al=80) modified with Mg or B (toluene conversion 5.5–6.2 %; toluene to

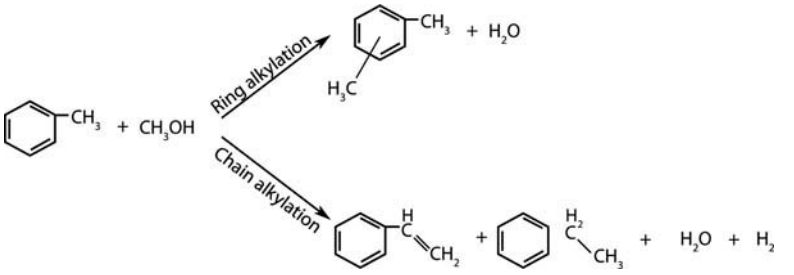

Scheme 1: Two paths of toluene alkylation with methanol.

methanol molar ratio 8:1). The catalyst may be prepared in situ by loading a physical mixture of hydroboric acid and MFI zeolite into the reactor prior to reaction or placing a bed of hydroboric acid upstream in front of a bed of MFI. High *para*-selectivity was achieved by these authors by minimizing the undesirable isomerization of *p*-xylene by operating at very short contact time equal to 0.4 s (89). External mass transfer was a key parameter in controlling selectivity and high toluene/methanol feed ratio was beneficial in minimizing methanol dehydration.

p-Xylene selectivity above 85% was achieved at toluene conversion of 8–9% over a pore-size-controlled Ga/MFI composite catalyst (58). The process was successfully scaled-up in a pilot-plant to simulate multi-bed catalyst operation. Toluene conversion was increased to about 28% at 85% *p*-xylene selectivity. Several kinetic models were tested and compared concluding a simple power law model was satisfactory in predicting toluene conversions and *p*-xylene selectivities (90).

La_2O_3-MgO/MFI showed improved *p*-xylene selectivity (93%) at a toluene conversion of 20%. The authors concluded that the reduction in pore dimension of MFI catalyst affected the *p*-xylene selectivity enhancement more importantly than the suppression of strong acid sites and inactivation of external surface acid sites (91). It was reported that the pore volume of MFI dropped from 0.22 ml/g to 0.1 ml/g for 20%La_2O_3-8%MgO/MFI. In another study, Zhang et al. (92) found that the addition of La_2O_3 during the hydrothermal synthesis of MFI did not change the basic structure of MFI but obviously decreased the crystallinity. Figure 8 shows that the initial toluene conversions over modified catalysts were similar but they decreased with TOS in the following order: 0.22%La/MFI>MFI>0.49%La/MFI > 0.13%La/MFI > 0.87%La/MFI. The La/MFI samples exhibited much slower conversion declines compared with parent MFI, especially for 0.22%La/MFI and 0.49%La/MFI (92).

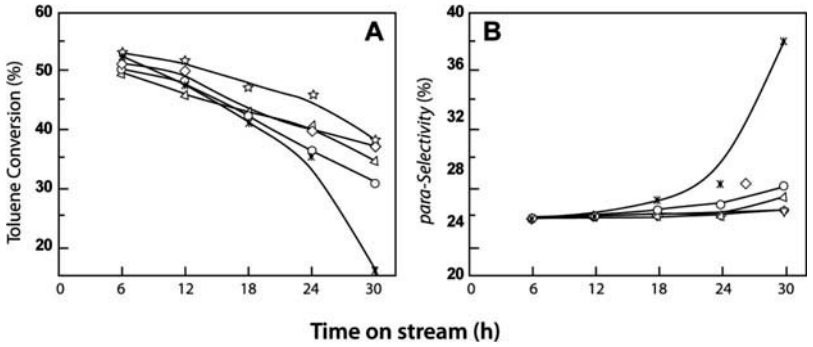

Figure 8: Catalytic performance of MFI (x), 0.13%La/MFI (○), 0.22%La/MFI (☆), 0.49%La/MFI (◊), 0.87%La/MFI (△), A: Toluene conversion, B: Para-selectivity. Reproduced from Zhang et al. (92), Copyright 2009, with permission from Springer.

Guo and co-workers (93,94) investigated the effects of reaction temperature, WHSV, and flow rate of N_2 over Si-P-Mg/MFI zeolite. Under optimized conditions (WHSV=2 h^{-1}, 460°C, toluene/methanol molar ratio = 8.0), *p*-xylene selectivity over 97% was achieved at toluene conversion of 10% even after 100–400 h of TOS (93). Modification with metals inhibited coke formation and significantly improved the stability under the condition providing high *para*-selectivity. The effect of Pt on stability of Si-P-Mg/MFI was studied for more than 500 h TOS reaching more than 98% of *para*-selectivity at 22–23% of toluene conversion (see Fig. 9 (94)).

Aboul-Gheit and co-workers (95,96,97) studied toluene methylation over Pt (0.2, 0.4, and 0.6 wt.%) on H-MFI and MOR with Pt (0.2, 0.4, and 0.6 wt.%), respectively, at 300–500°C in a stream of hydrogen. The selectivity to *p*-xylene depended on the Pt content in the catalysts, particularly for H-MFI. However, the *p*-xylene selectivity was not strictly controlled by Pt content in the MOR catalysts. The conversion over 0.2% Pt/MFI was increased after doping with HF concentrations (from 1.0–4.0%), most probably due to the formation of some mesopores as a result of a partial dissolution of the zeolite crystals (97).

Svelle et al. (98) reviewed reaction mechanism of zeolite catalyzed methylation of aromatics based on spectroscopy, quantum chemistry, and kinetic measurements. They proposed that the activation barrier for the formation of methoxy groups was substantially higher than the barriers of further consecutive reactions and direct methylation. Hence, they concluded that the formation of the surface methoxy groups is the rate determining step of the overall reaction mechanism.

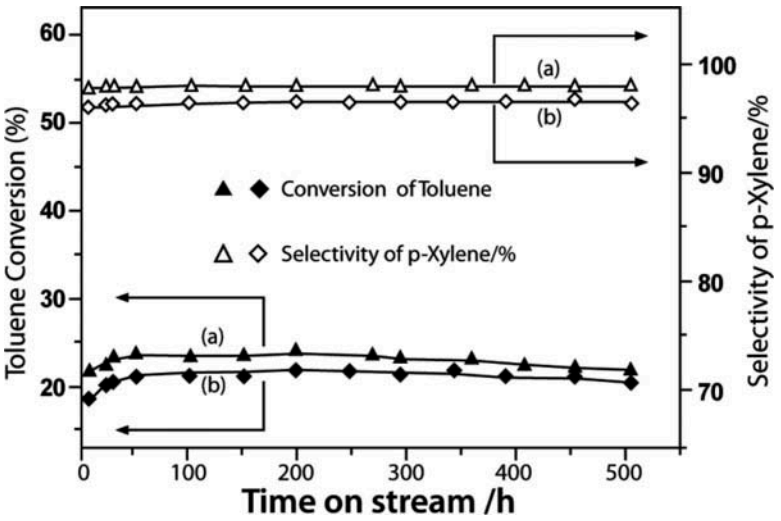

Figure 9: Performance 500 h long-run on catalysts: (a) (3% SiO_2 + 5% P_2O_5 + 3% MgO + 3% SiO_2 + 0.3% Pt)/nano-scale MFI and (b) (3% SiO_2 + 5% P_2O_5 + 3% MgO + 3% SiO_2 + 1.0% Pt)/nano-scale MFI. Reproduced from Zhao et al. (94), Copyright 2011, with permission from Elsevier.

Al-Khattaf and co-workers (99,100) determined the kinetic parameters of toluene alkylation with methanol in a riser simulator over H-MFI and H-FAU. The apparent activation energies of 68 and 24 kJ/mol were found for the methylation of toluene and xylenes over H-MFI zeolite, respectively, whereas the analogous values were found to be 43 and 41 kJ/mol for the same reactions carried out using zeolite H-Y. In another kinetic study of toluene methylation over H-MFI, physical mixture of MOR/MFI, and composite mixture of MFI/MCM-41, the activation energies were found as 57 kJ/mol, 21 kJ/mol, and 15 kJ/mol, respectively (101). The low values of activation energies can be explained by the diffusion control. The activity of the three catalyst samples decreased in the following order: MFI/MCM-41 > MFI > MOR/MFI due to the combined effect of the presence of mesopores and medium acidity strength. Similarly, the co-crystalline zeolites MFI/MTW (102) and MFI/BEA (103) were studied. The MFI/BEA provided 44.5% xylene yield compared with 34.1% for the physical mixture.

The growth of silicalite onto MFI zeolite resulted in higher *p*-xylene selectivity in toluene methylation while maintaining very good activity and stability (104,105,106,107).The silicalite/MFI composite with a crystal size of 5 μm showed a lower conversion (40 %) than parent MFI zeolite with a crystal size of about 1 μm (54%) while the *p*-xylene selectivity reached almost 100%. The authors concluded that smaller MFI crystals coated with a thin silicalite layer were required to attain both high activity and selectivity. The silicalite coating inhibited coke formation near the surface of MFI. In addition, zeolites possessing small crystal sizes were very stable with TOS, while the catalysts with large crystals deactivated more rapidly (see Fig. 10) (107).

The activity of various zeolites and zeotypes (MOR, MWW, CHA, AEL, AFI, and MFI) was found approximately proportional to the number of acidic

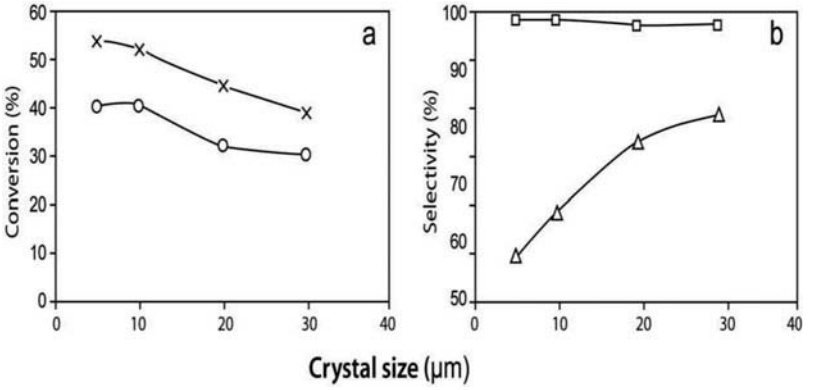

Figure 10: Toluene conversion and para-xylene selectivity in toluene alkylation as a function of crystal size of the zeolite catalysts: uncoated MFI (x, △), silicalite-1/MFI (○, □), at 400°C, methanol/toluene=1.0, reaction time = 60 min. Reproduced from Van Vu et al. (107), Copyright 2008, with permission from Elsevier.

sites exhibiting medium strength determined from ammonia desorption at 300–450 °C, except for CHA with small channels and MOR with higher acid strength (108). Toluene conversion decreased in the following order: MOR > MFI(25) > MFI (48) > MWW > MFI(136) > AEL = AFI > CHA. Zeolites with 10- ring channels (MFI, AEL and MWW) and medium acid strength showed the highest selectivity to *p*-xylene (>70%) at toluene conversion higher than 30%. Zeolites with 12-ring channels promoted secondary alkylation of xylene and rapid deactivation by coking, whereas zeolites with 8-ring channels restricted toluene alkylation and favored the formation of non-aromatic hydrocarbons from methanol.

3.3. Disproportionation of Trimethylbenzenes

Another possibility for increasing the production of the desired xylenes relies on the transformation of low-value C_9 aromatic streams. It is a rather complex task as, for instance, the transformation of 1,2,4-TMB over acidic catalysts involves isomerization, disproportionation, and transalkylation, as illustrated in Scheme 2 (109). The isomerization reaction produces other bulkier TMB isomers while disproportionation reaction yields xylenes and tetramethylbenzenes (TeMBs) from 1,2,4-TMB. Subsequently, the xylenes may react with the TMBs to form a transalkylation product, toluene. Table 6 lists catalysts and their performance in the disproportionation of TMBs.

The disproportionation reaction was investigated over medium, large, and extra-large pore zeolites aiming at enhancing the conversion of 1,2,4-TMB and the selectivity to *p*-xylene (8,58). Large pore zeolites are potential candidates for the isomerization reaction while medium pore zeolites are suitable for the disproportionation reaction since the desired xylenes have dimensions comparable with that of 1,2,4-TMB (110).

Large-pore zeolites MOR and CON and medium-pore zeolites MFI and TUN were investigated in the transformation of 1,2,4-TMB at 300–400°C

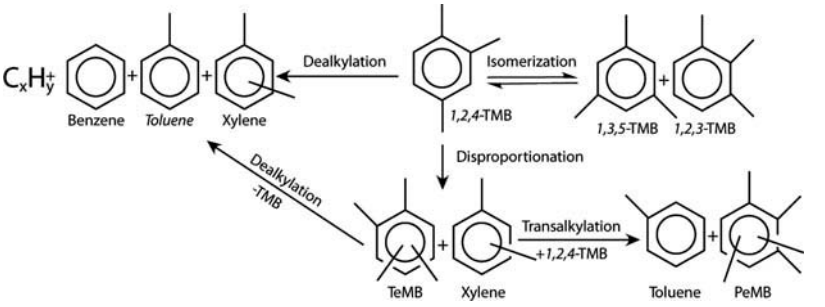

Scheme 2: Reaction scheme showing different probable reactions during disproportionation of 1,2,4-TMB. Reproduced from Al-Khattaf et al. (109), Copyright 2011, with permission from Elsevier.

Table 6: List of catalysts and their performance in disproportionation of TMB.

Catalyst	1,2,4-TMB Conversion, %	PX Selectivity, %	Conditions			Ref.
			T, °C	P, MPa	WHSV, h^{-1}	
CON	72.7	24.0	400	0.1	–	(109)
BEA	50.9	10.5	400	0.1	5.0	(111)
LTL	7.0	8.4	400	0.1	5.0	(111)
MOR	45.7	10.6	400	0.1	5.0	(111)
FAU (low acidity)	31.2	20.0	400	0.1	–	(113)
FAU (high acidity)	37.0	23.3	400	0.1	–	(113)
Ni–Pt/H–FAU	53.0	24.5	400	0.1	–	(115)
Al-MWW	17.8	14.8	300	0.1	–	(117)
Al,B-MWW	16.1	12.4	300	0.1	–	(117)
MFI/MCM-41	36.4	–	400	0.1	–	(118)

aimed at the evaluation of the reaction kinetics (109). Zeolite structure was found to control primarily the diffusion of reactants and products while the acidity of zeolites was of secondary importance. Although TUN has a 3D 10-ring channel system, its slightly larger pores compared with MFI provided sufficient reaction space to behave like large-pore zeolites. Čejka and coworkers (111) investigated the effect of large pore zeolites (MOR, BEA, LTL, and FAU) on the activity, selectivity to xylenes and TOS stability. Significant differences in conversion and TOS stability were observed among these zeolites. BEA and FAU zeolites exhibited the highest stability, while LTL and MOR deactivated much faster, most probably due to only 1D 12-ring channels. To achieve a high and stable conversion around 50%, the optimum reaction conditions were 400°C and WHSV = 5–20 h^{-1}. Differences in diffusion coefficients of TMBs and TeMBs (several orders of magnitude) influenced the apparent rate of disproportionation reaction due to the different coverage of acid sites by individual TMBs and TeMBs molecules (111).

The catalytic transformation of 1,2,4-TMB was investigated over FCC catalysts (HY and USY catalysts) in a riser simulator under different operating conditions to calculate adsorption constants, heats of adsorption, energies of activation and pre-exponential factors (112). The effect of reaction conditions on the variation of the isomerization to disproportionation products ratio, distribution of isomers (1,2,3-TMB and 1,3,5-TMB) and values of *p*-xylene/*o*-xylene ratios were studied (113). While FAU with a lower concentration of acid sites provided mainly xylenes and TeMBs, FAU with a higher concentration of acid sites catalyzed preferentially demethylation reactions. Simultaneously, higher amounts of C_3-C_4 hydrocarbons were formed, probably via paring reaction (114).

The effectiveness factor (η_{ss}) was estimated using the quasi-steady state approximation modeling of the experimental data involving a decay function based on TOS. The effectiveness factor was less than unity under all reaction conditions applied (115). The disproportionation and isomerization

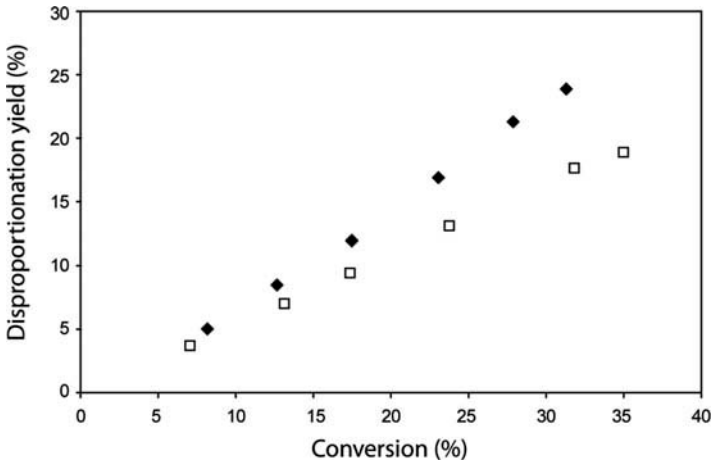

Figure 11: Disproportionation yield vs conversion for 1,2,4-TMB (♦) and 1,3,5-TMB (□) over FAU at 400°C. Reproduced from Tukur and Al-Khattaf (116), Copyright 2007, with permission from the American Chemical Society.

of 1,2,4-TMB were compared with the transformation of 1,3,5-TMB over USY zeolite (116). While 1,3,5-TMB consistently gave higher isomerization yields, 1,2,4-TMB produced more disproportionation products than the 1,3,5-TMB molecule as shown in Fig. 11. Diffusion limitations were observed for the 1,3,5-TMB transformation reactions, while very mild transport effects were seen for the 1,2,4-TMB molecule. The apparent activation energies were found to decrease in the following order: $E_{(1,3,5\text{-TMB,disproportionation})} > E_{(1,3,5\text{-TMB,isomerization})} = E_{(1,2,4\text{-TMB,isomerization})} > E_{(1,2,4\text{-TMB,disproportionation})}$.

The catalytic performance of (Al)MWW and boron-containing (Al,B)MWW zeolites was compared in view of the impact of their cage/channel pore structure on TMBs diffusion (117).The diffusion of 1,2,4-TMB is significantly limited within the pores of MWW and its conversion proceeds mainly on the external surface.

The distinctive catalytic performance of MFI/MCM-41 composite material was attributed to the excellent accessibility of the active sites provided by the mesopores for 1,2,4-TMB and product molecules (118). The product distribution and selectivity for xylenes over MFI and composite materials are presented in Fig. 12. The MFI/MCM-41 composite catalysts (ZM41A1 and ZM41A2) were prepared by disintegrating MFI using sodium hydroxide solution at a pH condition of 12.1 and 13, respectively, followed by vigorous stirring at 100°C for 24 h in the presence of 4.5 wt% cetyltrimethylammonium bromide. The results showed that modifying a purely zeolitic material to a meso-structured one increased the rate of the disproportionation reaction of 1,2,4-TMB due to the easier access to active centers of the composite catalyst.

Comparison of TMBs conversion and selectivity compared with isomerization, dealkylation and transalkylation over (Al) and (Ga)UTL, BEA, and MFI

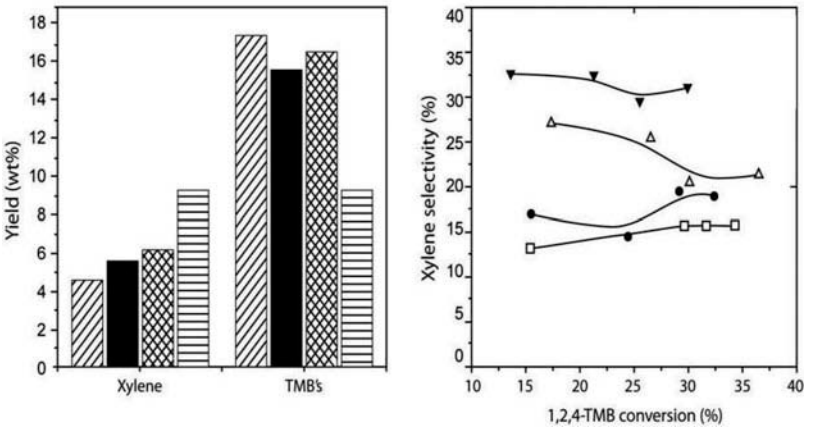

Figure 12: Product distribution in the transformation of 1,2,4-TMB over MFI (□) and composite materials MFI/MCM-41: ZM41A1 (●), ZM41A2 (△) and ZM4A3 (▼) at 30% 1,2,4-TMB conversion and xylene selectivity at 400°C and catalyst:feed ratio = 3.8. Reproduced from Odedario et al. (118), Copyright 2012, with permission of The Royal Society of Chemistry.

evidenced the importance of crystal shapes. Both (Al) and (Ga)UTL zeolites exhibit sheet-like crystals with much less entrances to the channel systems compared with zeolite BEA (37). As a result, BEA shows a higher conversion of TMBs under the same reaction conditions. Higher acid strength of acid sites in (Al)UTL is responsible for higher TMB conversion when compared with (Ga)UTL.

3.4. Transalkylation of Toluene with Trimethylbenzenes

Transalkylation of TMBs with toluene offers the possibility to utilize two lower value aromatic streams (C7 and C9) to maximize the efficiency of C8 aromatics production. As a model system, transalkylation of toluene with 1,2,4-TMB to xylenes has been investigated extensively over various types of zeolites and under different reaction conditions. Generally, transalkylation and/or disproportionation reactions occur on acid sites with higher acid strength while the isomerization of xylenes and TMBs predominates on weaker acid sites. The reaction is thermodynamically controlled; the equilibrium composition depends on the methyl/ring ratio with the maximum xylene product selectivity at a methyl/ring ratio of around 2.0 for equal molar ratio of toluene-TMB mixture. There are several commercial processes that supply about 17% of world *p*-xylene production (9) via toluene transalkylation such as UOP's Tatoray and ExxonMobil's TransPlus processes (57). More detailed discussion on the conversion of heavy reformate (C9+ aromatics) to xylenes is presented in Sec. 7. Table 7 presents a list of catalysts and their performance in the transalkylation of toluene with TMBs.

Table 7: List of catalysts and their performance in transalkylation of toluene with TMBs.

Catalyst	1,2,4,TMB Conversion, %	PX Selectivity, %	Conditions			Ref.
			T, °C	P, MPa	WHSV, h^{-1}	
BEA	52.1	26.8	300	0.1	5.0	(119)
MFI/MOR	52.3	24.0	400	0.1	–	(120)
USY	31.8	26.8	400	0.1	–	(122)
Pt/MOR	38.5	–	400	0.1	–	(123)
MFI(150)/MOR(180)	41.2	24.0	400	0.1	–	(121)

High activity, selectivity, and long-term stability remain the main challenges to be tackled in transalkylation zeolite catalysts. Large pore zeolites are effective in this reaction, however, they tend to deactivate rapidly due to excessive coke formation. Compared with MFI and MOR, zeolite BEA/alumina yielded higher xylene yields from the 50:50 toluene and C9+ aromatics mixture (60). The xylene yield followed the same trend as observed with the individual trimethylbenzene isomers. Krejčí et al. (119) reported that BEA zeolite exhibited the highest conversion and higher stability in TOS compared with MOR and FAU. The effect of Si/Al ratio in zeolite BEA was evaluated and it was found that transalkylation activity and xylene yields increased with decreasing Si/Al ratio. Zeolite BEA with the lowest Si/Al ratio (12.5) exhibited the highest 1,2,4-TMB conversion around 50% and the maximum xylene yield of 37% (119).

Using a riser-simulator reactor, the performance of MFI, MOR and dual MFI/MOR catalysts was compared under different reaction conditions (120). At 400°C, the dual zeolitic catalyst exhibited maximum toluene conversion, higher xylene yield and lower formation of undesired products (benzene and TeMBs). Figure 13 shows the effect of the reaction temperature (300°C and 400°C) and the addition of 1,2,4-TMB in the feed mixture (30, 50, 70, 100%) on the xylene yield over the MFI/MOR catalyst. The results were used to develop comprehensive kinetic models for isomerization, disproportionation, and transalkylation reactions over MFI/MOR (121) and FAU (122) catalysts.

Tsai and coworkers (123) reviewed recent investigations of different catalytic systems, selective pre-coking (124) and a versatile dual-bed catalyst system design for aromatic transformations containing zeolite BEA or MOR (125). Figure 14 compares the performance of the parent and desilicated MOR catalysts mostly having similar initial conversion (126). MOR-base treated catalyst with Pt resulted in a stable conversion for at least 100 h. NMR and adsorption data confirmed that the base treatment preferentially removed framework silica and re-inserted octahedral aluminum into the MOR with the formation of a hierarchical porous system (126).

The partial substitution of Al by Ga in EMT-type zeolite provided a catalyst with a lower strength of acid sites. As a result, lower conversion and

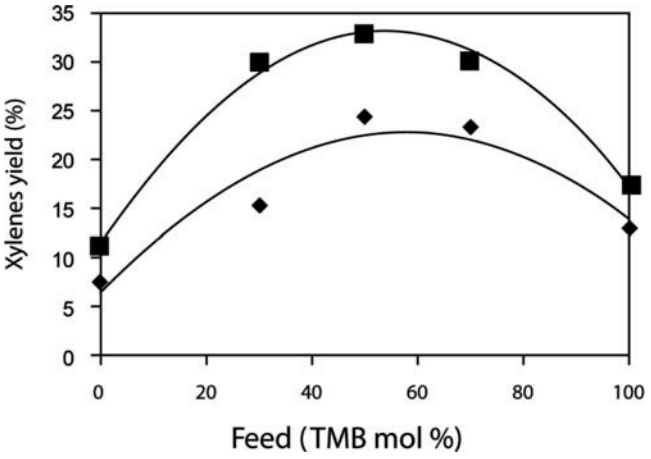

Figure 13: Yields of xylenes as a function of temperature: 300°C (♦), 400 °C (■), and mol.-% of 1,2,4-TMB in the toluene and 1,2,4-TMB feed mixture over dual MFI/MOR catalyst and 20s TOS. Reproduced from Aitani et al. (120), Copyright 2010, with permission from John Wiley and Sons.

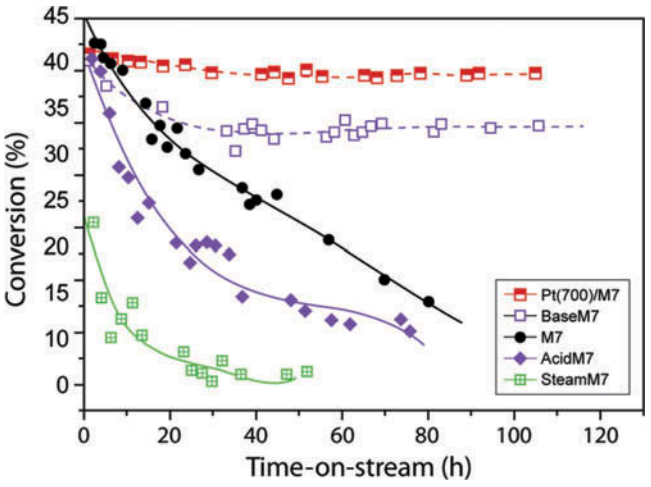

Figure 14: Catalytic performances of various mordenite samples in transalkylation of toluene and 1,2,4-TMB at 380°C, 2480 kPa, 3.0 h^{-1} WHSV and 3.0 H_2/HC (M7: parent mordenite, BaseM7: treated with 0.1 N NaOH, AcidM7: treated with 6 N HCl, SteamM7: treated with water saturated nitrogen, Pt(700)/M7: mordenite impregnated with H_2PtCl_6 precursor). Reproduced from Tsai et al. (126), Copyright 2009, with permission of The Royal Society of Chemistry.

higher selectivity towards xylenes were obtained when comparing with the parent (Al)EMT (127). The distribution of xylene isomers was close to that of the thermodynamic equilibrium due to the fact that xylene isomerization proceeded faster than any other reaction involved in the transalkylation process. In addition, large-pore system of EMT zeolite should not differentiate among xylene isomers based on the different diffusion rates.

3.5. Xylene Isomerization

Industrially, xylene isomerization is conducted in a fixed-bed reactor in the presence of hydrogen at temperatures between 350 and 400°C and about 1.0 MPa. Investigations of acid-catalyzed isomerization of *m*-xylene focus mainly on the role of different structural types of zeolites and their modification aiming to improve the activity and selectivity to *p*-xylene (8,128). Table 8 summarizes zeolite catalysts and their performance in m-xylene isomerization.

Shape selectivity usually plays critical role in xylene isomerization over zeolites. While the P/O ratio (*para*/*ortho*) is typically 1.0–1.5 for multidimensional 12-ring zeolites, the P/O ratio is > 2 for 10-ring zeolites exhibiting higher *p*-xylene selectivity. Molecular dynamics simulations verified that the diffusivity ratio for P/O is much higher for MFI (7.4) than for BEA (2.3), being consistent with the higher *p*-xylene selectivity obtained over MFI (129).

Reaction mechanisms of xylene transformations were described previously (8) and in references therein. Further mechanistic studies proposed the monomolecular route as the most effective one to achieve high yields of *p*-xylene (130,131). The influence of reaction conditions on the selectivity of *m*-xylene transformation over FAU zeolite (132) showed that both isomerization and disproportionation were primary reactions. Some in situ time-resolved spectroscopic methods have been used to look at how modification of MFI zeolite affects the monomolecular mechanism by constraining the diffusion of *m*-xylene (133). Theoretical studies of mechanistic aspects of xylene isomerization over large pore zeolites suggested that the initiation step involves a defect site rather than an acidic proton (134). On the other hand, one cannot exclude the contribution of the bimolecular pathway over medium-pore MFI zeolite (135).

Table 8: List of catalysts and their performance in *m*-xylene isomerization.

Catalyst	*m*-xylene Conversion, %	*p*/*o* Ratio	Conditions			Ref.
			T, °C	P, MPa	WHSV, h^{-1}	
MCM-56	10.0	2.2	350	0.1	–	(138)
MWW Dealuminated	5.0	2.5	350	0.1	–	(136)
MFI	28.9	1.5	300	0.1	–	(129)
MOR	51.9	1.0	300	0.1	–	(129)
CON	56.9	1.1	300	0.1	–	(129)
NES	70.0	1.0	350	0.1	–	(129)
EU-1	50.0	1.1	350	0.1	–	(135)
MWW	40.0	1.5	350	0.1	10.7	(140)
ITQ-2	20.0	1.5	350	0.1	10.7	(140)
IMF	50.0	1.0	350	0.1	10.7	(141)
TUN	58.4	1.2	300	0.1	10.7	(141)
MFI	50.0	1.0	350	0.1	10.7	(141)

Rather contradicting results were obtained for xylene isomerization over MWW zeolites. Guisnet and coworkers proposed a reaction scheme on fresh H-MWW zeolites where isomerization and disproportionation products were primary products (136,137). It was suggested that about 30% of isomerization took place in the supercages and 70%, without any deactivation, in the sinusoidal channels and in the external pockets. In contrast, in the case of MWW zeolite prepared in the presence of hexamethonium cations, the authors relate its higher isomerization activity and increased selectivity to the accessible protonic sites located in the surface 12-ring half-cavities (138). One can believe that varying the structure and charge of the template together with synthetic conditions can result in various MWW-related materials with different location of aluminum and acidity (139). Dealuminated MWW was tested for *m*-xylene conversion showing that extra-framework aluminum (EFAl) species blocked the zeolite micropores making the remaining Brønsted acid sites isolated and inefficient (140). The presence of such species reduced adsorption capacity and catalytic activity, modified reaction products distribution, and altered mode of coke formation and composition of the coke precursors.

Catalytic experiments as well as molecular dynamics were used to interpret the behavior of NU-87, BEA, CON, and MFI zeolites for *m*-xylene isomerization and disproportionation (Fig. 15, (129)). The presence of cavities allowed more space for the formation of bulky intermediates and/or products, and also trapped the molecules, allowing consecutive reactions leading to thermodynamic equilibrium composition. Channels, on the other hand, allowed diffusion without trapping, if their free diameter was large enough. 10-ring channels in NU-87 were smaller than 10-ring channels in MFI. Zeolites MFI, MOR, CON, and TUN were also investigated in a riser simulator reactor in *m*-xylene isomerization and disproportionation in the temperature range 300–400°C (141). CON, TUN, and MOR gave higher *m*-xylene conversions compared with MFI. At 400°C and reaction time of 20 s, *m*-xylene conversion was 43.7% over MFI while around 63% over the other three zeolites. The P/O

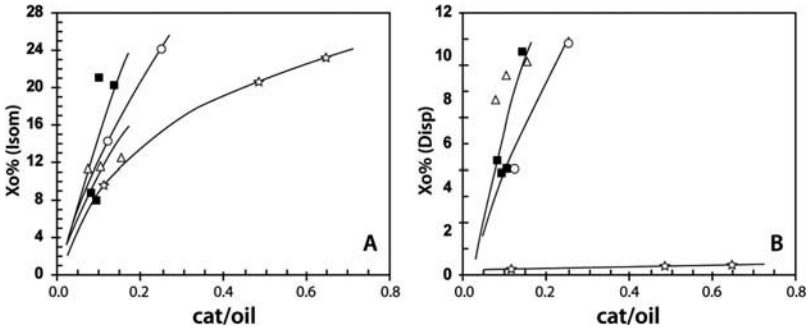

Figure 15: Initial conversion in the isomerization (a) and disproportionation (b) of *m*-xylene at 350°C and 20.3 kPa partial pressure, over MFI (x), NES (■), CON (△) and BEA (○) versus cat/oil (g of catalyst.h/mol *m*-xylene in feed). Reproduced from Llopis et al. (129), Copyright 2004, with permission from Elsevier.

and I/D ratios over the catalysts were found to decrease in the order: MFI > TUN > CON > MOR; thus, in the order of the decreasing pore dimensions.

Min et al. studied the mechanisms of *m*-xylene isomerization and disproportionation over 13 medium-pore zeolites with different framework topologies and three large-pore ones (142). While TUN and ZSM-57 (intersecting 10- and 8-ring channels) showed considerably higher P/O ratios than MFI, a commercial *m*-xylene isomerization catalyst, the ex situ gas chromatography–mass spectrometry (GC-MS) results demonstrated the intrazeolitic build-up of tri- and tetramethylated diphenylmethane species. High *p*-xylene selectivity found over some medium-pore zeolites was largely due to the product shape selectivity rather than to transition state one. The GC-MS results of *m*-xylene isomerization over TNU-10 catalyst provided clear experimental evidence supporting the bimolecular mechanism of *m*-xylene isomerization as presented in the scheme of Fig. 16. A thermodynamically favorable route was the transalkylation between 2,4-dimethylphenylmethane (species F) and another *m*-xylene molecule. As soon as the species F was formed, transalkylation operated by itself to produce a xylene mixture (L).

Single-event microkinetic methodology was applied towards "ethylbenzene dealkylation/xylene isomerization" under industrially relevant conditions (143). The model was able to reproduce the experimental observations in terms of ethylbenzene conversion, xylenes conversion, benzene selectivity, toluene, and C_9+ mass fraction, approach to equilibrium. Protonation enthalpies and activation energies of the considered reactions were estimated by model regression of experimental data acquired on a bifunctional Pt/H-MFI catalyst, while the remaining parameters were determined from the first principles or retrieved from literature information (143). Dealkylation was found to be energetically the most demanding with activation energy of 198 kJ/mol, while the alkyl shift and transalkylation reactions exhibited the lowest activation energies of 134 and 124 kJ/mol, respectively. Entropic effects resulted in the lowest rate coefficient for transalkylation and rate coefficients of a similar order of magnitude for alkyl shift and dealkylation. The catalyst was shown to have an adequate acid strength quantified by the standard protonation enthalpy between -70 and -90 kJ/mol.

Similarly to toluene disproportionation and methylation, many attempts have been made to improve the *para*-selectivity of zeolites by treatment with cations on MOR (144), pre-coking (145) or TEOS on MFI (146). Xylene loss can be prevented by inhibition of bimolecular reactions, which tend to dominate on the strongest acid sites located in the zeolite channels and on the external surfaces, where no rate-limiting steric constraints exist. The contribution of surface reactions increases with the decreasing crystal size of the zeolite catalyst. Experiments with ^{13}C labeled toluene confirmed that disproportionation products enable a supplementary, intermolecular pathway of xylene isomerization via transmethylation on the medium pore zeolite MFI (135).

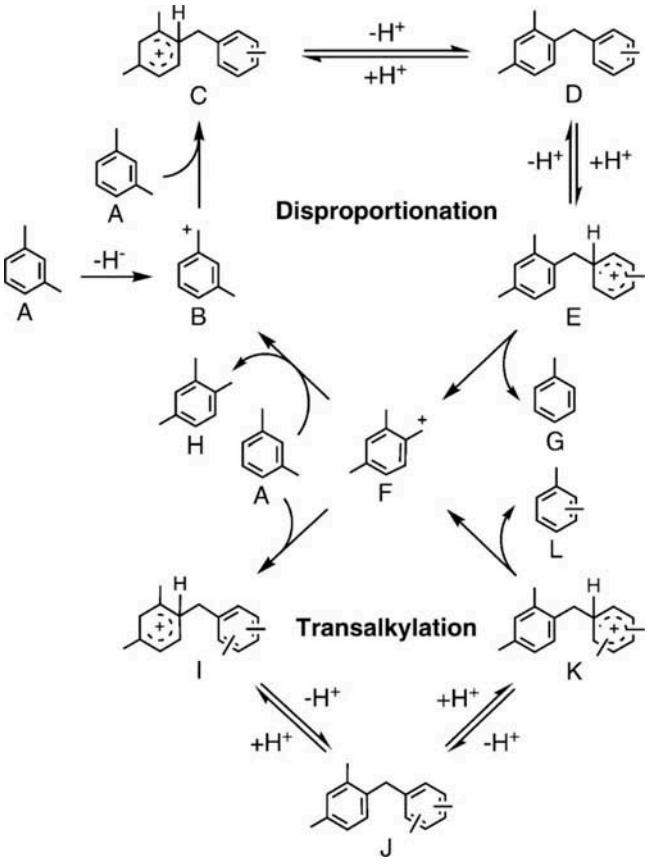

Figure 16: Bimolecular diphenylmethane-mediated reaction pathway of the zeolite-catalyzed m-xylene isomerization proposed based on the overall GC-MS results. Reproduced from Min et al. (142), Copyright 2012, with permission from the American Chemical Society.

The utilization of an in situ infrared reactor-cell for *o*-xylene isomerization on MFI zeolite allowed to detect traces of coke on the catalyst and to determine the OH groups specifically perturbed by the coke molecules (147). In fact, coke was not perturbing Brønsted acid bridging OH groups, but it was mainly located on silanol groups at defects inside the pore system. Lercher and coworkers found that the surface modification of MFI with TEOS enhanced the differences in diffusivity between *p*-xylene and *o*- or *m*-xylene via increased tortuosity of the transport pathway (133). Xylene isomerization catalyzed by Brønsted acid sites was largely suppressed by silylation. The reaction rate of *m*-xylene isomerization was controlled by reactant diffusion; the selectivity, by restricted transition state selectivity (8).

Further attempts to increase para-selectivity in *m*-xylene isomerization in the presence of ethylbenzene were performed with 5,6-benzoquinoline

(BQ) (148) adsorbed on the external surface of MFI zeolite. It suppressed substantially both disproportionation and transalkylation side reactions while the isomerization selectivity increased. Figure 17 shows the effect of this multiple modification procedure exceeding in terms of xylene loss (only 0.7 wt.%) at EB conversion level of 90.6 wt.% the state-of-art technology (148).

A hierarchical MFI zeolite prepared by treatment with NaOH and followed by mild HCl washing increased *p*-xylene selectivity and reduced the deactivation rate in *o*-xylene isomerization (149). The HCl-washed MFI displayed about two-fold increase in the *p*-xylene yield compared with the parent MFI. In situ infrared spectroscopy under reaction conditions allowed simultaneous monitoring of the catalytic performance and the buildup of carbonaceous deposits on the zeolite surface. The results showed that the interplay between activity, selectivity, and stability in modified zeolites can be optimized by relatively simple post-synthesis base treatment introducing mesopores and acid washing (surface acidity modification). ^{27}Al MAS NMR and IR spectroscopy enabled to conclude that the nature of the aluminum in mesoporous MFI zeolites was of greater importance than that of purely microporous zeolites. It was concluded that Lewis and Brønsted acid sites located close to the pore mouths are detrimental to the *para*-selectivity and stability of *o*-xylene isomerization (149).

Al-Khattaf and co-workers found that integrating MFI zeolite into mesostructured materials Al-MCM-41 and Al-MCM-48 led to high *p*-xylene

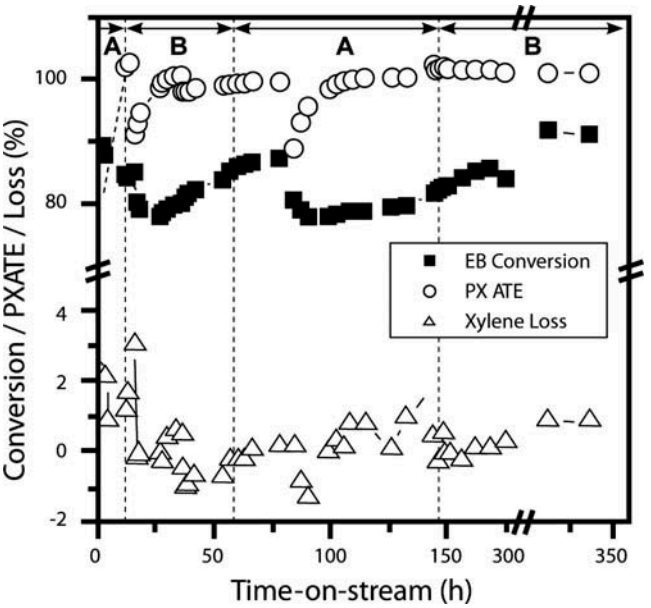

Figure 17: Catalytic performances of Pt300/Si/MFI with intermediated 5,6-benzoquinoline addition (feed: 15% EB + 85% m-xylene; rxn. temperature: 390°C; pressure: (A) 1.4 MPa, (B) 2.8 MPa; WHSV: 10 h^{-1}; H_2/aromatics: 2 mol/mol). Reproduced from Thibault-Starzyk et al. (147), Copyright 2001, with permission from Elsevier.

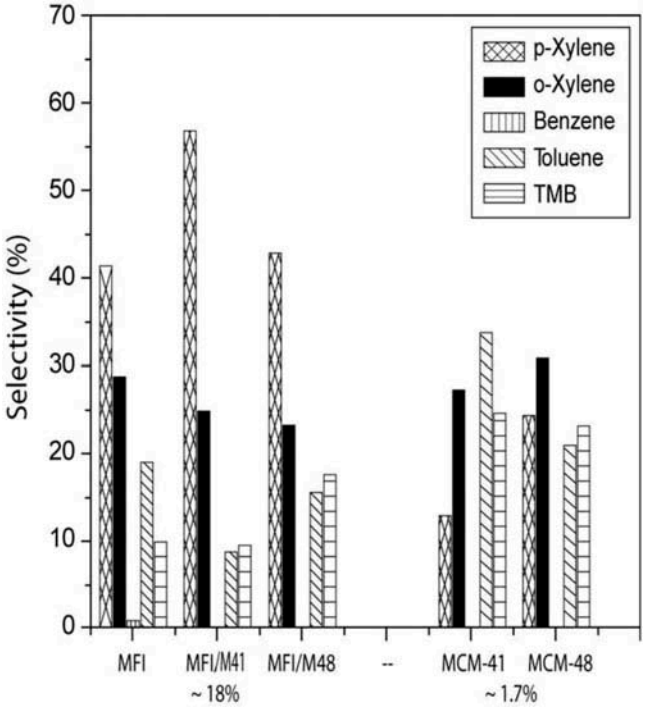

Figure 18: Product selectivity of transformation of m-xylene over MFI, MFI/MCM-41 (MFI/M41), MFI/MCM-48 (MFI/M48) at ~18% m-xylene conversion and Al-MCM-41 and Al-MCM-48 at ~1.7% m-xylene conversion (catalyst/feed = 3.8, reaction temperature: 350 °C. Reproduced from Balasamy et al. (150), Copyright 2011, with permission from Elsevier.

selectivity in the transformation of *m*-xylene (150). A bimolecular pathway involving disproportionation and transalkylation, together with the presence of MFI units in the composite materials, was responsible for this high *p*-xylene selectivity. The selectivity towards *p*-xylene over the different catalysts under study increased in the order: conventional MFI < MFI/MCM-48 < MFI/MCM-41. Figure 18 evidences high selectivity to toluene in the disproportionation of *m*-xylene occurring to a greater extent over MCM-48 and MCM-41 catalysts probably due to a large reaction volume available.

Catalytic membranes were also tested to improve *p*-xylene yield, selectivity and separation rate in xylene isomerization (151,152,153,154,155,156,157). MFI zeolite/alumina extractor type catalytic membrane reactor (CMR) was used to enhance *p*-xylene selectivity (157). The yield of p-xylene in CMR was 23% and *p*-xylene selectivity was to 65%. The operation of the CMR at lower temperatures was advantageous for higher *p*-xylene permeance.

Tarditi et al. conducted xylene isomerization in a Ba^{2+} ion-exchanged MFI using a membrane rector. The authors found that *p*-xylene yield increased from 52% in fixed-bed reactor to 69% in a membrane reactor at 370°C (156).

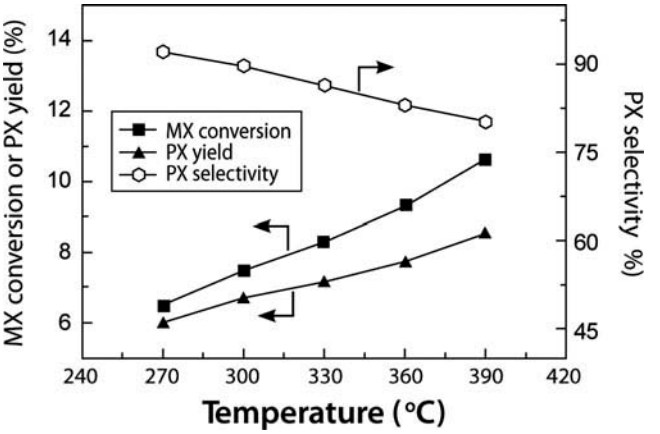

Figure 19: m-Xylene isomerization results of an H-MFI zeolite membrane as a function of the temperature (feed flow rate: 20 ml/min; sweep flow rate: 20 ml/min). Reproduced from Zhang et al. (157), Copyright 2012, with permission from Elsevier.

However, the quality of MFI membranes was difficult to control due to the introduction of Al in the MFI zeolite framework. The membranes used in this study were stable after 1000 h on stream, which included several thermal cycles between 25 and 400°C with no change in selectivity or permeation. Studies at higher pressures are required to further explore the applicability of CMR in industrial practice. An MFI CMR on α-alumina revealed the best performance in xylene isomerization among these membranes (156). Figure 19 shows a high *p*-xylene selectivity of 92.1% at m-xylene conversion of 6.5% achieved at 270°C over the MFI/α-Al_2O_3 membrane. In order to enhance the conversion of *m*-xylene, the number of active sites and membrane packing density must be improved. Catalytic zeolite membranes with hollow fiber structures could be an option to obtain high *p*-xylene productivity.

Diffusion studies were performed to understand the role of surface adsorption over MFI zeolites with different crystal sizes (158). Frequency response experiments with benzene, toluene and *p*-xylene were performed. It was found that rate-determining step depends on the size of MFI crystals; with particles around 1 μm overall diffusion was rate determining while for particles around 100 nm reaction rate was controlled by surface effects. Post-synthetic modification of MFI crystals with mesoporous silica significantly increased the sorption rate for benzene in contrast to toluene and *p*-xylene (159).

4. ETHYLBENZENE

Ethylbenzene is an important intermediate product in the petrochemical industry for the production of styrene further used for making polystyrene.

Over 99% of the world's ethylbenzene production is consumed in the manufacture of styrene, while minor applications include paint solvents and pharmaceuticals. World ethylbenzene demand is expected to increase from 27.5 million tons in 2008 to 31.7 million tons in 2013, which reflects a global average annual rate of 2.9%. The consumption is expected to grow the fastest in the Middle East (about 18%) and China (about 16%) during this period (160).

Commercially, almost all ethylbenzene (> 99 %) is produced by alkylation of benzene, except for a very small fraction being recovered from the mixed C_8 aromatics (xylenes) stream by superfractionation. Transalkylation is often combined with alkylation in order to convert polydiethylbenzenes into ethylbenzene, improving the efficiency of the process. The use of ethanol as the alkylating agent is favored in countries producing cheap bioethanol like India. Moreover, improved catalyst stability is reported when ethanol is used as an alkylating agent because of the formation of water enhancing proton-transfer reactions (161).

The reaction pathways for the acid-catalyzed alkylation of benzene with ethylene are presented in Fig. 20 (4). The first step is the formation of the ethyl carbocation, which then undergoes one of the following two pathways.

i. It reacts with benzene to form ethylbenzene. The subsequent alkylation of ethylbenzene results in the formation of diethylbenzenes (DEBs) and triethylbenzenes (TEBs).

ii. It reacts with ethylene to form a C_4 carbocation, which can then undergo alkylation, oligomerization, isomerization, and cracking to yield other alkyl benzenes and olefins.

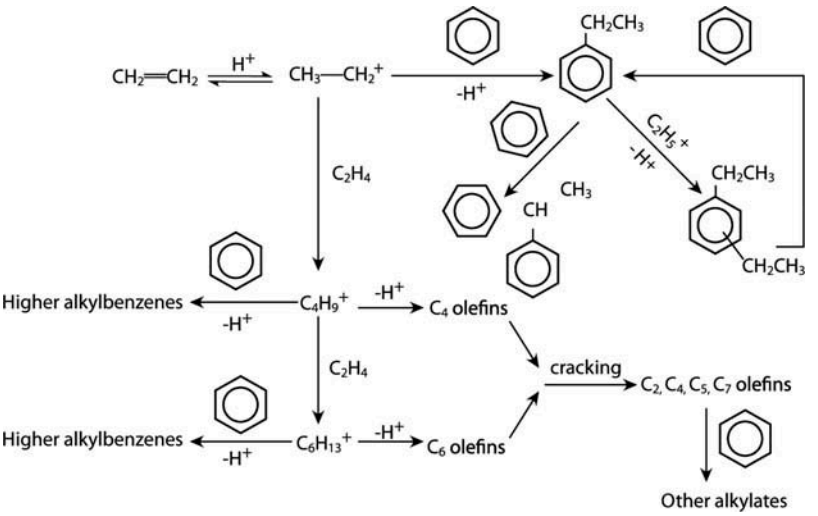

Figure 20: Reaction pathways for benzene alkylation with ethylene. Reproduced from Perego and Ingallina (4), Copyright 2004, with permission of The Royal Society of Chemistry.

To some extent, ethylbenzene also undergoes alkylation to diphenylethane. It must be noted that DEBs and TEBs are easily converted by their transalkylation with benzene to ethylbenzene, which also takes place at the same reaction conditions. At benzene-to-ethylene molar ratios above 4, the transalkylation can proceed to near equilibrium resulting in ethylbenzene yield of 99%, similarly to cumene (57). In contrast, the formation of olefins and higher alkylbenzenes (such as butylbenzenes) negatively affects the efficiency of the process by reducing ethylbenzene yield as well as its quality.

A possible mechanism of the ethylation of benzene with ethanol over MFI was proposed by Odedairo and Al-Khattaf, as illustrated in Fig. 21 (162). Proton from Brønsted acid sites attacks ethanol to form water and surface ethoxy groups. The ethoxy groups react with benzene molecules to form protonated ethylbenzene species on the surface. When desorbing, the protonated ethylbenzene returns a proton to the Brønsted site and forms ethylbenzene. In a consecutive manner, ethylbenzene can be further ethylated at *ortho* or *para* positions to form the respective diethylbenzenes.

Earlier processes for production of ethylbenzene using $AlCl_3$-HCl and BF_3/Al_2O_3 as catalysts were reviewed by Perego and Pollesel (57). Although liquid-phase $AlCl_3$ plants will continue to operate in future, all new plants are based on vapor-phase zeolite technology. In the widely used ExxonMobil/Badger process, gas-phase production of ethylbenzene takes place over a MFI based catalyst in a fixed-bed reactor. The reactor is operated under high temperature (390–450°C) and pressure (1.5–2 MPa). The process was subsequently improved by the addition of another reactor dedicated to the

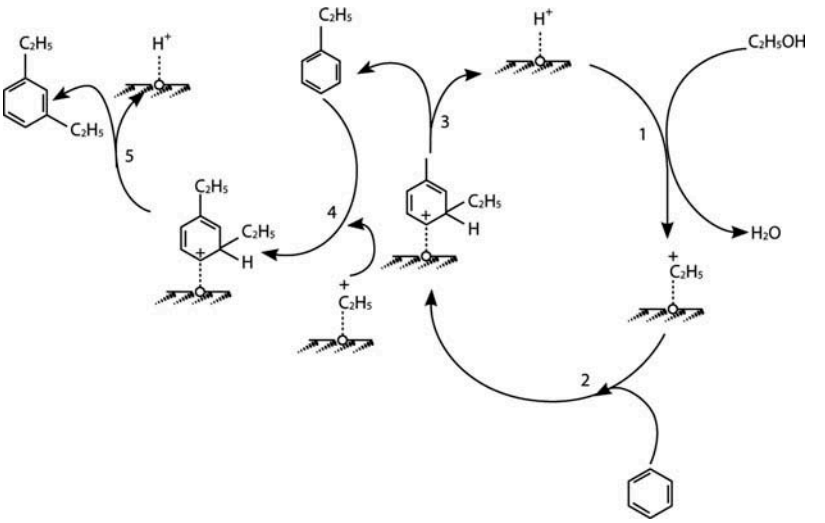

Figure 21: Proposed overall reaction scheme during benzene ethylation over MFI catalyst. Reproduced from Odedario and Al-Khattaf (162), Copyright 2010, with permission from Elsevier.

transalkylation of the polyethylbenzenes, resulting in an improvement in the yield and catalyst life (163). Another process, named Albene, was developed to alkylate benzene with ethanol in a single-step reaction by the National Chemicals Ltd. of India and Hindustan Polymers Ltd. It uses an MFI-like zeolite containing iron instead of aluminum in its framework (164). Any DEB formed is transalkylated with benzene in a separate reactor to produce more ethylbenzene.

A considerable improvement was achieved by UOP/Lummus/Unocal with the development of a liquid-phase process which resulted in better thermal control and an extension of the catalyst life. Consequently, less frequent regenerations are required that can be carried out ex situ. The introduction of new zeolite catalysts together with the process up-grading resulted in significant yield improvements to over 99% (165). An improved version of the UOP/Lummus process, called *EBOne,* uses catalysts UZM-8 for alkylation and transalkylation (166). In addition, CDTECH uses the process based on catalytic distillation, which is more suitable for processing dilute streams of ethylene (57).

The liquid-phase process developed by ExxonMobil, called EBMax, can process both polymer grade ethylene and dilute ethylene feed streams. The ethylbenzene unit has three subsystems: alkylation, transalkylation, and distillation. The process uses MWW, a zeolite of medium-pore size, in the liquid-phase, while the transalkylation is operated in the vapor-phase with a MFI-based catalyst. MWW demonstrates a catalytic activity comparable to FAU but inferior to that of BEA. In contrast, the selectivity is higher, with respect to both FAU and BEA zeolites, as the formation of DEBs and TEBs is particularly reduced (167).

A BEA-zeolite-based catalyst was reported by Polimeri Europa to exhibit exceptional performance, in terms of consumption of raw materials as well as the quality of the ethylbenzene produced (57). In this process, the catalyst is distributed in the reactor over several beds, and the supply of ethylene is directed over these in such a way as to create a much higher local ratio of benzene/ethylene with respect to the global ratio.

Further research in this area is focused on modification of zeolite structures and their textural properties. Mesoporous zeolite single crystals were reported by Christensen et al. in alkylation of benzene with ethylene (168). An increase in turn-over frequencies in the range of 15–20% compared with the parent MFI was observed due to improvement in the mass transport in the zeolite crystallites. It was proposed that the diffusion paths are shorter in mesoporous MFI crystals suppressing substantially secondary alkylation. As a result, both higher activity and higher selectivity to ethylbenzene were achieved (168).

Although MCM-49 zeolite is considered isostructural with MCM-22 (both are of MWW topology) (169), MCM-49 exhibits higher selectivity to

ethylbenzene in the alkylation of benzene with ethylene (170). Liu et al. (171) elucidated the role of different pore systems in MCM-49 zeolite (pocket, supercage, and sinusoidal pore) in liquid alkylation of benzene with ethylene by precoking to block the supercages and poisoning the surface pockets. The effect of alkali treatment on different pore systems of MCM-49 has been studied to improve the catalytic performance for the alkylation of benzene. Most Lewis acid sites (ca. 73%) were located within the supercages, while 38% of Brønsted acid sites were located in the surface pockets, 28% in the sinusoidal pores and only 34% in the supercages, respectively. The authors concluded that the alkylation of benzene with ethylene mainly occurs in the surface pockets, and the contribution from the sinusoidal pores is limited (171). This result is in good agreement with previous reports for benzene alkylation with propylene by the groups of Corma and Čejka (172,173).

Promising results were reported by the group of Wu using modified MWW nanosheets (MCM-56 analogs (174)) or mesoporous MWW (175). The MCM-56 analogues exhibited a higher conversion (33%) of benzene and a higher catalytic stability than MCM-22 (28%) in liquid-phase benzene alkylation with ethylene (174). This is in a good agreement with earlier report of Cheng et al. (176). Even better performance was achieved with the mesoporous MWW prepared using carbon black pearls. Mesoporous MWW had a larger accessible external surface and contained a substantial amount of mesopores (175).

Odedairo and Al-Khattaf investigated the ethylation of benzene with ethanol over two USY zeolite catalysts with different acid site concentrations (177). Higher benzene conversion was observed over the USY zeolite possessing a higher concentration of acid sites (Si/Al = 5.3 and 16). As expected, among side reactions cracking of ethylbenzene dominated at temperatures 350 and 400°C while ethylbenzene ethylation was significant at reaction temperature of 300°C.

CON and TUN show usually higher activities in transformations of aromatics than, e.g., MFI zeolite. Zeolite CON possesses a unique channel system consisting of intersecting 12-ring and 10-ring pores; it is the first synthetic zeolite having 4-4 = 1 SBU (secondary building unit) in the structure (30). Corma et al. (172) studied the alkylation of benzene with ethanol over CON and compared it with other zeolite catalysts. CON zeolite exhibited the highest conversion of benzene among the zeolites studied, MFI, BEA, IWW. The following ethylbenzene selectivity order was achieved at benzene conversion between 17–20%: IWW (86.3%) > MFI (82.1%) > CON (75.3%) > BEA (62.5%). The high selectivity of IWW was explained, on the one hand, by the multi-pore structure itself, which enhances diffusion of the primary products before being involved in consecutive reactions, and on the other hand, by taking into account that according to theoretical calculations only 1/6 of the total Brønsted acid sites are located in the 12-ring channels. The remaining OH groups are located in the intersections of the 10- and 12-ring pores, or in the

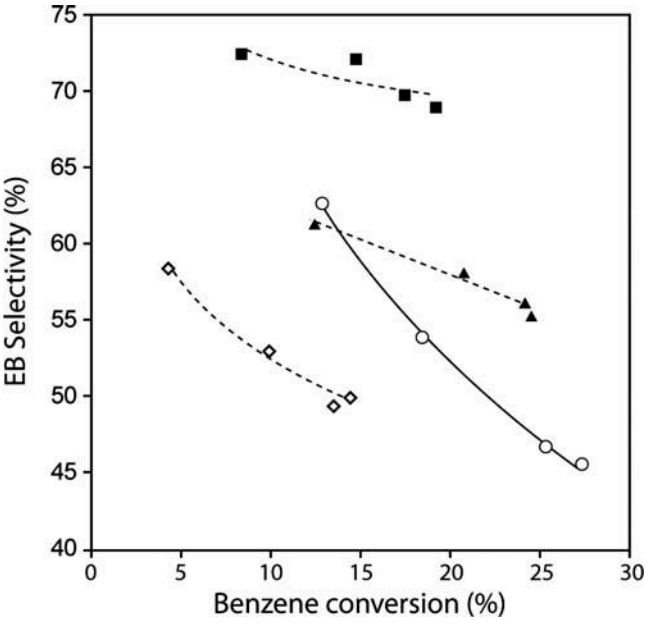

Figure 22: Effect of benzene conversion on ethylbenzene selectivity at 275°C over MOR (◊), MFI (■), CON (○), TUN (▲). Reproduced from Odedario and Al-Khattaf (162), Copyright 2010, with permission from Elsevier.

10-ring channels close to the intersections. Therefore, the formation of heavier compounds leading to a selectivity reduction and/or to catalyst deactivation is sterically hindered. Hence, IWW, with its multi-pore structure containing connected 10- and 12-ring pores, shows a unique behavior as a multipurpose alkylation catalyst.

Odedairo and Al-Khattaf (162) compared the behavior of MFI, TUN, CON, and MOR in benzene ethylation with ethanol. The conversion of benzene follows the order: CON > TUN > MFI > MOR due to the high acidity of CON combined with increased mass transport through its large pores. Ethylbenzene selectivity follows the order: MFI > TUN > CON > MOR, at the same benzene conversion. The effect of benzene conversion on ethylbenzene selectivity at 275°C over zeolite-based catalysts studied is given in Fig. 22. EB selectivity over CON, MOR, and TUN zeolite catalysts shows a high dependence on benzene conversion and it decreased with increasing benzene conversion.

5. DIETHYLBENZENE

The catalytic transformation of ethylbenzene over zeolite-based catalysts to produce diethylbenzene isomers has recently gained more importance due to a wide range of applications of diethylbenzenes in various industrial processes (178). *p*-Diethylbenzene (*p*-DEB) is an important desorbent in adsorptive separation processes such as UOP Parex, in the separation of xylene isomers.

Moreover, it is an important monomer for the production of copolymers, such as ion exchange resins and viscosity modifiers of lubricant oil (178).

5.1. Ethylation of Ethylbenzene

DEBs can be prepared by shape selective alkylation of ethylbenzene with ethylene, ethyl chloride, or ethanol. The use of ethanol as the alkylating agent is increasing because of its industrial availability in countries like India or Brasil. In situ dehydration of alcohols prolongs also the catalyst activity since the water formed suppresses coke formation (179). Primary and secondary reactions occurring during ethylation of ethylbenzene with ethanol are presented in Fig. 23. The primary reaction pathway is ethylation of ethylbenzene with ethanol to produce DEB and water. This is accompanied by disproportionation of ethylbenzene resulting in the formation of DEB and benzene. A cracking reaction of DEB also occurs at elevated temperatures (180).

Conventional catalysts are not highly selective to the *para* DEB isomer providing selectivities close to the thermodynamic equilibrium composition of DEBs (para:meta:ortho) 30:54:16 (178). A number of studies deals with catalyst modification techniques for promoting the para selectivity, the earlier ones are summarized in reviews by Čejka and Wichterlova (8) and Perego and Ingallina (4).

One way to enhance the para selectivity is through post-synthesis modifications removing the unselective acid sites located in the pore mouth regions

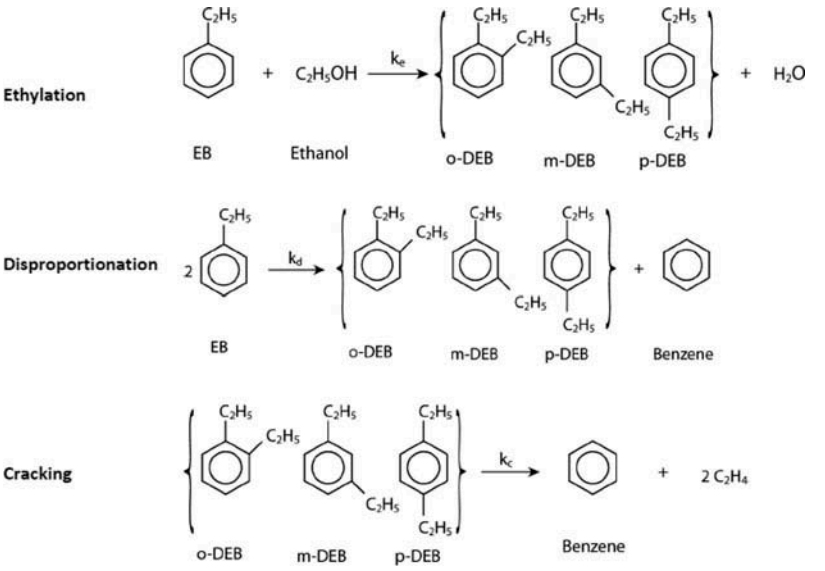

Figure 23: Primary and secondary reactions occuring during ethylation of ethylbenzene with ethanol Reproduced from Waziri and Al-Khattaf (180), Copyright 2009, with permission from the American Chemical Society.

and/or by narrowing the pore openings. Halgeri and Das (178) reported a significant improvement in *para*-selectivity to *p*-DEB by pore size modification of MFI zeolite through chemical vapor deposition of tetraethyl ortho-silicate (TEOS). It narrows the pore openings, coats the external surface, and eliminates the external acid sites without affecting the internal ones. It should be mentioned that although different authors concluded that narrowing of the pore entrances or annihilation of the acid sites on the external surface are critical conditions to improve the *para*-selectivity, so far nobody succeeded in decoupling these two effects.

The CVD treatment increased the *p*-DEB selectivity from 50% to 97% while the conversion decreased from 24% to 14%. It indicates that the yield of *para*-DEB was almost the same. Čejka and Wichterlová (8) noted that the effect of zeolite coking on *para*-selectivity in ethylation reactions of ethylbenzene was analogous to that observed with xylenes. Coke was formed preferentially on the external surface sites, resulting in narrowing of the pore openings and increasing the *para*-selectivity. Similarly, Bauer et al. (181) found that, in terms of inactivation of the external surface acidity of MFI, samples modified by precoking possessed improved shape selectivity during xylene isomerization as compared with those by one-cycle silica deposition.

The effect of precoking is not yet fully understood, studies by, e.g., Čejka et al. (182) for toluene ethylation reported that precoking has no positive effect on the *para*-selectivity of zeolites. The main reason of these discrepancies could be in different reaction conditions used by different authors. The agreement seems to be in the role of acid sites in MFI. Zheng et al. (183) noted that the reduction of strong Brønsted acid sites suppressed the isomerization of *p*-DEB and lead to enhancement of *para*-selectivity.

Waziri et al. (180) investigated the kinetics of ethylation of ethylbenzene with ethanol over an MFI catalyst. Ethylbenzene conversions between 7-21 % were observed at temperatures of 300–500°C. The yield of DEBs increased with increasing reaction temperature. At 400°C, maximum DEBs yield (12.4%) was achieved. Other products included benzene (1.1%) and negligible amounts of xylenes, triethylbenzenes, and gaseous hydrocarbons. The yield of DEB decreased at the reaction temperatures above 400°C. While alkylation was dominant in the temperature range 300–400°C, the rates of disproportionation and dealkylation increased at temperatures above 400°C leading to an increase in the benzene/DEB ratio and yield of gases.

5.2. Disproportionation of Ethylbenzene

The disproportionation of ethylbenzene to benzene and diethylbenzene is also an acid-catalyzed reaction frequently studied over medium-pore (e.g., MFI, TON, MWW) or large-pore zeolites (e.g. MTW, ZSM-34, FAU (both Y and EMT), LTL, BEA) (57). It was noted that mostly strong Brønsted acid sites catalyze this reaction.

Based on experimental study using in situ MAS NMR spectroscopy, Huang et al. (184) proposed a bimolecular reaction mechanism of ethylbenzene disproportionation on large pore zeolites (Fig. 24, Scheme ***A***) and a monomolecular reaction pathway on medium pore zeolites (Fig. 24, Scheme ***B***) via the ethoxy-mediated intermolecular ethyl group transfer. On the medium-pore zeolite MFI, after adsorption of **A** on the zeolite surface, the aromatic ring

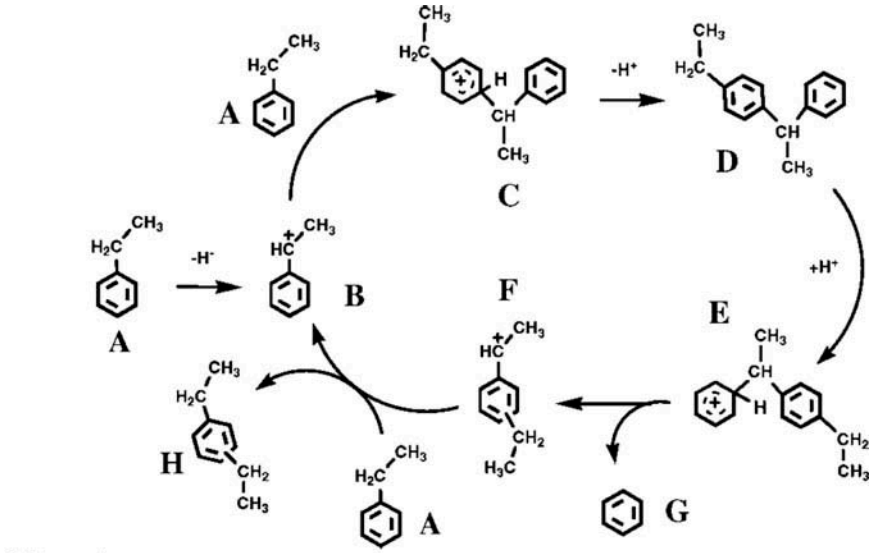

Scheme A

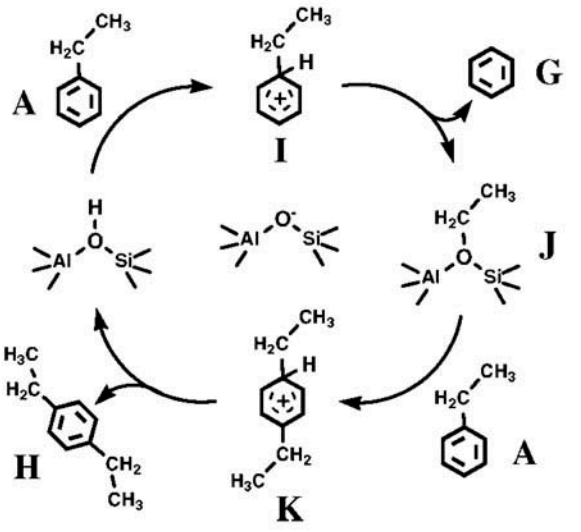

Scheme B

Figure 24: Proposed reaction pathways for ethylbenzene disproportionation. Reproduced from Huang et al. (184), Copyright 2008, with permission from the American Chemical Society.

is rapidly protonated to form the ethylcyclohexadienyl carbenium ion **I** even at room temperature**.** The proton is added to the carbon atom holding the ethyl group to form a σ-complex. At higher temperatures, the σ-complex **I** splits off an ethyl cation from the aromatic ring to produce the benzene molecule **G**. The alkyl cation is stabilized by a nearby SiO-Al site and forms a ethoxy group **J**. Subsequently, **J** combines with a second **A** to yield the diethylbenzylium cation with an additional proton at the aromatic ring (**K**). This proton can migrate back to the nearby SiO-Al site to complete the catalytic cycle, and diethylbenzene **H** is produced as the final product. On large-pore zeolites FAU (ca. 0.74 nm), the bulky diphenylethane species **(C, D, E,** and **F)** are produced, but this type of transition state is too large to be formed on medium-pore zeolite MFI (ca. 0.56 nm). This study provided NMR spectroscopic evidence that the pore shape of zeolite catalysts strongly affects the transition states of ethylbenzene disproportionation and results in different reaction mechanisms.

The products obtained in the disproportionation of ethylbenzene normally give the thermodynamic equilibrium composition and therefore require energy intensive operations for *para*-DEB recovery. Park and Rhee (185) investigated ethylbenzene disproportionation over parent and dealuminated MWW zeolites. *p*-DEB is supposed to be formed inside the micropores of dealuminated MWW zeolite as the primary reaction product. The *m*-DEB and *o*-DEB are mainly produced via the secondary isomerization of the *para*-isomer on the external surface of the MCM-22 catalyst. *Para*-selectivity of MWW increased with the increasing degree of dealumination as a result of preferential removal of Brønsted acid sites from the external surface.

Chen et al. (186) studied the effects of coking and surface modification of MFI zeolites (Si-CVD or lutidine adsorption) on the enhancement of *p*-diethylbenzene selectivity in ethylbenzene disproportionation. Similarly to studies of other *para*-selective reactions, diffusion limitations and inactivation of the external active sites were found to be responsible for changes in conversion and selectivity. Similar results were obtained by Zhu et al. (187) using Si-CLD or loading with MgO. Recently, Tsai et al. (148) succeeded to deactivate the external surface of MFI zeolite by 5,6-benzoquinoline adsorption. As a result, consecutive reactions were deeply suppressed.

FAU-based zeolite catalysts were investigated by Al-Khattaf (188). Fresh catalyst (0.55 mmol/g of acid sites) was modified by steaming (0.033 mmol/g of acid sites). EB disproportionation over FAU catalysts was a strong function of acidity and acid sites strength. The fresh catalyst exhibited significantly higher conversion (7–45% depending on the contact time) than the steamed catalyst and selectivity to DEBs increased with decreasing conversion. With medium pore MFI (189), ethylbenzene conversion increased from 9 to 30% as the reaction temperature was raised from 350 to 500°C with simultaneous decrease in DEB selectivity from 48 to 13%.

In summary, ethylbenzene disproportionation over MFI-type and FAU-type catalysts strongly depends on the catalyst acidity and acid sites strength—zeolites with higher acidity generally exhibit higher ethylbenzene conversion. This is accompanied by a decrease in DEBs selectivity. DEBs selectivity is also highly dependent on reaction temperatures—lower temperatures (<400°C) promote formation of DEBs while higher temperatures (>400°C) promote dealkylation and coke formation.

6. CUMENE AND CYMENES

Alkylation of benzene and toluene with propylene or C_3 alcohols is an important reaction producing cumene (an intermediate in phenol production) or cymenes. While the first reaction is of a particular industrial importance, the second reaction is frequently used as a model reaction to investigate the acidity and inner channel structure of zeolite catalysts (190,191).

6.1. Alkylation of Benzene with Propylene

Investigation of different zeolites with unique topology of their channel systems (NES, CON, and MFI) in alkylation with different alcohols showed that the presence of cavities allows for the formation of bulky intermediates and/or products (129). The cavities also trap molecules affording consecutive reactions leading to thermodynamic equilibrium. Molecular dynamic study confirmed that larger pores enable faster diffusion of reactants and products. Any new zeolite having medium or large-pore system is worth investigating in transformation of aromatic hydrocarbons. TUN zeolite is a medium pore zeolite with a complex 3D channel system (192). As for cumene synthesis, the selectivity over TUN is higher than over MFI but lower than of MWW. Lower selectivity of TUN in comparison with MWW is due to the formation of larger amounts of *n*-propylbenzene in the pore intersections of TUN. On the other hand, high activity without formation of *n*-propylbenzene was observed over of ITQ-33 zeolites. It was attributed to its unique 18-10-10-ring channel system (35,193).

Benzene alkylation with isopropyl alcohol was investigated from the point of view of the role of crystallinity over zeolite BEA (194) in a liquid phase. Benzene conversion increased with the increasing void volume of zeolite BEA accessible for benzene molecules.

Recently, Ryoo and coworkers (195) evaluated the catalytic behavior of lamellar MFI zeolites synthesized using tailored surfactants. The results evidenced high resistance of lamellar MFI against coking due to a fast desorption of reaction products, which are mostly formed on the external surface of the zeolite lamellas. Benzene alkylation with propylene can be also used aiming at

decreasing concentration of benzene in gasoline. MWW with optimized ratio of Brønsted to Lewis acid sites is highly active in this reaction (196).

6.2. Alkylation of Toluene with Propylene

Toluene alkylation with propylene is not only an important model reaction but serves as the first reaction step to selective synthesis of cresols (8). The obtained conversions, selectivities to cymenes, *p*-cymene, and *n*-propyltoluenes allow us to gain deep insight into the acidity and structural/textural properties of zeolites under study.

A series of zeolites with one- to three-dimensional 10-ring and 12-ring channels with and without cages, and those having 12-12-10 and 12-10-10-ring channel systems was investigated in toluene alkylation with isopropyl alcohol (77). The authors showed that the general relationship of increasing zeolite activity with the increasing pore diameter and pore connectivity is not valid as the size of some 12-ring channels (BEA, MSE) is comparable with 10-ring channels (MFI, STF). Zeolites STF and MCM-58 behaved in toluene alkylation like 3D large-pore zeolites due to the presence of cages. The presence of 18-ring cages in the channels of 10-ring zeolite STF gives rise to an unusual catalytic behavior of this zeolite in comparison with the other 10-ring zeolites. STF, possessing channels of 0.54 x 0.57 nm in diameter, i.e., of comparable size to the medium-pore MFI zeolite, exhibits catalytic activity in transformation of aromatic hydrocarbons similar to large-pore zeolites. 18-Ring cages enable the formation of relatively bulky transition states without restricting diffusion of the product molecules out of the 10-ring channel system (193).

Presence of mesopores in MFI crystals achieved via addition of secondary template (carbon black pearls) to the reaction mixture modified substantially the catalytic behavior of this zeolite (70). Toluene conversion in its alkylation with isopropyl alcohol increases with increasing mesopore volume in parallel with the selectivity to primary alkylation products. In contrast, products of consecutive reactions as well as *para*-selectivity decreased due to a short "real contact time" caused by the presence of mesopores.

Desilication of MWW zeolites by sodium silicate solution substantially influenced their catalytic behavior. Under milder conditions, conversion of toluene increased. In contrast, severe desilication resulted in destruction of the MWW structure accompanied by decrease in toluene conversion (83).

Controlled synthesis of MFI with a specially designed surfactant-based template performed by group of Ryoo enabled the synthesis of MFI in the form of nanosheets (71). Adsorption of 2,6-di-tert-butyl pyridine evidenced that most of the acid sites are located on the external surface of the MFI nanosheets. As a result, the MFI nanosheets were more active than conventional MFI crystals. Surprisingly, the MFI nanosheet-crystals exhibited higher *para*-selectivity than the thermodynamic one despite their thickness was only 1.5 nm.

While zeolite activity and selectivity clearly depends on the textural properties of zeolites under investigation, Davis et al. (197) showed that the void volume of channel intersections of zeolite STI is also of a high importance. The channel intersections of 10- and 8-rings in STI are larger in size than the intersecting channels of MFI (two 10-rings). It results in a much higher *iso*-/*n*-propyltoluene ratio obtained over STI zeolite (197).

7. CONVERSION OF HEAVY REFORMATE TO XYLENES

While alkylations of benzene with ethylene or propylene are reactions performed with "pure" components, different situation arises in the case of industrial applications in which mixtures of aromatics are involved. From a practical point of view, studies using "real" feed address more complex issues. Conversion of heavy reformate into value-added xylenes by dealkylation-transalkylation process is an important example of such an application (123).

7.1. Reactions of Heavy Reformate

Heavy reformate consists mainly of C_9^+ stream (aromatics with carbon number nine and higher). Composition of a typical heavy reformate stream is presented in Table 9. Among the C_9 components, trimethylbenzenes (TMBs; 50–60%) and methylethylbenzenes (MEBs; 30–40%) are the major constituents.

Due to the presence of a variety of other aromatic compounds in the heavy reformate, multiple parallel and consecutive reactions take place. Main

Table 9: Composition of a typical heavy reformate feed (198).

Major Compound	Short Name	wt.%
Iso-propyl benzene	iPB	1.7
n-propyl benzene	nPB	4.3
1-methyl 2-ethyl benzene	1M2EB	6.5
1-methyl 3-ethyl benzene	1M3EB	18.5
1-methyl 4-ethyl benzene	1M4EB	9.1
1,2,3-tri-methyl benzene	123TMB	6.6
1,2,4-tri-methyl benzene	124TMB	39.1
1,3,5-tri-methyl benzene	135TMB	10.1
Total A_9		**95.9**
n-butyl benzene	nBB	0.5
1,4-diethyl benzene	14DEB	0.8
1,3-diethyl benzene	13DEB	0.4
1,3-dimethyl, 5-ethyl benzene	13DM5EB	0.8
1,4-dimethyl, 2-ethyl benzene	14DM2EB	0.4
Others A_{10}		1.2
Total A_{10}		**4.1**

reactions during its conversion include disproportionation (re-arrangement of alkyl groups between two identical molecules), transalkylation (transfer of alkyl groups between different molecules), dealkylation (removal of alkyl group) and isomerization (conversion of one isomer into another). The conversion process is carried out in hydrogen atmosphere in order to minimize coke formation on the catalyst. The parallel and consecutive reaction network is also accompanied by multiple chemical equilibria, including isomerization of xylenes, TMBs, and MEBs. The disproportionation, transalkyation, and isomerization reactions are equilibrium constrained while the dealkylation reactions are kinetically controlled (198, 199).

Heavy reformate can be subjected to transalkylation either alone (200) or with toluene for the production of xylenes and benzene. Table 10 lists principal reactions occurring during the conversion of heavy reformate to xylenes. Each reaction has been assigned an identification code for easy reference.

When heavy reformate is processed alone, in situ production of toluene is required for the xylene-forming reactions (***X-1, X-2***) to proceed. Toluene formation occurs, mainly from hydrodealkylation of MEBs (***T-1***), prior to the formation of xylenes. Toluene can be formed by disproportionation of MEBs (***T-2***) but this reaction is not desirable as it produces also C_{11} alkylaromatics. The highly desirable reaction is the transalkylation of TMBs and toluene to produce xylenes (***X-1***). Xylene formation may also occur from disproportionation of toluene (***X-2).*** Hydrodealkylation of dimethylethyl benzenes (***X-3***) and disproportionation of TMBs (***X-4***) are other routes for direct production of xylenes. However, disproportionation of TMBs also produces tetramethylbenzenes (TeMBs) which may form coke precursors by secondary reactions. Ethylbenzene formation (***E-1*** to ***E-3***) is also not desirable as the boiling point of ethylbenzene (136°C) is too close to *p*-xylene (138°C) causing difficult downstream separation by distillation. The C_{10} and C_{11} aromatic compounds can be formed via reactions ***H-1*** to ***H-7***. Heavy aromatics act as coke precursors, thus, their formation should be limited. The isomerization of xylenes, TMBs and MEBs (***I-1*** to ***I-3***, respectively) also occur and tend to readjust the isomers into their thermodynamic equilibrium proportion.

Commercial transalkylation processes generally use a mixture of heavy reformate and toluene as feedstock. Most of the published reaction studies were carried out using mixtures of 124-TMB and toluene as the feedstock, which partially models the industrial heavy reformate. A few published studies were conducted using a mixture of heavy reformate and toluene as feedstock (111,201,202,203). A mixture containing 20–30% toluene and 70–80% heavy reformate was reported to improve the xylene yield from 22.5 to 25.3%.

Table 10: List of principal reactions occuring during the conversion of heavy reformate (198).

Reactants	Reaction	Products	Reaction No.
Toluene Forming Reactions			
MEB	Dealkylation	Toluene + Ethane	***T-1***
MEB + MEB	Disproportionation	Toluene + C_{11}	***T-2***
Xylenes Forming Reactions			
Toluene + TMB	Transalkylation	Xylene + Xylene	***X-1***
Toluene + Toluene	Disproportionation	Xylene + Benzene	***X-2***
DMEB	Dealkylation	Xylenes + Ethane	***X-3***
TMB + TMB	Disproportionation	Xylene + TeMB	***X-4***
Benzene Forming Reactions			
Toluene + Toluene	Disproportionation	Benzene + Xylene	***B-1***
Propylbenzene	Dealkylation	Benzene + Propane	***B-2***
Ethylbenzene	Dealkylation	Benzene + Ethane	***B-3***
Ethylbenzene Forming Reactions			
Toluene + MEB	Transalkylation	Ethylbenzene + Xylene	***E-1***
DEB	Dealkylation	Ethylbenzene + Ethane	***E-2***
MEB + MEB	Disproportionation	Ethylbenzene + DMEB	***E-3***
Heavy Aromatics (C_{10} and C_{11}) Forming Reactions			
Toluene + MEB	Transalkylation	C_{10} + Benzene	***H-1***
MEB + MEB	Disproportionation	C_{11} + Toluene	***H-2***
MEB + MEB	Disproportionation	C_{10} + Ethylbenzene	***H-3***
TMB + TMB	Disproportionation	C_{10} + Xylene	***H-4***
MEB + TMB	Transalkylation	C_{11} + Toluene	***H-5***
Propylbenzene + Toluene	Transalkylation	C_{10} + Benzene	***H-6***
Isomerization Reactions			
Xylenes	Isomerization	*o*-xylene + *m*-xylene + *p*-xylene	***I-1***
TMBs	Isomerization	123-TMB + 124 TMB + 135TMB	***I-2***
MEBs	Isomerization	1M2EB + 1M3EB + 1M4EB	***I-3***

Abbreviations: TMB = Trimethylbenzene(s); MEB = Methylethylbenzene(s); DEB = Diethylbenzene; DMEB = Dimethylethylbenzene(s); TeMB = Tetramethylbenzene(s).

7.2. Thermodynamic Aspects

7.2.1. *Isomerization of TMBs and MEBs*

The thermodynamic equilibrium composition of the TMB isomers at 400°C is 67:25:8 for 1,2,4-TMB:1,3,5-TMB:1,2,3-TMB (204), while that of MEB isomers is 16:50:34 for 1M2EB:1M3EB:1M4EB (205). As the TMBs and MEBs react during the heavy reformate conversion, their isomers also re-adjust themselves towards thermodynamic equilibrium concentrations.

7.2.2. *Transalkylation of TMBs with toluene*

Krejčí et al. (119) reported the thermodynamic equilibrium conversions of TMBs and toluene. The equilibrium composition data at 400°C from this publication are presented in Fig. 25. The thermodynamic equilibrium composition depends largely on the TMB/toluene ratio, whereas the dependence on temperature is not so dominant. When the TMB/toluene ratio is >3, the disproportionation of TMB predominates and the major products are xylenes and TeMBs. When the TMB/toluene ratio is <0.1, the disproportionation of toluene dominates and the major products are benzene and xylenes. However, when the TMB/toluene ratio is 0.7–1.7, transalkylation of TMB and toluene becomes significant resulting in higher amounts of xylenes (206).

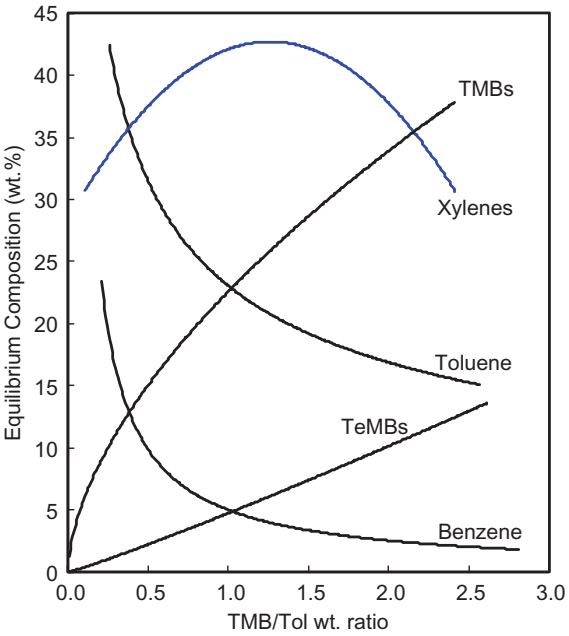

Figure 25: Thermodynamic equilibrium composition of aromatic compounds at 400°C. Reproduced from Krejčí et al. (119), Copyright 2010, with permission from Elsevier.

When the feedstock is equimolar mixture of TMB and toluene, almost equal amounts of benzene and TeMB are formed. Higher amounts of benzene are formed if the toluene content is higher than the content of TMBs. On the other hand, higher amounts of TeMB will be formed if the toluene content is lower than that of TMBs. Therefore, the thermodynamic limitations imply that, if heavy reformate alone is used as feedstock, higher xylene yield can be obtained if the amount of toluene produced from MEB dealkylation matches the TMB content present in the heavy reformate feedstock.

7.2.3. Overall yield of xylenes from heavy reformate

For a typical heavy reformate with a composition of 55% TMBs, 33% MEBs, and 3% C_{10}^{+}, Serra et al. (200,207) calculated the equilibrium product distribution when different amounts of toluene were added (Fig. 26). The authors included only dealkylation of ethyl groups and transalkylation reactions while all other parallel or consecutive reactions were not considered. The effect of change in heavy reformate composition was not studied (200).

The results of this thermodynamic study show, for instance, for a feedstock having 50% heavy reformate and 50% toluene, the xylene yield is 38%, and TMB conversion is about 64 %, whereas the benzene and TeMB yields are 8.8 and 0.5%, respectively. The maximum yield of xylenes is achieved at about

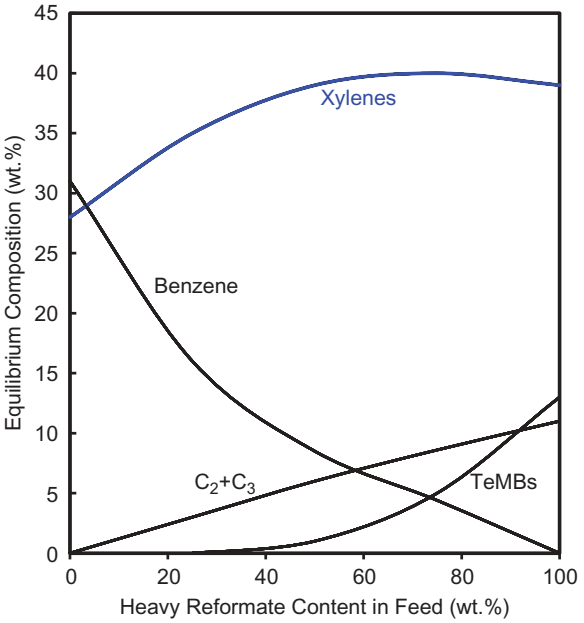

Figure 26: Equilibrium composition of transalkylation products as a function of heavy reformate content in feed (mixed with toluene). Reproduced from Serra et al. (200), Copyright 2005, with permission from Elsevier.

75% reformate and 25% toluene. However, in this situation the TeMB yield at equilibrium was about 5%. Therefore, from a thermodynamic point of view, the optimum reformate content is about 50%, which maximizes the ratio of xylenes to TeMBs in the product. When heavy reformate is processed without any addition of toluene, the maximum content of xylenes can reach up to about 40 wt.%, but at the same time the yield of undesired TeMBs exceeded 12 wt.% (200).

7.3. Reaction Schemes

1,2,4-TMB is the most commonly used model compound representing heavy reformate composition due to its highest content in the typical industrial heavy reformate. A transalkylation reaction network reported by Tsai et al. (208) is shown in Fig. 27. The typical reaction network of transalkylation over acidic zeolites consists of transalkylation of toluene and TMB (Route A); disproportionation of toluene (Route B); and disproportionation of TMB (Route C). Isomerization of TMB into MEB also takes place (Route D). The reaction network over metal-supported zeolite catalysts, such as Pt/MOR, includes also hydrogenation of all the aromatics compounds in the reaction system into naphthenes of various carbon numbers (Routes E and F). Dealkylation or ring-opening of naphthenes may also take place over acid catalysts (Route G)—especially at high temperatures. The reaction selectivity

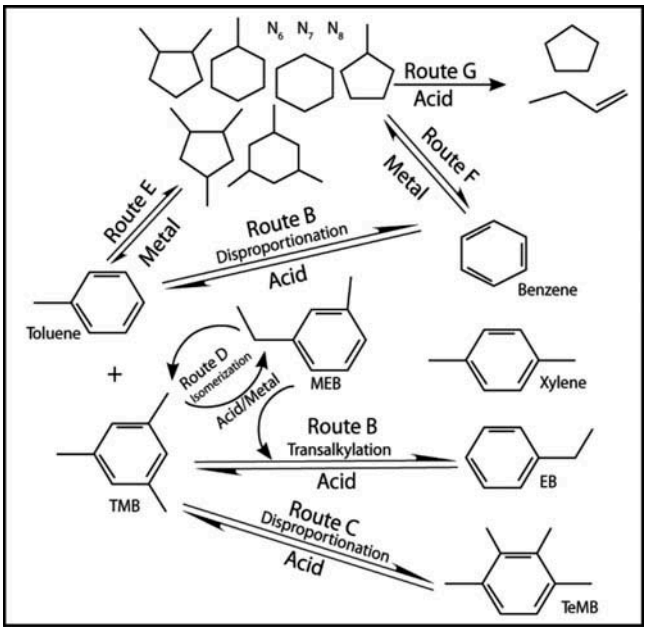

Figure 27: Reaction network of toluene-TMB transalkylation. Reproduced from Tsai et al. (208), Copyright 2007, with permission from Elsevier.

of transalkylation, disproportionation, and hydrogenation can be elucidated from the corresponding product ratios of xylene/benzene, xylene/TeMB and naphthene/aromatics (N/A).

A reaction scheme covering the most likely sequence of reactions during the conversion of heavy reformate without addition of toluene was proposed by Ali et al. (199) based on a detailed analysis of products obtained over four catalysts at various process conditions:

i. isomerization of TMBs and MEBs;
ii. transalkylation of TMBs with MEBs;
iii. disproportionation of MEBs;
iv. dealkylation of MEBs;
v. transalkylation of toluene and TMBs; and
vi. dealkylation of A_{10}.

With the exception of dealkylation reactions, all reactions are thermodynamically controlled. A linear relation between MEBs conversion (mainly dealkylation) and xylene yield from the transalkylation of heavy reformate was obtained, as shown in Fig. 28 (198). Hence, the dealkylation of MEBs, was postulated as the rate-determining step in the overall reaction scheme of xylene production from heavy reformate.

7.4. Catalysts for Conversion of Heavy Reformates to Xylenes

Transformation of heavy aromatics to xylenes was tested over zeolites such as MFI (209), NU-87 (200,210), and MWW (123), as well as large-pore zeolites

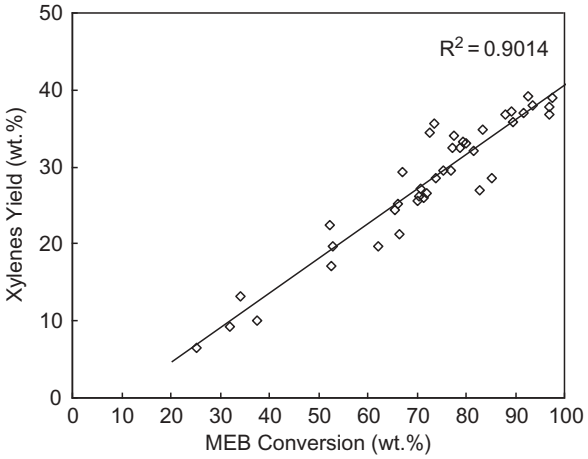

Figure 28: General correlation between MEB conversion and xylene yield. Reproduced from Ali et al. (198), Copyright 2011, with permission from Elsevier.

such as MTW (201), FAU (112), BEA (211,212), MOR (119,123,198,199), zeotype AFI (203), and LTL (111). These studies show that activity and selectivity towards the dealkylation and transalkylation of C_9^+ is significantly influenced by the pore dimensions and channel architecture of zeolite catalysts. The highest yield of xylenes was obtained with zeolites containing a combination of 10- and 12-rings (NU-87) or 12-rings (MOR). These types of zeolites were also reported to possess considerable concentrations of Brønsted acid sites promoting carbon-carbon bond scission (200).

A weak hydrogenation function is introduced in the zeolitic catalyst by incorporating suitable metal or a combination of metals (such as Ni, Pt, or Re) to promote desirable reactions such as hydrogenation of coke precursors, dealkylation of certain C_9+ compounds, saturation of cracking products, and their subsequent alkylation (203). Incorporation of Ni (200,207), Pt (212), Re (198), Ag, Bi, Cu, Pb (200), Cr, W, Co (213) into MOR has been reported .

Serra et al. (200,207) optimized conversion of heavy reformate streams into xylenes with zeolite catalysts using high-throughput experimentation techniques. The authors tested zeolites (MFI, IMF, MOR, NU-87, ITQ-23, BEA, and FAU) differing in channel types after impregnation with <1% of one of the seven metals (Re, Ni, Mo, Ga, Pt, La, and Bi). MFI and IMF were the most active in dealkylation of MEBs. With the increasing pore-size of zeolites, the dealkylation activity decreases. High TMBs conversion is achieved with 3D large-pore zeolites such as BEA or FAU. TMBs diffusion and the formation of the bimolecular transition states required for transalkylation of the methyl group from TMBs to toluene is favored inside the large pores. The best-performing zeolite structures (BEA or FAU) are reported to combine a high de-ethylation activity with a high trans-methylation activity.

The incorporation of the metal into zeolites increases the yield of xylenes obtained with all zeolites in the order Mo > Re > Ni > Ga > Bi > La > Pt (207). Addition of Mo, Re, and Ni resulted in the highest increase (up to 12%) of the xylene yield. The incorporation of Pt increased yield of cracking products (methane and C_3-C_4 alkanes), because of the improved hydrogenolysis and aromatic ring hydrogenation activity. MOR and NU-87 were the best performing zeolites in combination with Re and Mo providing a high activity and a medium-high selectivity (low ethyl benzene and $C_{11}+$ yield), although the dealkylation activity and selectivity were still lower than those observed for Re, Mo, Ga, or Ni over MFI.

The fabrication and modification of various 12-ring zeolites and their catalytic performance during transalkyaltion of heavy aromatics was investigated by Tsai et al. (201). In addition to investigation of metal-free zeolites, platinum (0.06-5 wt.%) was incorporated into zeolites BEA, FAU, MTW, and MOR with Si/Al ratio of 12.5, 14.0, 120.0, and 22.9, respectively, either by ion-exchange or impregnation methods. The catalytic performances were determined at 400°C using toluene and 1,3,5-TMB in the weight ratio of 2. The conversion

of TMBs was about 48% over BEA and MTW while it was only about 38% over MOR and FAU. The yields of xylenes followed the trend: MTW > BEA > MOR ≫ FAU while the stability followed the order: FAU > MTW > BEA ≫ MOR. Upon incorporating 5% Pt onto MOR, a marked increase in activity and stability was observed. However, it also resulted in deterioration of purity of aromatic products due to formation of some naphthenes which are co-boilers of aromatics. Improvement of catalyst performance of metal zeolites was demonstrated by combined procedures of metal incorporation, steaming, and continuous sulfurization treatments.

The conversion of heavy reformate into xylenes over a series of MOR-based catalysts was studied by Ali et al. (199). The results showed that MEBs were more reactive than TMBs. MOR catalysts with higher acid site concentration favored dealkylation of MEBs while MOR catalysts with lower acid site concentration favored disproportionation of TMBs. Combining a MOR catalyst with lower acid site concentration with MFI enhanced MEBs conversion and, in turn, xylenes yield. Tests with mixtures of 1,2,4-TMB/toluene and heavy reformate/toluene indicate that catalyst acid site concentration plays a key role in promoting desirable transalkylation reactions needed to enhance xylenes yield. The amount of coke formed increased with the acid site concentration of catalysts and more coke deposition was observed during conversion of heavy reformate than 1,2,4-TMB, which supports the conclusion that with the increasing molecular mass of reactants/products the zeolite catalysts are more prone to coking.

In another study, Ali et al. (198) investigated the effects of Mo content (3 vs. 1 wt.%), MOR content (80 vs. 67 wt.%; with alumina binder as balance), and metal type (Re vs. Mo) in the catalysts for dealkylation-transalkylation of heavy reformate. Higher Mo content enhanced the MEBs dealkylation as well as TMBs transalkylation, resulting in increased toluene and xylene formation. Higher MOR content in the catalyst had an insignificant effect on either MEBs or TMBs conversion. When compared with Mo-containing catalysts, Re-containing catalyst exhibited higher MEBs dealkylation and TMBs transalkylation, but also resulted in a higher hydrogen consumption and methane formation. A stability test (500 h) of the most active catalyst (3%Mo/67%MOR) showed that the initial high activity requires 2–3 days for stabilization, after which the catalyst performance remains stable.

7.5. Kinetic Modeling

Two approaches were used for kinetic modeling of heavy reformate conversion to xylenes: (i) using the data obtained by model compound studies; or (ii) using a simplified reaction network to describe heavy reformate conversion.

Waziri et al. (121) developed a kinetic model accounting for disproportionation of toluene, 1,2,4-TMB, and their transalkylation over MOR and MFI catalysts. A significant difference between the apparent

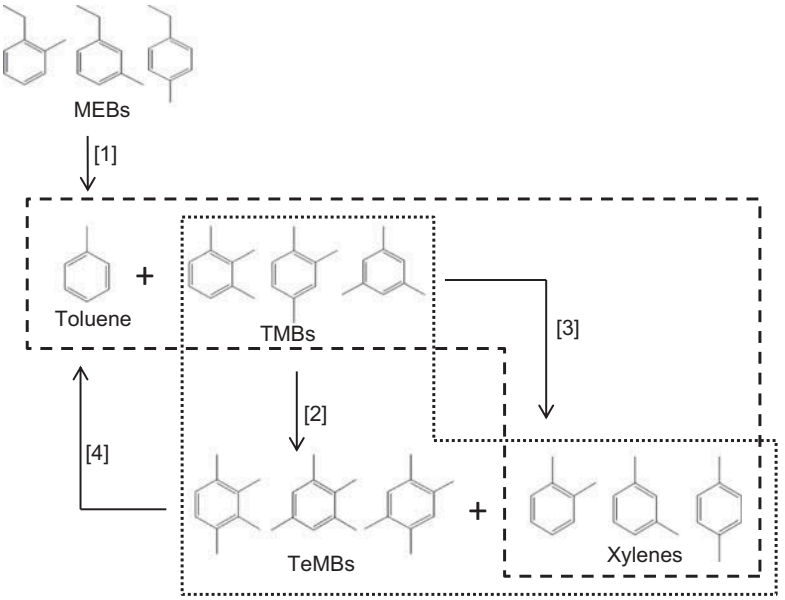

Figure 29: Simplified reaction network for kinetic modeling: (1) dealkylation of MEBs to form toluene; (2) disproportionation of TMBs to form TeMBs and xylenes; (3) transalkylation of toluene and TMBs to form xylenes; and (4) paring reaction of TeMBs to form toluene. Reproduced from Al-Mubaiyedh et al. (206), Copyright 2012, with permission from Elsevier.

activation energies over MOR (7–12 kJ/mol) and MFI (38–64 kJ/mol) for reactions involving 1,2,4-TMB was attributed to the increased reaction rate of bimolecular reaction over large pore MOR.

Kinetic modeling of the conversion of commercial heavy reformate into xylenes was recently published by Al-Mubaiyedh et al. (206). Catalysts containing equal amounts of MOR (Si/Al ratio: 18 or 180) and MFI (Si/Al ratio: 27) were used. A simplified reaction network (Fig. 29) was used for the kinetic modeling after justifying the simplification on the basis of reaction studies with model compounds. The order of apparent activation energies, $E_{paring} \gg E_{dealkylation} = E_{disproportionation} > E_{transalkylation}$, was ascribed to the relative size of the reactant molecules involved in these reactions.

8. EFFECTS OF ZEOLITE STRUCTURE AND MORPHOLOGY

Activity and selectivity of zeolites in transformations of aromatic hydrocarbons is generally controlled by two factors: (i) acidity of zeolites including its type (Brønsted or Lewis), concentration, location, and acid strength of acid sites; and (ii) textural properties as channel sizes (channel entrances), connectivity of channels, presence/absence of cages in the structure, size, and shape of the crystals. In addition, for any reaction, reactivity of substrate(s),

reaction conditions, experimental setup, type of reaction, mass transfer or thermodynamic considerations need to be taken into account. It becomes rather obvious that there are some parameters, which we are able to control (at least to some extent) while the others we cannot control at all. In addition, despite significant synthesis effort and improvements in understanding of synthetic mechanisms of zeolites, we are frequently not able to govern the size or shape of the crystals, and/or the acidity (location of acid sites in particular). Catalytic activities and selectivities obtained are the result of combination of these parameters with a limited possibility to separate them in model experiments.

8.1. Effect of the Structure of Zeolites

Transformations of aromatic hydrocarbons are catalyzed by both Brønsted and Lewis acid sites located either on the external surface of zeolite crystals or inside their channel systems. The external surface of zeolite crystals can be active in acid catalyzed reactions depending on the concentration of acid sites located there. Acid site concentration on the external surface accounts for about 1–3% of the total concentration varying with size and shape of the crystals. Despite the fact that these sites are easily accessible without any diffusion limitations in zeolite micropores, size of the entrances to the channel system controls accessibility of active sites due to *reactant shape selectivity*. Generally, zeolites with larger entrance windows exhibit higher activity. This can be clearly documented when increasing the number and length of alkyl group substituents on the benzene ring. The activity of zeolites in transalkylation reactions or heavy aromatic upgrading increases from 10- to 12-ring zeolites. Zeolites with 14-ring have been also investigated, however, the results are not completely clear and understood. Mostly, 12-ring zeolites with 3D channel systems are more active than 14-ring zeolites, plausibly due to their 1D channels architecture. This is related to much lower number of channel entrances in 1D 14-ring zeolites (usually these zeolites crystallize as tiny sheets with channel entrances parallel to the smallest crystal sizes). Simultaneously, channel entrances for 14- and 12-ring zeolites are rather comparable in the size.

In the case of 2D zeolites (e.g., 2D MFI, ITQ-2, MCM-56, and pillared MCM-36), the activity is mainly proportional to the zeolite external surface (in other words, to the concentration of acid sites on the external surface). The reactions proceed only to limited extent in the channel system of the 2D zeolites. This is similar to the performance of hierarchic zeolites, in which any modification or synthetic approach leads to the formation of mesopores increasing the concentration of surface acid sites.

Size of the zeolite channels controls primarily the activity of zeolites, and secondarily in some cases also the selectivity (*shape selectivity*).

In the case of reactions leading to xylenes, two effects need to be considered. To achieve high conversions of reactants larger channel sizes are preferred. This is of particular importance in the case of trimethylbenzene + toluene transalkylation or even reactions of heavier aromatics. On the other hand, selectivity to the mainly desired *p*-xylene is clearly related to *product shape selectivity*. This can be partly reached with 10-ring zeolites, more precisely with MFI or MEL zeolites, under optimized reaction conditions. *p*-Xylene selectivities higher than 90 % require modification of zeolite either with metal oxides or organics to annihilate the non-selective active sites on the external surface and to decrease/narrow (to plug partly) the channel entrances. These two factors can hardly be separated from each other. The necessary modification can be successful only for reactions involving reactants smaller than xylenes, it means in the case of toluene alkylation with methanol or toluene disproportionation. With bulkier reactants severe diffusion limitations exist due to the modification of zeolite external surface.

Hierarchical and 2D zeolites exhibit lower *para*-selectivity at the same conversion level than conventional zeolites. Certain diffusion length is required to separate individual di-alkyl benzene isomers according to their diffusion coefficients (usually *para* $\gg$ *ortho* > *meta*). This can be achieved with zeolite crystals of dimensions of about 0.5 μm and larger and particularly after modification of the external surface (*vide supra*). In contrast, investigations of 2D zeolites or hierarchical zeolites evidenced lower *para*-selectivity for xylenes or cymenes due to a preferential reaction on the external surface catalyzed by non-selective sites and substantially limited reaction and diffusion inside the zeolite channels.

As a consequence, high activities can be achieved with large pore zeolites affording easy penetration of reactants to active sites followed by fast removal of products, while sufficiently long diffusion paths are necessary to reach high *para*-selectivity.

8.2. Effect of Active Site Properties

Transformations of aromatic hydrocarbons are catalyzed by acid sites, the type of which (Brønsted or Lewis), their concentration, location (accessibility), distribution, and acid strength influence the resulting activity or selectivity.

Brønsted acid sites catalyze primarily alkylation, isomerization, disproportionation, and transalkylation reactions if they are accessible for reactants differing in kinetic diameter. Lewis acid sites also catalyze reactions of aromatic hydrocarbons, however, it is assumed that they are active also in undesired oligomerizations/polymerizations of short olefins forming precursors of coke. Thus, their contribution to faster deactivation is inferred.

The effect of acid strength seems to be of a less importance. Comparing FAU zeolite (Brønsted acid sites with lower strength) with MFI or even MOR (Brønsted acid sites with the highest strength) all these zeolites catalyze easily all transformations of aromatic hydrocarbons. The most important is location of these sites, e.g., Brønsted acid sites located in 8-rings of MOR do not contribute to the overall activity of zeolites.

While location of acid sites can govern their accessibility for reactants controlling in fact the reaction rate, their distribution (individual distance in other words) can be also of a significant importance. This is related to different reaction mechanisms. In the case of alkylation reactions, the accepted mechanism involves the interaction of olefin (alcohol) with bridging Si-OH-Al group forming alkoxy group attached to the framework oxygen. Aromatic hydrocarbon (e.g., benzene, toluene) then reacts with this alkoxy group without being chemisorbed. In such cases, close proximity of acid sites is not necessarily advantageous due to possible steric limitations.

Different situation might arise in the case of transalkylation reactions carried out inside the channel system. The activity of zeolites in transalkylation reactions increases with increasing concentration of acid sites (decreasing Si/Al ratio). Although one cannot expect the reaction of two Wheland complexes reacting with each other, experimental data show higher activity of zeolites with higher concentration of acid sites.

The open question is the possible change of acid strength of Brønsted sites when moving from conventional 3D zeolites to their 2D counterparts. More experimental and theoretical work in this area is needed, although it can be assumed that the changes (if any) are not too significant to increase (decrease) substantially the rate of respective reactions.

8.3. Stability of Zeolites against Coking

Both textural as well as chemical factors influence the time-on-stream stability of zeolites in transformations of aromatic hydrocarbons. In addition, modification with metals could also play an important role. It seems that decreasing crystal size as well as changing of texture to 2D zeolites has positive effect on conversion stability in aromatic hydrocarbon reactions. This is probably connected with the fact that coke is mostly formed inside of the channels decreasing the accessibility to active sites by their plugging. When micropore volume is decreased on purpose via decreasing size of the crystals and increasing ratio of external/internal surface, zeolite catalysts with higher time-on-stream stability against deactivation are prepared.

Modification with metal (usually up to 1–2 wt.%) is used in combination with hydrogen as carrier gas. The metals can activate hydrogen to accelerate hydrogenation of olefins and precursors of coke. This again positively influences the long-term stability of zeolites.

9. SUMMARY AND OUTLOOK

There are three important aspects of transformations of aromatic hydrocarbons over zeolites.

i. Aromatics transformations form a group of industrially highly important reactions (toluene disproportionation, xylene isomerization, benzene alkylations with ethylene (ethanol) or propylene, trimethylbenzene plus toluene transalkylation).

ii. Several reactions are of potential interest to be applied industrially, depending on the price of reactants (toluene alkylation with methanol, toluene alkylation with propylene, heavier aromatic upgrading).

iii. Utilization of these reactions to characterize the internal architecture of zeolites.

Ad i. large-scale production of ethylbenzene, cumene, and xylenes (*p*-xylene in particular) are key industrial productions, in which these intermediates are prepared for further application in polymer industry. There is no doubt that zeolites are indispensable at present as catalysts for these processes providing high activities, selectivities, and environmental acceptability in comparison with previously (sometimes still) used aluminum trichloride or solid phosphoric acid.

Ad ii. industrial implementation of new processes depends primarily on their economic output, which in the case of toluene alkylation with methanol depends mainly on the price of methanol and stability of high *p*-xylene selectivity. Recent efforts of companies in this domain are clear signal about the industrial potential of this reaction.

While polystyrene is an extremely important commodity, analogous polymer prepared from methylstyrene looks very promising. In such case, modified MFI zeolites can be used for *para*-selective toluene alkylation providing *p*-ethyltoluene selectivity higher than 90%.

More and more important will be the selective treatment of polyalkyl benzenes (heavier aromatics) mainly to xylenes. Selective dealkylation seems to be the appropriate way. In that case extra-large pore zeolites or 2D ones can be the zeolite catalysts of choice.

Ad iii. Different reactions of aromatic hydrocarbons were proposed and are still used as model reactions to characterize pore sizes, their connectivity and channel architecture in general. o-Ethyltoluene was proposed by Csicsery (214), followed by xylene isomerization (215). Recently, toluene alkylation with propylene (isopropyl alcohol) was frequently used providing information about the size and connectivity of channels based on the

selectivities to isopropyl vs. *n*-propyl toluenes and *p*-isopropyl toluene (8). When studying new zeolites with not yet fully characterized structure, these reactions can be of significant help in addition to the standard adsorption measurements with nitrogen and argon.

From the material point of view, the perspective directions can be characterized as follows. For non *para*-selective reactions, easy accessibility to active sites not restricted by diffusion issues is critically important. New large pore (or even extra-large pore) zeolites could be efficient, however, nanosized zeolites (having problems with handling in large quantities) or 2D zeolites could be preferred. Here, one can expect that economic criteria will be important, considering particularly easy synthesis (handling) and cheap raw materials (limited amounts if no templates at all).

Synthesis of zeolites and their analogues without alkali metal cations giving after calcination directly protonic forms would be definitely interesting as they would limit ion-exchange in high quantities and waste water treatment.

MFI, with the exception of MEL, is the only zeolite providing nice para-selectivity, especially after modification with metal oxides (*vide supra*). Other 10-ring zeolites including TUN, -SVR, or IMF are much less effective due to the large dimensions of pores 0.55 vs. 0.6 nm. Synthesis of new 10-ring (9-ring?) zeolite(s) with preferentially 3D channel system of about 0.5 nm channels could be very helpful.

FUNDING

S.S.K., S.A.A., and A.M.A acknowledge the support provided by King Abdulaziz City for Science and Technology through the Science and Technology Unit at King Fahd University of Petroleum and Minerals (KFUPM) for funding the work through project No. 11-PET2201-04 as part of the National Science, Technology and Innovation Plan. They also acknowledge the Ministry of Higher Education, Saudi Arabia for establishing the Center of Research Excellence in Petroleum Refining and Petrochemicals at KFUPM. N.Ž., D.K., and J.Č thank the Czech Science Foundation for the financial support (Centre of Excellence – P106/12/G015).

REFERENCES

[1] Franck, H.G.; Stadelhofer, J.W. *Industrial Aromatic Chemistry*, Springer: Berlin, 1988.

[2] Čejka, J.; van Bekkum, H.; Corma, A.; Schüth, F. (Eds.), *Introduction to Zeolite Science and Practise, Stud. Surf. Sci. Catal.*; 3rd ed.; vol. 168 Elsevier: Amsterdam, 2007.

[3] Perego, C.; Ingallina, P. Recent advances in the industrial alkylation of aromatics: new catalysts and new processes, *Catal. Today* **2002**, *73*, 3–22.

[4] Perego, C.; Ingallina, P. Combining alkylation and transalkylation for alkylaromatic production, *Green Chem*. **2004**, *6*, 274–279.

[5] Vermeiren, W.; Gilson, J.-P. Impact of zeolites on the petroleum and petrochemical industry, *Top. Catal*. ***2009***, *52*, 1131–1161.

[6] Martinez, C.; Corma, A. Inorganic molecular sieves: Preparation, modification and industrial application in catalytic processes, *Coord. Chem. Rev*. **2011**, *255*, 1558–1580.

[7] Bellussi, G.; Carati, A.; Rizzo, C.; Millini, R. New trends in the synthesis of crystalline microporous materials, *Catal. Sci. Technol*. **2012**, *3*, 833–857

[8] Čejka, J.; Wichterlová, B. Acid-catalyzed synthesis of mono- and dialkyl benzenes over zeolites: Active sites, zeolite topology, and reaction mechanisms, *Catal. Rev. Sci. Eng*. **2002**, *44*, 375–421.

[9] Lidback, A. IHS Aromatics Update, Presented at the PEMEX Petrochemicals Forum, Mexico City, 2012.

[10] Čejka, J.; Centi, G.; Perez-Pariente, J.; Roth, W.J. Zeolite-based materials for novel catalytic applications: Opportunities, perspectives and open problems, *Catal. Today* **2012**, *179*, 2–15.

[11] Roth, W.J.; Nachtigall, P.; Morris, R.E.; Čejka, J. Two-Dimensional Zeolites: Current Status and Perspectives, *Chem. Rev*. 114, **2014**, 4807–4837.

[12] Hong, S.B.; Min, H.-K.; Shin, Ch.-H.; Cox, P.A.; Warrender, S.J.; Wright, P.A. Synthesis, crystal structure, characterization, and catalytic properties of TNU-9, *J. Amer. Chem. Soc*. **2007**, *129*, 10870–10885.

[13] Benazzi, E.; Guth, J.-L.; Rouleau, L. IM-5 zeolite, a process for its preparation and catalytic applications thereof, *US Patent 6,136,290*, 2000.

[14] Zones, S.I.; Burton A.W.; Ong K. Molecular sieve SSZ-74 composition of matter and synthesis thereof, *WO 079038 A2*, 2007.

[15] Roth W.J.; Nachtigall P.; Morris R.E.; Wheatley P.S.; Seymour V.; Ashbrook S.E.; Chlubná P.; Grajciar L.; Položij M.; Zukal A.; Shvets O.V.; Čejka J. A family of zeolites with controlled pore size prepared using a top-down method, *Nat. Chem*. **2013**, *5*, 628–633.

[16] Serrano, D.P.; Aguado, J.; Escola, J.M.; Rodríguez, J.M.; Peral, A. Hierarchical zeolites with enhanced textural and catalytic properties synthesized from organofunctionalized seeds, *Chem. Mater*. **2006**, *18*, 2462–2464.

[17] Tao, Y.; Kanoh, H.; Abrams, L.; Kaneko, K. Mesopore-modified zeolites: Preparation, characterization, and applications, *Chem. Rev*. **2006**, *106*, 896–910.

[18] Pérez-Ramirez, J.; Christensen, C.H.; Egeblad, K.; Christensen, C.H.; Groen, J.C. Hierarchical zeolites: enhanced utilisation of microporous crystals in catalysis by advances in materials design, *Chem. Soc. Rev*. **2008**, *37*, 2530–2542.

[19] Choi, M.; Na, K.; Kim, J.; Sakamto, Y.; Terasaki, O.; Ryoo, R. Stable single-unit-cell nanosheets of zeolite MFI as active and long-lived catalysts, *Nature* **2009**, *461*, 246–250.

[20] Roth, W.J.; Čejka, J. Two-dimensional zeolites: dream or reality? *Catal. Sci. Technol*. **2011**, *1*, 43–53.

[21] Čejka, J.; Mintova, S. Perspectives of micro/mesoporous composites in catalysis, *Catal. Rev. Sci. Eng*. **2007**, *49*, 457–509.

[22] Kresge, C.T.; Roth, W.J. The discovery of mesoporous molecular sieves from the twenty year perspective. *Chem. Soc. Rev*. **2013, *42***, 3663–3670.

[23] Perego, C.; Millini, R. Porous materials in catalysis: challenges for mesoporous materials, *Chem. Soc. Rev*. **2013**, *42*, 3956–3976.

[24] Kubů, M.; Zones, S.I.; Čejka. J. TUN, IMF and -SVR Zeolites; Synthesis, properties and acidity, *Top Catal*. **2010**, *53*, 1330–1339.

[25] Corma, A.; Triguero J.-M.; Valencia, S.; Benazzi, E.; Lacombe, S. IM-5: A highly thermal and hydrothermal shape-selective cracking zeolite, *J. Catal*. **2002**, *206*, 125–133.

[26] Baerlocher, Ch.; Gramm, F.; Massuger, L.; McCusker, L.B.; He, Z.; Hovmoeller, S.; Zou, X. Structure of the polycrystalline zeolite catalyst IM-5 solved by enhanced charge flipping, *Science* **2007**, *315*, 1113–1116.

[27] Baerlocher, C.; Weber, T.; McCusker, L.B.; Palatinus, L.; Zones, S.I. Unraveling the perplexing structure of the zeolite SSZ-57, *Science* **2011**, *33*, 1134–1137.

[28] Zones, S.I.; Ruan, J.; Elomari, S.; Terasaki, O.; Chen, C.Y.; Corma, A. Studies on zeolite SSZ-57: A structural enigma, *Solid State Sci*. **2011**, *13*, 706–713.

[29] Dorset, D.L.; Weston, S.C.; Dhingra, S.S. Crystal structure of zeolite MCM-68: A new three-dimensional framework with large pores, *J. Phys. Chem. B* **2006**, *110*, 2045–2050.

[30] Wagner, P.; Nakagawa, Y.; Lee, G.S.; Davis, M.E.; Elomari, S.; Medrud, R.C.; Zones, S.I. Guest/host relationships in the synthesis of the novel cage-based zeolites SSZ-35, SSZ-36, and SSZ-39, *J. Amer. Chem. Soc*. **2000**, *122*, 263–273.

[31] Shibata, T.; Suzuki, S.; Kawagoe, H.; Komura, K.; Kubota, Y.; Sugi, Y.; Kim, J.-H.; Seo, G. Synthetic investigation on MCM-68 zeolite with MSE topology and its application for shape-selective alkylation of biphenol, *Microporous Mesoporous Mater*. **2008**, *116*, 216–226.

[32] Corma, A.; Díaz Cabañas, M.J.; Rey, F.; Nicolooulas, S.; Boulahya, K. ITQ-15: The first ultralarge pore zeolite with a bi-directional pore system formed by intersecting 14- and 12-ring channels, and its catalytic implications, *Chem. Commun*. **2004**, 1356–1357.

[33] Shamzhy, M.V.; Shvets, O.V.; Opanasenko, M.V.; Kurfiřtová, L.; Kubička, D.; Čejka, J. Extra-large-pore zeolites with UTL topology: Control of the catalytic activity by variation in the nature of the active sites, *ChemCatChem* **2013**, *5*, 1891–1898.

[34] Corma, A; Díaz Cabañas, M.J.; Jorda, J.L.; Martinez, C.; Moliner, M. High-throughput synthesis and catalytic properties of a molecular sieve with 18-and 10-member rings, *Nature* **2006**, *443*, 842–845.

[35] Moliner, M; Díaz Cabañas, MJ; Fornes, V; Martinez, C; Corma, A. Synthesis methodology, stability, acidity, and catalytic behavior of the 18x10 member ring pores ITQ-33 zeolite, *J. Catal*. **2008**, *254*, 101–109.

[36] Shamzhy, M.; Shvets, O.V.; Opanasenko, M.V.; Procházková, D.; Nachtigall, P.; Čejka, J. The effect of synthesis conditions and nature of heteroelement on acidic properties of isomorphously substituted UTL zeolites, *Adv. Porous Mater*. **2013**, *1*, 103–113.

[37] Shamzhy, M.V.; Shvets, O.V.; Opanasenko, M.V.; Yaremov, P.S.; Sarkisyan, L.G.; Chlubná, P.; Zukal, A.; Marthala, V.R.; Hartmann, M.; Čejka, J. Synthesis of isomorphously substituted extra-large pore UTL zeolites, *J. Mater. Chem. A* **2012**, *22*, 15793–15803.

[38] Žilková, N.; Shamzhy, M.; Shvets, O.V.; Čejka, J. Transformation of aromatic hydrocarbons over isomorphously substituted UTL: Comparison with large and medium pore zeolites, *Catal. Today* **2013**, *204*, 22–29.

[39] Jiang, Xu, Y; Cheng, P.; Sun, Q.M.; Yu, J.H.; Corma, A. investigation of extra-large pore zeolite synthesis by a high-throughput approach, *Chem. Mater*. **2011**, *23*, 4709–4715.

[40] Koo, J.-B.; Jiang, N.; Saravanamurugan, S.; Bejblová, M.; Musilová, Z.; Čejka, J.; Park, S.-E. Direct synthesis of carbon-templating mesoporous ZSM-5 using microwave heating, *J. Catal*. **2010**, *276*, 327–334.

[41] Choi, M.; Cho, H.S.; Srivastava, R.; Venkatesan, C.; Choi, D.-H.; Ryoo, R. Amphiphilic organosilane-directed synthesis of crystalline zeolite with tunable mesoporosity, *Nat. Mater*. **2006**, *5*, 718–723.

[42] Choi, M.; Srivastava, R.; Ryoo, R. Organosilane surfactant-directed synthesis of mesoporous aluminophosphates constructed with crystalline microporous frameworks, *Chem. Commun*. **2006**, 4380–4382.

[43] Serrano, D.P.; García, R.A.; Vicente, G.; Linares, M.; Procházková, D.; Čejka, J. Acidic and catalytic properties of hierarchical zeolites and hybrid ordered mesoporous materials assembled from MFI protozeolitic units, *J. Catal*. **2011**, *279*, 366–380.

[44] Morris, R.E.; James, S.L. Solventless synthesis of zeolites, *Angew. Chem. Int. Ed*. **2013**, *52*, 2163–2165.

[45] Ramos, F.S.O.; De Pietre, M.K.; Pastore, H.O. Lamellar zeolites: an oxymoron? *RSC Adv*. **2013**, 3, 2084–2111.

[46] Puppe, L.; Weisser, J. (Bayer Aktiengesellschaft) Crystalline aluminosilicate PSH-3 and its process of preparation, U.S. Patent, 4,439,409, March 27, 1984.

[47] Zones, S.I. (Chevron Research and Technology Company), New zeolite SSZ-25, EP0231860 January 27, 1987 (filing date).

[48] Bellussi, G.; Perego, G.; Clerici, M.G.; Giusti, A. (ENIRICERCHE S.p.A.) Synthetic, crystalline, porous material containing oxides of silicon and boron, EP0293032, November 5, 1988 (filing date).

[49] Rubin, M.K.; Chu, P. (Mobil Oil Corp.), Composition of synthetic porous crystalline material, its synthesis and use, U.S. Patent, 4,954,325, September 4, 1990.

[50] Millini, R.; Perego, G.; Parker Jr., W.O.; Bellussi, G.; Carluccio, L. Layered structure of ERB-1 microporous borosilicate precursor and its intercalation properties towards polar-molecules. *Microporous Mater*. **1995**, *4*, 221–230.

[51] Na, K.; Park, W.; Seo, Y.; Ryoo, R. Disordered assembly of MFI zeolite nanosheets with a large volume of intersheet mesopores, *Chem. Mater*. **2011**, *23*, 1273–1279.

[52] Corma, A.; Fornes, V.; Pergher, S.B.; Maesen, T.L.M.; Buglass, J.G. Delaminated zeolite precursors as selective acidic catalysts, *Nature* **1998**, *396*, 353–356.

[53] Roth, W.J.; Chlubna, P.; Kubů, M.; Vitvarová, D. Swelling of MCM-56 and MCM-22P with a new medium — surfactant-tetramethylammonium hydroxide mixtures, *Catal. Today* **2013**, *204*, 8–14.

[54] Chlubná, P.; Roth, W.J.; Greer, H.F.; Zhou, W.Z.; Shvets, O.; Zukal, A.; Čejka, J.; Morris, R. E. 3D to 2D routes to ultrathin and expanded zeolitic materials, *Chem. Mater*. **2013**, *25*, 542–547.

[55] Kubů, M.; Roth, W.J.; Greer, H.F.; Zhou, W.; Morris, R.E.; Přech, J.; Čejka, J. A New family of two-dimensional zeolites prepared from the intermediate layered precursor IPC-3P obtained during the synthesis of TUN zeolite, *Chem. Eur. J*. **2013**, *19*, 13937–13945.

[56] Alario, F.; Giusnet, M. In: *Zeolites for Cleaner Technologies*, Guisnet, M.; Gilson, J. P., Eds., Imperial College Press, London, 2002, pp. 189–207.

[57] Perego, C.; Pollesel, P. Advances in aromatics processing using zeolite catalysts. In: *Advances in Nanoporous materials*, Ernst, S., Ed., **2009**, *1*, 97–149.

[58] Al-Khattaf, S.; Ali, M.A.; Čejka, J. Recent development in transformations of aromatic hydrocarbons over zeolites. In: Ze*olites and Catalysis Synthesis, Reactions and Applications*, Čejka, J.; Corma, A.; Zones, S.; Eds., Wiley-VCH, Weinheim, 2010, pp. 623–648.

[59] Fechete, I.; Wang, Y.; Védrine, J.C. The past, present and future of heterogeneous catalysis, *Catal. Today*, **2012**, *189*, 2–27.

[60] Das, J.; Halgeri, A. Design and development of zeolite-based catalytic processes for aromatics production, *Catal. Surv. Asia* **2003**, *7*, 3–9.

[61] Wang, K.; Wang, X.; Li, G. A study on acid sites related to activity of nanoscale ZSM-5 in toluene disproportionation, *Catal. Commun*. **2007**, *8*, 324–328.

[62] Wang, K.; Wang, X.; Li, G. Quantitatively study acid strength distribution on nanoscale ZSM-5, *Microporous Mesoporous Mater*. **2006**, *94*, 325–329.

[63] Zheng, S.; Heydenrych, H.R.; Roeger, H.P.; Jentys, A.; Lercher, J.A. On the enhanced selectivity of HZSM-5 modified by chemical liquid deposition, *Top. Catal*, **2003**, *22*, 101–106.

[64] Teng, H.; Wang, J.; Ren, X.; Chen, D. Disproportionation of toluene by modified ZSM-5 zeolite catalysts with high shape-selectivity prepared using chemical liquid deposition with tetraethyl orthosilicate, *Chin. J. Chem. Eng*. **2011**, *19*, 292–298.

[65] Zhu, Z.; Xie, Z.; Chen, Q.; Kong, D.; Li, W.; Yang, W.; Li, C. Chemical liquid deposition with polysiloxane of ZSM-5 and its effect on acidity and catalytic properties, *Microporous Mesoporous Mater*. **2007**, *101*, 169–175.

[66] Nishiyama, N.; Miyamoto, M.; Kamei, T.; Egashira, Y.; Ueyama, K. Selective formation of p-xylene over single crystal-like zeolite composite, *Stud. Surf. Sci. Catal*. **2006**, *162*, 275–282.

[67] Teng, H.; Wang, J.; Chen, D.; Liu, P.; Wang, X. Silicalite-1 membrane on millimeter-sized HZSM-5 zeolite extrudates: Controllable synthesis and catalytic behavior in toluene disproportionation, *J. Memb. Sci*. **2011**, *381*, 197–203.

[68] Zheng, S.; Jentys, A.; Lercher, J.A. On the enhanced para-selectivity of HZSM-5 modified by antimony oxide, *J. Catal*. **2003**, *219*, 310–319.

[69] Al-Khattaf, S.; Ali, M.A.; Al-Amer, A. Effect of reaction pressure and carrier gas on toluene disproportionation over molybdenum/ZSM-5 catalyst, *Energy Fuels* **2008**, *22*, 243–249.

[70] Musilová, Z.; Žilková, N.; Park, S.E.; Čejka, J. Aromatic transformations over mesoporous ZSM-5: Advantages and disadvantages, *Top. Catal*. **2010**, *53*, 1457–1469.

[71] Jo, C.; Ryoo, R.; Žilková, N.; Vitvarová, D.; Čejka, J. The effect of MFI zeolite lamellar and related mesostructures on toluene disproportionation and alkylation, *Catal. Sci. Technol*. **2013**, *3*, 2119–2129.

[72] Na, K.; Jo, C.; Kim, J.; Cho, K. Jung, J.; Seo, Y.; Messinger, R. J.; Chmelka, B.F. Ryoo, R. Directing zeolite structures into hierarchically nanoporous architectures, *Science* **2011**, *333*, 328–332.

[73] Park, W.; Yu, D.; Na, K.; Jelfs, K.E.; Slater, B.; Sakamoto, Y.; Ryoo, R. Hierarchically structure-directing effect of multi-ammonium surfactants for the generation of MFI zeolite nanosheets, *Chem. Mater*. **2011**, *23*, 5131–5137.

[74] Mitra, B.; Chakraborty, J.P.; Kunzru, D. Disproportionation of toluene on ZSM-5 washcoated monoliths, *AIChE J*. **2011**, *57*, 3480–3495.

[75] Mitra, B.; Kunzru, D. Disproportionation of toluene on monoliths washcoated with metal oxide modified ZSM-5, *Catal. Lett*. **2011**, *141*, 1569–1579.

[76] Yang, C.; Zhao, T.; Zhou, H. Molecular simulation on the diffusion characteristics of toluene disproportionation reactants and products in the channel of ZSM series zeolites, *Acta Petrolei Sinica*. **2006**, *22*, 14–19.

[77] Žilková, N.; Bejblová, M.; Gil, B.; Zones, S.I.; Burton, A. W.; Chen, C.; Musilová, Z.; Košová, G.; Čejka, J. The role of the zeolite channel architecture and acidity on the activity and selectivity in aromatic transformations: The effect of zeolite cages in SSZ-35 zeolite, *J. Catal*. **2009**, *266*(1), 79–91.

[78] Odedairo, T.; Balasamy, R.J.; Al-Khattaf, S. Toluene disproportionation and methylation over zeolites TNU-9, SSZ-33, ZSM-5, and mordenite using different reactor systems, *Ind. Eng. Chem. Res*. **2011**, *50*, 3169–3183.

[79] Al-Khattaf, S.; Musilová, Z.; Ali, M.A.; Čejka, J. Comparison of activity and selectivity of SSZ-33 based catalyst with other zeolites in toluene disproportionation, *Top. Catal*. **2009**, *52* 140–147.

[80] Baduraig. A.; Odedairo, T.; Al-Khattaf, S. Disproportionation and methylation of toluene with methanol over zeolite catalysts, *Top. Catal*. **2010**, *53*, 1446–1456.

[81] Kubů, M.; Žilková, N.; Čejka, J. Post-synthesis modification of TUN zeolite: Textural, acidic and catalytic properties, *Catal. Today*, **2011**, *168*, 63–70.

[82] Park, S.H.; Rhee, H.K. Catalytic properties of zeolites MCM-22 and NU-87 in disproportionation of toluene, *React. Kinet. Catal. Lett*. **2003**, *78*, 81–89.

[83] Miltenburg, A.; Pawlesa, J.; Bouzga, A.M.; Žilková, N.; Čejka, J.; Stöcker, M. Alkaline modification of MCM-22 to a 3D interconnected pore system and its application in toluene disproportionation and alkylation, *Top. Catal*. **2009**, *52*, 1190–1202.

[84] Ji, Y.; Zhang, B.; Xu, L.; Wu, H.; Peng, H.; Chen, L.; Liu, Y.; Wu, P. Core/shell-structured al-MWW/B-MWW zeolites for shape-selective toluene disproportionation to para-xylene, *J. Catal*. **2011**, *283*, 168–177.

[85] Jan, D.; Barger, P. Processes on industrial C-C bond formation, In: *Zeolites in Industrial Separation and Catalysis*, Kulprathipanja, S.; Ed., Wiley-VCH, Weinheim, 2010, pp. 505–528.

[86] Dave, D. New routes to Styrene and para-Xylene, IHS Chemical Process Economics Program, *PEP Report 289*, IHS, Englewood, CO, October 2013.

[87] Dumitriu, E.; Fechete, I.; Caullet, P.; Kessler, H.; Hulea, V.; Chelaru, C.; Hulea, T.; Bourdon, X. Conversion of aromatic hydrocarbons over MCM-22 and MCM-36 catalysts, *Stud. Surf. Sci. Catal*. **2002**, *142*, 951–958.

[88] Breen, J.P.; Burch, R.; Kulkarni, M.; McLaughlin, D.; Collier, P.J.; Golunski, S.E. Improved selectivity in the toluene alkylation reaction through understanding and optimizing the process variables, *App. Catal. A* **2007**, *316*, 53–60

[89] Breen, J.; Burch, R.; Kulkarni, M.; Collier, P.; Golunski, S. Enhanced para-xylene selectivity in the toluene alkylation reaction at ultralow contact time, *J. Amer. Chem. Soc*. **2005**, *127*, 5020–5021.

[90] Das, J.; Char, P.R.; Halgeri A.A.; Mewada, R.K.; Subrahmanyam, N. Kinetics of toluene methylation over silica modified H-ZSM-5 zeolites, *Ind. J. Chem. Technol*. **2002**, *9*, 334–240.

[91] Zou, W.; Yang D, Zhu, Z, Kong, D.; Chen, Q.; Gao, Z. Methylation of toluene with methanol over metal oxide-modified H-ZSM-5 catalysts, *Chin. J. Catal*. **2005**, *26*, 470–474.

[92] Zhang, L.; Gao, J.; Hu, J.; Li, W.; Wang, J. Lanthanum oxides-improved catalytic performance of ZSM-5 in toluene alkylation with methanol, *Catal. Lett*. **2009**, *130*, 355–361.

[93] Zhao, Y.; Wu, H,; Tan, W.; Zhang, M.; Liu, M.; Song, C.; Wang, X.; Guo, X. Effect of metal modification of HZSM-5 on catalyst stability in the shape-selective methylation of toluene, *Catal. Today*. **2010**, *156*, 69–73.

[94] Zhao, Y.; Tan, W.; Wu, H.; Zhang, A.; Liu, M.; Li, G.; Wang, X.; Song, C.; Guo, X. Effect of Pt on stability of nano-scale ZSM-5 catalyst for toluene alkylation with methanol into p-xylene, *Catal. Today* **2011**, *160*, 179–83.

[95] Aboul-Gheit, A.K.; Aboul-Fotouh, S.M.; Emam, E.A.; Ahmed, S.M. Catalytic para-xylene maximization. Part V. Toluene methylation with methanol and disproportionation of toluene using Pt/ZSM-5 and Pt/mordenite catalysts, *J. Chin. Chem. Soc*. **2004**, *51*, 817–826.

[96] Aboul-Gheit, A.K.; Hanafi, S.A, Ghoneim, S.A. Para-xylene maximization, Part VI: Shape-selective platinum-promoted methylation of toluene, *Petrol. Sci. Technol*. **2010**, *28*, 248–61.

[97] Aboul-Gheit, A. K.; Aboul-Enein, A.A.; Awadallah, A.E.; Ghoneim, S.A.; Emam, E.A. Para-xylene maximization. Part VIII: Promotion of H-ZSM-5 zeolite by Pt and HF doping for use as catalysts in toluene alkylation with methanol, *Chin. J. Catal*. **2010**, *31*, 1209–1216.

[98] Svelle, S.; Visur, M.; Olsbye, U.; Bjørgen, M. Mechanistic aspects of the zeolite catalyzed methylation of alkenes and aromatics with methanol: A review, *Top. Catal*. **2011**, *54*, 897–906.

[99] Al-Khattaf, S, Rabiu, S.; Tukur N.M.; Alnaizy, R. Kinetics of toluene methylation over USY-zeolite catalyst in a riser simulator, *Chem. Eng. J*. **2008**, *139*, 622–630.

[100] Rabiu, S.; Al-Khattaf, S. Kinetics of toluene methylation over ZSM-5 catalyst in a riser simulator, *Ind. Eng. Chem. Res*. **2008**, *47*, 39–47.

[101] Alabi, W.; Atanda, L.; Jermy, R.; Al-Khattaf, S. Kinetics of toluene alkylation with methanol catalyzed by pure and hybridized HZSM-5 catalysts, *Chem. Eng. J*. **2012**, *195–196*, 276–288.

[102] Joshi, P.N.; Niphadkar, P.S.; Desai, P.A.; Patil, R.; Bokade, V.V. Toluene alkylation to selective formation of p-xylene over co-crystalline ZSM-12/ZSM-5 catalyst, *J. Nat. Gas Chem*. **2007**, *16*, 37–41.

[103] Zhao, T.; Zhang, H.; Li, F.; Yang, C.; Zong, B. Synthesis and characterization of ZSM-5/β co-crystalline zeolite, *J. Nat. Gas Chem*. **2005**, *14*, 95–100.

[104] Miyamoto, M.; Kamei, T.; Nishiyama, N.; Egashira, Y.; Ueyama, K. Single crystals ZSM-5/silicalite composites, *Adv. Mater*. **2005**, *17*, 1985–1988.

[105] Van Vu D.; Miyamoto, M.; Nishiyama N.; Egashira Y.; Ueyama K. Selective formation of para-xylene over H-ZSM-5 coated with polycrystalline silicalite crystals, *J. Catal*. **2006**, *243*, 389–94.

[106] Van Vu, D.; Miyamoto, M.; Nishiyama, N.; Egashira, Y.; Ueyama, K. Morphology control of silicalite/HZSM-5 composite catalysts for the formation of para-xylene, *Catal. Lett*. **2009**, *127*, 233–8.

[107] Van Vu, D.; Miyamoto, M.; Nishiyama, N.; Ichikawa, S.; Egashira, Y.; Ueyama, K. Catalytic activities and structures of silicalite-1/H-ZSM–5 zeolite composites, *Microporous Mesoporous Mater*. **2008**, *115*, 106–112.

[108] Zhu, Z.; Chen, Q.; Xie, Z.; Yang, W.; Li, C. The roles of acidity and structure of zeolite for catalyzing toluene alkylation with methanol to xylene, *Microporous Mesoporous Mater*. **2006**, *88*, 16–19.

[109] Al-Khattaf, S.; Akhtar, M. N.; Odedairo, T.; Aitani, A.; Tukur, N. M.; Kubů, M.; Musilová-Pavlačková, Z.; Čejka, J. Catalytic transformation of methyl benzenes over zeolite catalysts, *Appl. Catal. A*. **2011**, *394*, 176–190.

[110] Millini, R.; Perego, C. The role of molecular mechanics and dynamics methods in the development of zeolite catalytic processes, *Top. Catal*. **2009**, *52*, 42–66.

[111] Čejka, J.; Kotrla, J.; Krejčí, A. Disproportionation of trimethyl benzenes over large pore zeolites: Catalytic and adsorption study, *Appl. Catal. A*. **2004**, *277*, 191–199.

[112] Atias, J. A.; Tonetto, G.; De Lasa, H. Catalytic conversion of 1,2,4-trimethylbenzene in a CREC riser simulator. A heterogeneous model with adsorption and reaction phenomena, *Ind. Eng. Chem. Res*. **2003**, *42*, 4162–4173.

[113] Al-Khattaf, S. Effect of Y- Zeolite acidity on 1,2,4 trimethyl benzenes reactions, *Energy Fuels* **2007**, *21*, 646–652.

[114] Sullivan, R.F.; Egan, C.J.; Langlois, G.E.; Sieg, R.P. A new reaction that occurs in the hydrocracking of certain aromatic hydrocarbons, *J. Amer. Chem. Soc*. **1961**, *83*, 1156–1160.

[115] Al-Khattaf, S.; Tukur, N.M.; Al-Amer, A.; Al-Mubaiyedh, U.A. Catalytic transformation of C7-C9 methyl benzenes over USY-based FCC zeolite catalyst, *Appl. Catal. A*. **2006**, *305*, 21–31.

[116] Tukur, N. M.; Al-Khattaf, S. Catalytic transformation of 1,3,5-trimethylbenzene over a USY zeolite catalyst, *Energy Fuels* **2007**, *21*, 2499–2508.

[117] Kollár, M.; Kolev, I.; Mihályi, M.R.; Mavrodinova, V. Transformations of alkyl aromatics over delaminated MCM-22 zeolites and their composites with mesoporous MCM-41 silicate, *Appl. Catal. A*. **2011**, *393*, 59–70.

[118] Odedairo, T.; Balasamy, R.J.; Al-Khattaf, S. Aromatic transformations over aluminosilicate micro/mesoporous composite materials, *Catal. Sci. Tech*. **2012**, *2*, 1275–1286.

[119] Krejčí, A.; Al-Khattaf, S.; Ali, M.A.; Bejblová, M.; Čejka, J. Transalkylation of toluene with trimethylbenzenes over large-pore zeolites, *Appl. Catal. A*. **2010**, *377*, 99–106.

[120] Aitani, A. M.; Ali, A. M.; Waziri, S. M.; Al-Khattaf, S. Production of xylenes from toluene and 1,2,4-trimethylbenzene over ZSM-5 and mordenite catalysts in a fluidized-bed reactor, *Chem. Eng. Tech*. **2010**, *33*, 1193–1202.

[121] Waziri, S.M.; Aitani, A.M.; Al-Khattaf, S. Transformation of toluene and 1,2,4-trimethylbenzene over ZSM-5 and mordenite catalysts: A comprehensive kinetic model with reversibility, *Ind. Eng. Chem. Res*. **2010**, *49*, 6376–6387.

[122] Al-Khattaf, S.; Tukur, N.M.; Al-Amer, A. 1,2,4-trimethylbenzene transformation reaction compared with its transalkylation reaction with toluene over USY zeolite catalyst, *Ind. Eng. Chem. Res*. **2007**, *46*, 4459–4467.

[123] Tsai T.; Liu S.; Wang I. Metal supported zeolite for heavy aromatics transalkylation process, *Catal. Surv. Asia*. **2009**, *13*, 94–103.

[124] Chao P.; Lin H.; Chen C.; Wang P.; Chen Y.; Sei H.; Tsai T. Precoking selectivation for improving benzene product purity in heavy aromatics transalkylation, *Appl. Catal. A* **2008**, *335*, 15–19.

[125] Tsai, S.; Chao, P.; Wang, I.; Tsai, T. Dual-bed catalyst system for improving product purity and catalytic stability in alkylbenzene transalkylation, *Appl. Catal. A* **2010**, *385*, 73–79.

[126] Tsai, S.; Chen, C.; Tsai, T. Base treated H-mordenite as stable catalyst in alkylbenzene transalkylation, *Green Chem*. **2009**, *11*, 1349–1356.

[127] Fechete, I.; Caullet, P.; Dumitriu, E.; Hulea, V.; Kessler, H. Study of the conversion of aromatic hydrocarbons on EMT-type zeolite influence of the partial substitution of al by Ga, *Appl. Catal. A* **2005**, *280*, 245–254.

[128] Bauer, J.E.; Xu, F.; Bogdan, P.L.; Gajda, G.J. Industrial isomerization. In: *Zeolites in Industrial Separation and Catalysis*, Kulprathipanja, S., Ed.; Wiley-VCH, Weinheim, 2010, 479–504.

[129] Llopis, F.; Sastre, G.; Corma, A. Xylene isomerization and aromatic alkylation in zeolites NU-87, SSZ-33, β, and ZSM-5: molecular dynamics and catalytic studies, *J. Catal*. **2004**, *227*, 227–241.

[130] Traa, Y.; Sealy, S.; Weitkamp, J. Characterization of the pore size of molecular sieves using molecular probes, *Mol. Sieves* **2007**, *5*, 103–154.

[131] Al-Khattaf, S.; Iliyas, A.; Al-Amer, A.; Inui, T. The effect of Y-zeolite acidity on m-xylene transformation reactions, *J. Mol. Catal. A* **2004**, *225*, 117–124.

[132] Iliyas, A.; Al-Khattaf, S. Gas phase isomerization of meta-xylene over USY zeolite in a riser simulator: a simplified kinetic model, *Chem. Eng. J*. **2005**, *107*, 127–132.

[133] Zheng, S.; Jentys, A.; Lercher, J.A. Xylene isomerization with surface-modified HZSM-5 zeolite catalysts: An in situ IR study. *J. Catal*. **2006**, *241*, 304–311.

[134] Demuth, T.; Raybaud, P.; Lacombe, S.; Toulhoat, H. Effects of zeolite pore sizes on the mechanism and selectivity of xylene disproportionation - A DFT study, *J. Catal*. **2004**, *222*, 323–337.

[135] Bauer, F.; Bilz, E.; Freyer, A. C-14 studies in xylene isomerization on modified HZSM-5, *Appl. Catal. A* **2005**, *289*, 2–9.

[136] Laforge S.; Martin D.; Paillaud, J.L.; Guisnet, M. m-Xylene transformation over H-MCM-22 zeolite, *J. Catal*. **2003**, *220*, 92–103.

[137] Laforge, S.; Martin, D.; Guisnet, M. m-Xylene transformation over H-MCM-22 zeolite. 2. Method for determining the catalytic role of the three different pore systems, *Microporous Mesoporous Mater*. **2004**, *67*, 235–244.

[138] Goergen, S.; Fayad, E.; Laforge, S.; Magnoux, P.; Rouleau, L.; Patarin, J. Synthesis of layered MCM-22(P) in the presence of hexamethonium cations and

its transformation into EUO- and MWW-type zeolites, *J. Porous Mater*. **2011**, *18*, 639–650.

[139] Gil, B.; Makowski, W.; Marszalek, B.; Roth, W.J.; Kubů, M.; Čejka, J.; Olejniczak, Z. High acidity unilamellar zeolite MCM-56 and its pillared and delaminated derivatives, *Dalton Trans*. doi:10.1039/C4DT00130C.

[140] Mihályi, R.M.; Kollár, M.; Király, P.; Karoly, Z.; Mavrodinova, V. Effect of extra-framework al formed by successive steaming and acid leaching of zeolite MCM-22 on its structure and catalytic performance, *App. Catal. A* **2012**, *417–418*, 76–86

[141] Tukur, N.; Al-Khattaf, S. Comparison studies of xylene isomerization and disproportionation reactions between SSZ-33, TNU-9, mordenite and ZSM-5 zeolite catalysts, *Chem. Eng. J*. **2011**, *166*, 348–357.

[142] Min, H.; Cha, S.H.; Hong, S.B. Mechanistic insights into the zeolite-catalyzed isomerization and disproportionation of m-xlene, *ACS Catal*. **2012**, *2*, 971–981.

[143] Toch, K.; Thybaut, J.W.; Vandegehuchte, B.D.; Narasimhan, C.S.L.; Domokos, L.; Marin, G.B. A single-event MicroKinetic model for ethylbenzene dealkylation/xylene isomerization on Pt/H-ZSM-5 zeolite catalyst, *Appl. Catal. A* **2012**, 425–426, 130–144.

[144] Moreau, F.; Gnep, N.S.; Lacombe, S.; Merlen, E.; Guisnet, M. Ethylbenzene transformation on bifunctional Pt/Al2O3-NaHMOR catalysts: Influence of Na exchange on their activity and selectivity in ethylbenzene isomerization. *Appl. Catal. A* **2002**, *230*, 253–262.

[145] Al-Khattaf, S. Enhancing p-xylene selectivity during m-xylene transformation using mildly pre-coke ZSM-5 catalyst, *Chem. Eng. Proc*. **2007**, *46*, 964–974.

[146] Bauer, F.; Chen, W.-H.; Ernst, H.; Huang, S.-J.; Freyer, A.; Liu, S.-B. Selectivity improvement in xylene isomerization, *Microporous Mesoporous Mater*. **2004**, *72*, 81–89.

[147] Thibault-Starzyk, F.; Vimont, A.; Gilson, J-P. 2D-COS IR study of coking in xylene isomerisation on H-MFI zeolite, *Catal. Today* **2001**, *70*, 227–241.

[148] Tsai, T-C.; Wang, I.; Huang, C-K.; Liu, S-D. Study on ethylbenzene and xylene conversion over modified ZSM-5, *Appl. Catal. A* **2007**, *321*, 125–134.

[149] Fernandez, C.; Stan, I.; Gilson, J.; Thomas, K.; Vicente, A.; Bonilla, A.; Pérez-Ramírez, J. Hierarchical ZSM-5 zeolites in shape-selective xylene isomerization: Role of mesoporosity and acid site speciation, *Chem. Eur. J*. **2010**, *16*, 6224–33.

[150] Balasamy, R.; Odedario,T.; Al-Khattaf, S. A unique catalytic performance of mesoporous molecular sieves containing zeolite units in transformation of m-xylene, *Appl. Catal. A* **2011**, *409–410*, 223–233.

[151] Daramola, M.O.; Burger, A.J.; Pera-Titus, M.; Giroir-Fendler, A.; Miachon, S.; Dalmon, J.-A.; Lorenzen, L. Separation and isomerization of xylenes using zeolite membranes: a short overview, *Asia-Pacific J. Chem. Eng*. **2010**, *5*, 815–837.

[152] Van Dyk, L.; Lorenzen, L.; Miachon, S.; Dalmon, J. Xylene isomerization in an extractor type catalytic membrane reactor, *Catal. Today* **2005**, *104*, 274–280.

[153] Deshayes, A.L.; Miró, E.E.; Horowitz, G.I. Xylene isomerization in a membrane reactor. Part II. simulation of an industrial reactor, *Chem. Eng. J*. **2006**, *122*, 149–157.

[154] Xu, O.; Su, H.; Jin, X.; Chu, J. Kinetic model for hydroisomerization reaction of C8-aromatics, Front, *Chem. Eng. China* **2008**, *2*, 10–16.

[155] Yeong, Y.; Abdullah, A.; Ahmad, A.; Bhatia, S. Xylene isomerization kinetic over acid-functionalized silicalite-1 catalytic membranes: Experimental and modeling studies, *Chem. Eng*. J. **2010**, *157*, 579–589.

[156] Tarditi, A.M.; Horowitz, G.I.; Lombardo, E.A. Xylene isomerization in a ZSM-5/SS membrane reactor, *Catal. Lett*. **2008**, *123*, 7–15.

[157] Zhang, C.; Hong, Z.; Chen, J.; Gu, X.; Jin, W.; Xu, N. Catalytic MFI zeolite membranes supported on α-Al2O3 substrates for m-xylene isomerization, *J. Membr. Sci*. **2012**, *389*, 451–458.

[158] Gobin, O.C.; Reitmeier, S.J.; Jentys, A.; Lercher, J.A. Comparison of the transport of aromatic compounds in small and large MFI particles, *J. Phys. Chem. C* **2009**, *113*, 20435–20444.

[159] Reitmeier, S.J.; Gobin, O.C.; Jentys, A.; Lercher, J.A. Influence of postsynthetic surface modification on shape selective transport of aromatic molecules in HZSM-5, *J. Phys. Chem. C* **2009**, *113*, 15355–15363.

[160] Davis, S. Ethylbenzene, Marketing Research Report, *Chemical Economics Handbook* (CEH), December 2009, pp. 5–8.

[161] Barman, S.; Pradhan N.C.; Basu, J.K. Alkylation of benzene with ethyl alcohol over Ce exchanged 13X zeolite catalyst, *Ind. Chem. Eng*. **2006**, *48*, 10–17.

[162] Odedario, T.; Al-Khattaf, S. Ethylation of benzene: Effect of zeolite acidity and structure, *Appl. Catal. A Gen*. **2010**, *385*, 31–45.

[163] Wang, S.H. Styrene, *PEP Report 33C, Supplement C*, Process Economics Program, Menlo Park, California, SRI International, 1993.

[164] Ratnasamy, P.; Kumar, R. Ferrisilicate analogs of zeolites, *Catal. Today* **1991**, *9*, 329–416.

[165] Wight, C.G. Manufacture of ethylbenzene, US Patent 4,169,111 (to Union Oil Company of California, 1979).

[166] Zones, S.I. Translating new materials discoveries in zeolite research to commercial manufacture, *Microporous Mesoporous Mater*. **2011**, *144*, 1–8.

[167] Millini, R.; Perego, C.; Parker, W.O.; Flego, C.; Girotti, G. Stability upon thermal treatement of coked zeolite, *Stud. Surf. Sci. Catal*. **2004**, *154B*, 1214–1221.

[168] Christensen, C.H.; Johannsen, K.; Schmidt, I.; Christensen, C.H. Catalytic benzene alkylation over mesoporous zeolite single crystals: Improving activity and selectivity with a new family of porous materials, *J. Amer. Chem. Soc*. **2003**, *125*, 13370–13371.

[169] Lawton, S.; Fung, A.; Kennedy, G.; Alemany, L.; Chang, C.; Hatzikos, G.; Lissy, D.; Rubin, M.; Timken, H.; Steuernagel, S. Zeolite MCM-49: A three-dimensional MCM-22 analogue synthesized by in-situ crystallization, *J. Phys. Chem*. **1996**, *100*, 3788–3798.

[170] Cheng, J.; Smith, C.; Walsh, D. Liquid phase ethylbenzene synthesis with MCM-49, US Patent 5493065, 1996 (to Mobil Oil Corporation).

[171] Liu, K.; Xie, S.; Liu, S.; Xu, G.; Gao, N.; Xu, L. Catalytic role of different pore systems in MCM-49 zeolite for liquid alkylation of benzene with ethylene, *J. Catal*. **2011**, *283*, 68–74.

[172] Corma, A.; Llopis, F.J.; Martinez, C.; Sastre, G.; Valencia, S The benefit of multipore zeolites: Catalytic behavior of zeolites with intersecting channels of different sizes for alkylation reactions, *J. Catal*. **2009**, *268*, 9–17.

[173] Čejka, J.; Krejčí, A.; Žilková, N.; Kotrla, J.; Ernst, S.; Weber, A., Activity and selectivity of zeolites MCM-22 and MCM-58 in the alkylation of toluene with propylene, *Microporous Mesoporous Mater*. **2002**, *53*, 121–133.

[174] Zhang, B.; Ji, Y.J.; Wang, Z.D.; Liu, Y.M.; Sun, H.M.; Yang, W.M.; Wu, P. Liquid-phase alkylation of benzene with ethylene over postsynthesized MCM-56 analogues, *Appl. Catal. A* **2012**, *443*, 103–110.

[175] Zhang, B.; Wang, Z.D.; Ji, P.; Liu, Y.M.; Sun, H.M.; Yang, W.M.; Wu, P. Efficient liquid-phase ethylation of benzene with ethylene over mesoporous MCM-22 catalyst, *Microporous Mesoporous Mater*. **2013**, *179*, 163–168.

[176] Cheng, J.C.; Fung, A.S.; Klocke, D.J.; Lawton, S.L.; Lissy, D.N.; Roth, W.J.; Smith, C.M.; Walsh, D.E. Manufacture of short-chain alkylaromatic compounds with a zeolite catalyst, U.S.Patent 5453554 (to Mobil Oil Corporation).

[177] Odedairo, T.; Al-Khattaf, S. Kinetic investigation of benzene ethylation with ethanol over USY zeolite in a riser simulator, *Ind. Eng. Chem. Res*. **2010**, *49*, 1642–1651.

[178] Halgeri, A.B.; Das, J. Recent advances in selectivation of zeolites for para-distributed aromatics, *Catal. Today*, **2002**, *73*, 65–73.

[179] Yadav, G. D.; Kamble, S. B. Alkylation of xylenes with isopropy alcohol over acidic clay supported catalysts: Efficacy of 20% w/w $Cs_{2.5}H_{0.5}PW_{12}O_{40}$/K-10 clay, *Ind. Eng. Chem. Res*. **2009**, *48*, 9383–9393.

[180] Waziri, S.M.; Al-Khattaf, S. Kinetics of ethylbenzene ethylation with ethanol over a ZSM-5-based catalyst in a riser simulator, *Ind. Eng. Chem. Res*. **2009**, *48*, 8341–8348.

[181] Bauer, F.; Chen, W. H.; Bilz, E.; Freyer, A.; Sauerland, V.; Liu, S. B. Surface modification of nano-sized HZSM-5 and HFER by pre-coking and silanization, *J. Catal*. **2007**, *251*, 258–270.

[182] Čejka, J.; Žilková, N.; Wichterlová, B.; Eder-Mirth, G.; Lercher, J.A. Decisive role of transport rate of products for zeolite paraselectivity: Effect of coke deposition and external surface silylation on activity and selectivity of HZSM-5 in alkylation of toluene, *Zeolites*, **1996**, *17*, 265–271.

[183] Zheng, X.; Li, Q.; Fu, J. Alkylation of ethylbenzene with ethanol over zeolite-β, *Beijing Fuzhuang Xueyuan Xuebao, Ziran Kexueban* **2006**, *26*, 59–66.

[184] Huang, J.; Jiang, Y.; Marthala, V.R.R.; Hunger, M. Insight into the mechanisms of the ethylbenzene disproportionation: Transition state shape selectivity on zeolites, *J. Amer. Chem. Soc*. **2008**, *130*, 12642–12644.

[185] Park, S-H.; Rhee, H-K. Shape selective properties of MCM-22 catalysts for the disproportionation of ethylbenzene, *App. Catal. A Gen*. **2001**, *219*, 99–105.

[186] Chen, W-H.; Tsai, T-C.; Jong, S-J.; Zhao, Q.; Tsai, C-T.; Wang, I.; Lee, H-K.; Liu, S-B. Effects of surface modification on coking, deactivation and para-selectivity of H-ZSM-5 zeolites during ethylbenzene disproportionation, *J. Mol. Catal. A Chem*. **2002**, *181*, 41–55.

[187] Zhu, Z.; Chen, Q.; Xie, Z.; Yang, W.; Kong, D.; Li, C., Shape-selective disproportionation of ethylbenzene to para-diethylbenzene over ZSM-5 modified by chemical liquid deposition and MgO, *J. Mol. Catal. A* **2006**, *248*, 152–158.

[188] Al-Khattaf, S.; Catalytic transformation of ethylbenzene over Y-Zeolite-based catalysts, *Energy Fuels* **2008**, *22*, 3612–3619.

[189] Tukur, N. M.; Al-Khattaf, S. Comparative study between ethylbenzene disproportionation reaction and its ethylation reaction with ethanol over ZSM-5, *Catal. Lett*. **2009**, *131*, 225–233.

[190] Čejka, J.; Vondrová, A.; Wichterlová, B.; Vorbeck, G.; Fricke, R. The effect of Al, Fe, and In substitution in the MFI silicate structure on the aromatic hydrocarbon transformations: Si-OH-M site strength, *Zeolites* **1994**, *14*, 147–153.

[191] Wichterlová, B.; Čejka, J.; Žilková, N. Selective synthesis of cumene and p-cymene over Al and Fe silicates with large and medium pore zeolites, *Micropor. Mater*. **1996**, *6*, 405–414.

[192] Portilla, M.T.; Llopis, F.J.; Martinez, C.; Valencia, S.; Corma, A. Structure-reactivity relationship for aromatics transalkylation and isomerization process with TNU-9, MCM-22 and ZSM-5 zeolites, and their industrial implications, *App. Catal. A* **2009**, *373*, 257–268.

[193] Corma, A.; Díaz Cabañas, M.J.; Jorda, J.L.; Martinez, C.; Moliner, M. High-throughput synthesis and catalytic properties of a molecular sieve with 18-and 10-member rings, *Nature* **2006**, *443*, 842–845.

[194] Kasture, M.W.; Niphadkar, P.S.; Sharanappa, N.; Mirajkar, S.R.; Bokade, V.V.; Joshi, P.N. Isopropylation of benzene catalyzed by H/beta zeolite catalysts with different crystallinities, *J. Catal*. **2004**, *227*, 375–383.

[195] Kim, W.; Kim, J.C.; Kim, J.; Seo, Y.; Ryoo, R. External surface catalytic sites of surfactant-tailored nanomorphic zeolites for benzene isopropylation to cumene, *ACS Catal*. **2013**, *3*, 192–195.

[196] Laredo, G.C.; Quintana-Solorzano, R.; Castillo, J.J.; Armendariz-Herrera, H.; Garcia-Gutierrez, J.L. Benzene reduction in gasoline by alkylation with propylene over MCM-22 zeolite with a different Bronsted/Lewis acidity ratios, *Appl. Catal. A* **2013**, *454*, 37–45.

[197] Davis, T.M.; Chen, C.Y.; Zones, S.I.; Žilková, N.; Vitvarová, D.; Čejka, J. The Importance of Pore Intersections in the Catalytic Performance of SSZ-75, *J. Catal*. **2013**, *298*, 84–93.

[198] Ali, S.A.; Ali, M.A.; Al-Nawad, K.; Ercan, C.; Wang, Y. Parametric study of dealkylation-transalkylation reactions over mordenite-based bi-functional catalysts, *Appl. Catal. A*, **2011**, *393*, 96–108.

[199] Ali, S.A.; Aitani, A.M.; Ercan, C.; Wang, Y.; Al-Khattaf, S. Conversion of heavy reformate into xylenes over mordenite-based catalysts, *Chem. Eng. Res. Des*. **2011**, *89*, 2125–2135.

[200] Serra, J.; Guillon, E.; Corma, A. Optimizing the conversion of heavy reformate streams into xylenes with zeolite catalysts by using knowledge base high-throughput experimentation techniques, *J. Catal*. **2005**, *232*, 342–354.

[201] Tsai, T.C.; Chen, W.H.; Liu, S.B.; Tsai C.H.; Wang, I. Metal zeolites for transalkylation of toluene and heavy aromatics. *Catal. Today* **2002**, *73*, 39–47.

[202] Tsai, T.C.; Liu, S.B.; Wang, I., Disproportionation and transalkylation of alkylbenzenes over zeolite catalysts, *Appl. Catal. A* **1999**, *181*, 355–398.

[203] Dumitriu, E.; Guimon, C.; Hulea, V.; Lutic, D.; Fechete, I. Transalkylation of toluene with trimethylbenzenes catalyzed by various AFI catalysts, *Appl. Catal. A* **2002**, *237*, 211–221.

[204] Norval, G.W. Phillips, M.J. Alkylation of toluene with ethylene: An equilibrium approach, *React. Kinet. Catal. Lett*. **1989**, *38*, 261–264.

[205] Csicsery, S.M. Equilibrium distributions of the dimethylethylbenzene and methyldiethylbenzene isomers, *J. Chem. Eng. Data* **1967**, *12*, 118–122.

[206] Al-Mubaiyedh, U.; Ali, S.A.; Al-Khattaf, S. Kinetic modeling of heavy reformate conversion into xylenes over mordenite-ZSM5-based catalysts, *Chem. Eng. Res. Des*. **2012**, *90*, 1943–1955.

[207] Serra, J.M.; Guillon, E.; Corma, A. A rational design of alkyl-aromatics dealkylation–transalkylation catalysts using C8 and C9 alkyl-aromatics as reactants, *J. Catal*. **2004**, *225*, 459–469.

[208] Tsai, T.C.; Chao, P.H.; Zeng, W.L.; Tsai, S.T. Selective naphthene cracking over cascade dual catalyst in heavy aromatics transalkylation, *Stud. Surf. Sci. Catal*. **2007**, *170B*, 1611–1616.

[209] Roger, H. Moller, K.; O'Conner, C. The transformation of 1,2,4-trimethylbenzene A probe reaction to monitor external surface modifications of HZSM-5?, *Microporous Mater*. **1997**, *8*, 151–157.

[210] Park, S. H.; Rhee, H.K. Shape selective conversion of 1, 2, 4-trimethylbenzene over zeolite NU-87, *Catal. Today* **2000**, *63*, 267–273.

[211] Halgeri, A.; Das, J. Novel catalytic aspects of beta zeolite for alkyl aromatics transformation, *Appl. Catal. A* **1999**, *181*, 347–354.

[212] Ali, S.A.; Ogunronbi, K.; Al-Khattaf, S. Kinetics of dealkylation-transalkylation of C_9 alkyl-aromatics over zeolites of different structures, *Chem. Eng. Res. Des*. **2013**, *91*, 2601–2616.

[213] Nacamuli, G.; Vogel, R.; Zones, S.I. Aromatics and toluene/TMB gas phase transalkylation processes. US Patent 5,952,536, 1999 (for Chevron).

[214] Csicsery, S.M. Catalysis by shape selective zeolites — sceince and technology. *Pure Appl. Chem*. **1986**, *58*, 841–856.

[215] Martens, J.A.; Perez-Pariente, J.; Sastre, E.; Corma, A.; Jacobs, P.A. Isomerization and disproportionation of m-xylene: Selectivities induced by the void structure of the zeolite framework. *Appl. Catal*. **1988**, *45*, 85–101.